# INELASTIC INTERACTIONS IN THE DYNAMIC RESPONSE OF STRUCTURES

Thesis by

Navin Chandra Nigam

In Partial Fulfillment of the Requirements

For the Degree of

Doctor of Philosophy

California Institute of Technology

Pasadena, California

1967

(Submitted May 23, 1967)

# ACKNOWLEDGMENTS

The author wishes to thank Professor G. W. Housner for his guidance and assistance in the preparation of this thesis. The interest and help of Professors D. E. Hudson, R. T. Shield and P. C. Jennings is also appreciated.

The author is grateful for the teaching and research assistantships and tuition scholarships granted by the California Institute of Technology during the course of this work.

# ABSTRACT

The dynamic response of structures is examined under a general condition of loading. It is shown that the inelastic response of structures depends on the interaction between forces and displacements existing at a section during yielding. A theory of yielding is developed in terms of forces and displacements incorporating the effects of such interactions. Based on this theory, a force-displacement relationship is derived under a general condition of loading. The use of this relationship to study the response of structures is discussed and equations of motion are derived for a simple frame subjected to simultaneous base excitation along its principal directions.

To study the inelastic response of structures, under a general condition of loading, it is necessary to derive the equation of the yield surface in terms of forces acting at a section. For the special case of bending about the principal axes of a section, equations of yield surfaces are derived for various structural sections.

The response of a simple frame, subjected to sinusoidal base excitation, is obtained for elastic behavior, elasto-plastic behavior and elasto-plastic behavior with interaction. The response for these behaviors is compared and it is shown that interaction causes significant changes in the response. The response of the frame is also investigated for earthquake type excitation and a series of curves are presented to show the effect of interaction on various response parameters. Use of these curves for inelastic design of structures is indicated and the implications of the effects of interaction are examined.

TABLE OF CONTENTS

# CHAPTER I

# INTRODUCTION

The inelastic behavior of structures has been the object of considerable interest and extensive research during the last twenty years. For static loads, a large measure of confidence and understanding of inelastic behavior exists by now, and advantages and limitations of inelastic design are well recognised. Several excellent books[1,2,3], covering methods of inelastic design and analysis of different types of structures, are now available and building codes of most countries permit such designs. For dynamic loads, the interest in inelastic behavior is relatively recent. Though a large amount of work has been done in this area, much more work, both experimental and theoretical, needs to be done to develop proper understanding of inelastic behavior under dynamic loads.

Problems of structural dynamics arise due to vibrations induced by time varying loads, which can be classified under two broad categories: 1) Recurrent loads, which act on a structure during most of its life-span and over extended periods of time. Examples of such loads are the machine induced dynamic loads in support structures and machine components; and forces of aerodynamic and hydrodynamic origin; 2) Occasional loads, which are likely to act on a structure infrequently during its life-span and over short periods of time. Examples of such loads are the dynamic loads generated by blasts and earthquakes and occasional overloads in normally recurrent loads. For recurrent loads, the attempt more

often is to design the structure in such a way that inelastic deformations will not occur, so as to avoid the possibility of fatigue failure and cumulative damage. In such problems, it is of interest to study how inelastic deformations can occur and if they do occur, due to occasional overloads, what kind of response is to be expected. For occasional loads, on the other hand, it is being increasingly realized that inelastic deformations can be and should be permitted in order to produce economical and safe designs. This has stimulated interest in the study of the inelastic behavior of structures under dynamic loads, particularily in earthquake engineering.[4]

Analyses of common types of structures, under assumed elastic behavior, show that during strong-motion earthquakes they must experience lateral loads significantly larger than those specified by current building codes. Yet, studies of damage to structures during several of the past earthquakes have shown that many structures designed for lateral loads even lower than those prescribed by building codes have survived with little or no damage.[5] This anomaly is best explained by considering the energy input into the structure and the mechanism of its dissipation, if the structure is permitted to undergo inelastic deformations. It is found that inelastic deformations reduce the energy input to the structure[6] and through hysteresis provide a mechanism for large dissipation of energy.[5] Recognition of these facts forms the basis of current earthquake engineering research in understanding the response of structures during earthquakes and establishing methods and criteria for design.

In 1956, Housner[7] introduced the concept of inelastic design based on energy input to a structure during an earthquake and its capacity to dissipate energy by hysteresis, while undergoing inelastic deformations. Later, Housner used this concept to analyze the plastic failure of frames[8] and explain the anomalies in the response of structures during past earthquakes.[5] Housner's limit design[5,7,8] and Blume's reserve energy technique[9] provide simplified design procedures based upon energy dissipation through inelastic deformations, without considering a detailed response of the structure. The advent of high speed digital computers, permitting step by step integration, stimulated detailed studies of inelastic response of single and multi degree-of-freedom structures by a number of investigators--Newmark,[10,11] Berg,[6,12] Clough,[13] Penzien[14,15] Jennings,[16] Tanabashi,[17] and many others.[16,19,20] Such studies, coupled with experimental investigations,[21,22] have provided valuable insight into the feasibility and limitations of inelastic design. By now, a generally accepted design philosophy has emerged, which aims at an elastic behavior for small to moderate strong-motion earthquakes, which occur frequently, and permits inelastic response during infrequent large earthquakes, thus risking limited damage.

In the studies referred to above and known to the author, the inelastic response of a structure is obtained on the basis of a preassumed force-displacement relationship of either general yielding,[11] bilinear, or elastic-perfectly-plastic type, for each force-displacement pair independent of others. A more complex mechanism of

yielding invariably exists in almost all real structures and can arise in several ways, some of which are mentioned below for a simple structure.

1. The simple structure shown in Fig. 1.1 consists of a mass supported on a single column. Let a time varying force be applied to the mass in the direction 1-1. The mass vibrates in the direction 1-1 and at each section of the column there is a bending moment and a shear force, in the direction 1-1, and an axial force. Yielding will occur at a section when these forces attain a certain set of values and the yield behavior will change as these forces change with time. Thus the interaction between these forces determines the inelastic response of this simple structure.

2. Suppose we now apply time varying forces in directions 1-1 and 2-2 simultaneously. In addition to the forces of case 1, we now have a bending moment and a shear force, in the direction 2-2 also. If a torque is applied to the mass, a torsional moment will also exist at each section. The nature of yielding will depend on all these forces and moments.

The procedure of computing the inelastic response of structures, with a pre-assumed force-displacement relationship, neglects the effects of interaction between these forces on yielding. For static loads, the effects of such interactions have been investigated[2] for a

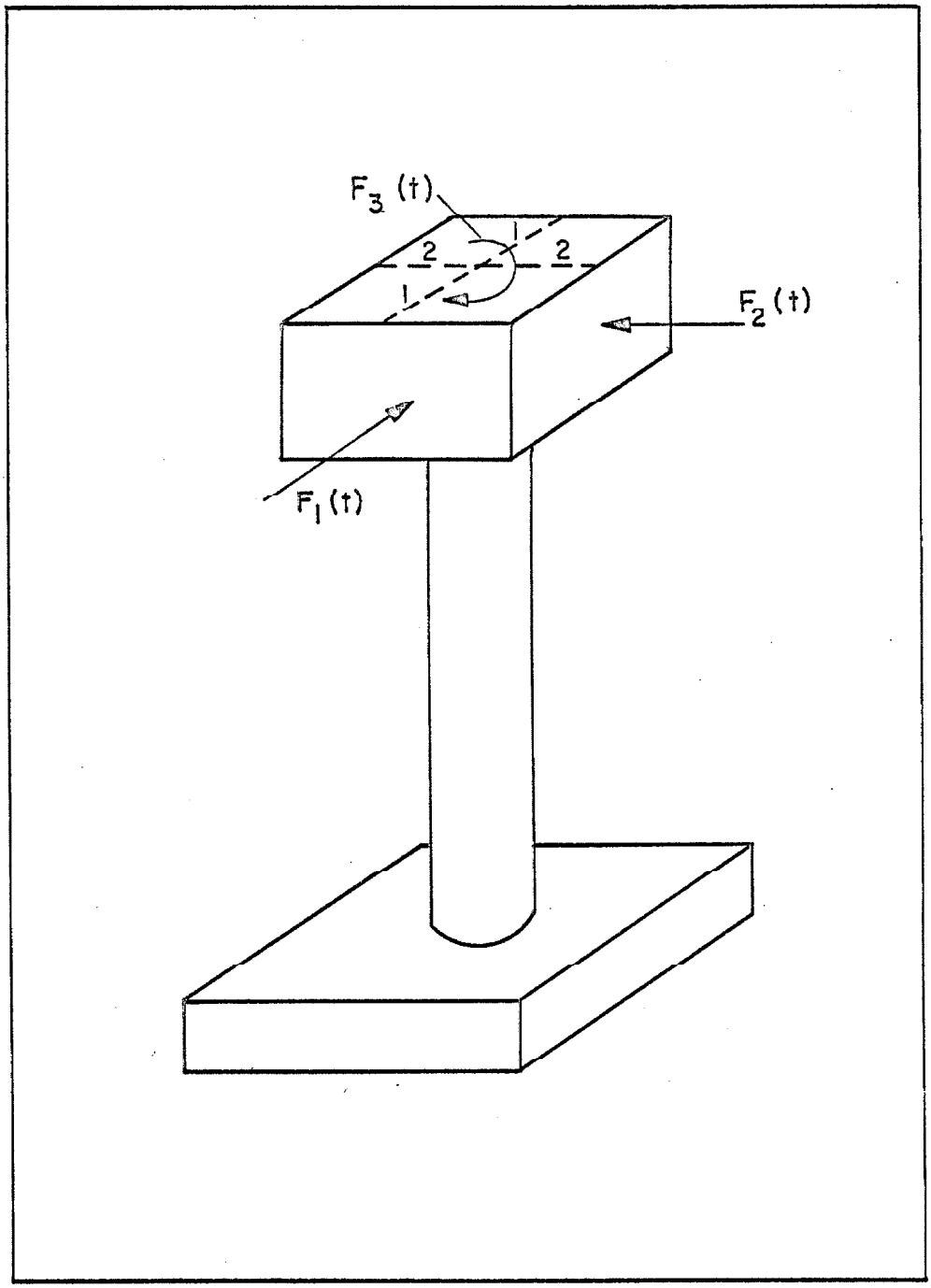


FIG. 1.1 A SIMPLE STRUCTURE

class of structures, but for dynamic loads, no such study is known to the author. Based on experience with static loads, it may be expected that in some cases effects of interaction due to axial and shear forces may be of secondary nature, but for earthquake and shock type excitation, the effects of bending in two directions are, in general, of the same order and, in particular cases, the effects of torsional moment may also be comparable.

The object of this study is to determine the inelastic response of structures, considering the effects of such interactions on yielding. Following the well established concepts of yielding in a continuum, under a complex state of stress and strain, it is possible to establish corresponding criteria for yielding of a structure in terms of forces and displacements,[2] and to derive a general force-displacement relationship. Once this is done, the equations of motion of a structure can be written and inelastic response can be computed under a general condition of loading.

This thesis is divided into five chapters. In the second chapter a general theory of yielding is developed in terms of forces and displacements under general conditions of loading. Based on this theory a general force-displacement relationship is derived and this is used to obtain the equations of motion of a simple frame. In the third chapter, the general problem of determining the yield surface under complex loading conditions is discussed and the equations of the yield surface are derived for the special case of bending in two directions. The fourth chapter deals with the inelastic

response of structures to sinusoidal excitation. Transient and steady-state response is obtained with and without interaction and these are compared to make clear the consequences of interaction. In chapter five the response of a simple frame is obtained for earthquake type excitation, using the Taft earthquake record and also an ensemble of pseudo-earthquakes. Response is again obtained with and without interaction and the implications of the effects of interaction are discussed.

In this thesis several terms already existing in technical literature are used, and some new terms are introduced. Some of these terms are often used with varying interpretations by different authors. For purposes of clarity, the specific sense in which such terms are used in this thesis is stated in Appendix I.

# CHAPTER II

# A THEORY OF YIELDING AND EQUATIONS OF MOTION OF DYNAMIC SYSTEMS

## 2.1 Introduction

In this chapter a general theory of yielding in framed structures is formulated in terms of forces and displacements at a section. Starting with assumed stress-strain relations for elasto-plastic materials the theory is built up step by step, following the basic ideas of the theory of plasticity. Based on this theory a force-displacement relationship is derived under the most general condition of loading. It is shown that the elastic-perfectly-plastic force-displacement relationship is a degenerate case of this more general relationship. For purposes of comparison, response of structures is divided into three cases:

1. Elastic response (E), with a linear force-displacement relationship.
2. Elasto-plastic response (EP), with an elastic-perfectly-plastic relationship for each force-displacement pair, independent of others.
3. Elasto-plastic response with interaction (EPI), with a dynamic force-displacement relationship incorporating the effects of interaction between various forces and displacements at a section.

For the special case of a simple frame the equations of motion and the expressions for energy input and energy loss are derived for

each of the above cases. In Chapters IV and V, these equations are used to study the effects of interaction for sinusoidal and earthquake type excitations.

A list of symbols to be used is given below and they are defined again where they first appear in the text.

| Symbol | Explanation or Definition |
|---|---|
| $a_y$ | yield acceleration |
| c | viscous damping coefficient |
| e | superscript denoting elastic behavior |
| i,j | subscripts |
| m | mass of a structure |
| p | superscript denoting plastic behavior |
| $\bar{p}$ | force ratio vector denoting the ratio of a generalized force and the corresponding yield force |
| $\bar{q}$ | generalized displacement vector |
| $\bar{q}_y$ | generalized yield displacement vector |
| $\bar{q}_o$ | displacement vector denoting current position of equilibrium |
| t | time |
| $\bar{u}$ | displacement ratio vector denoting the ratio of a generalized displacement and the corresponding yield displacement |
| w | internal work in stress-space |
| $w^p$ | plastic work in stress-space |
| y | subscript denoting yielding |
| $\bar{z}$ | vector denoting base displacement of a structure |

| Symbol | Explanation or Definition |
|---|---|
| $[C]$ | viscous damping matrix |
| DE | energy loss due to damping |
| E | Young's modulus |
| EI | energy input to a structure |
| $\overline{F}(t)$ | vector valued forcing function |
| G | shear modulus |
| HE | energy loss due to hysteresis |
| $[K]$ | stiffness matrix |
| $\overline{L}$ | bending moment vector at a section |
| $[M]$ | mass matrix |
| $\overline{P}(\overline{X})$ | vector valued restoring-force function |
| $\overline{Q}$ | generalized force vector |
| $\overline{Q}_y$ | generalized yield force vector |
| W | internal work in force-space |
| $W^p$ | plastic work in force-space |
| $\overline{X}$ | displacement vector defining the motion of a structure |
| $\epsilon$ | uniaxial strain |
| $\epsilon_{ij}$ | strain tensor |
| $\epsilon'_{ij}$ | deviatoric strain tensor |
| $\zeta$ | ratio of natural frequencies |
| $\lambda$ | positive scalar |
| $\mu$ | Poisson's ratio |
| $\xi$ | fraction of critical damping |
| $\sigma$ | uniaxial stress |
| $\sigma_{ij}$ | stress tensor |

| Symbol | Explanation or Definition |
|---|---|
| $\sigma'_{ij}$ | deviatoric stress tensor |
| $\omega$ | natural frequency |
| $\Delta$ | differential increment |
| $\| \|$ | symbol denoting absolute value |
| $\langle \rangle$ | symbol denoting inner product of vectors |
| $[\ ]$ | symbol denoting matrix |

## 2.2 Stress-Strain Relations for Elasto-Plastic Materials

### Uniaxial Loading

The stress-strain curve for an elasto-plastic material under uniaxial loading is shown in Fig. 2.1(a). For simple tension, with monotonically increasing strain, the stress $\sigma$ will be a monotonically increasing function of the strain $\epsilon$ from O to H after which it falls off until fracture occurs. From O to the proportional limit A, the material is linearly elastic and as the deformation is reversible, unloading takes place along AO. The elastic behavior, however, extends generally beyond A to yield limit B and stress-strain relationship is nonlinear between A and B. For loading beyond B, the deformation is irreversible, so that unloading from a point C to zero stress would leave a permanent plastic strain. Unloading from C to a point, say E, takes place along CDE. Reloading from E proceeds along EF to subsequent yielding at G and further loading proceeds along the path GH. We suppose that loading does not extend beyond H and disregard the portion HI.

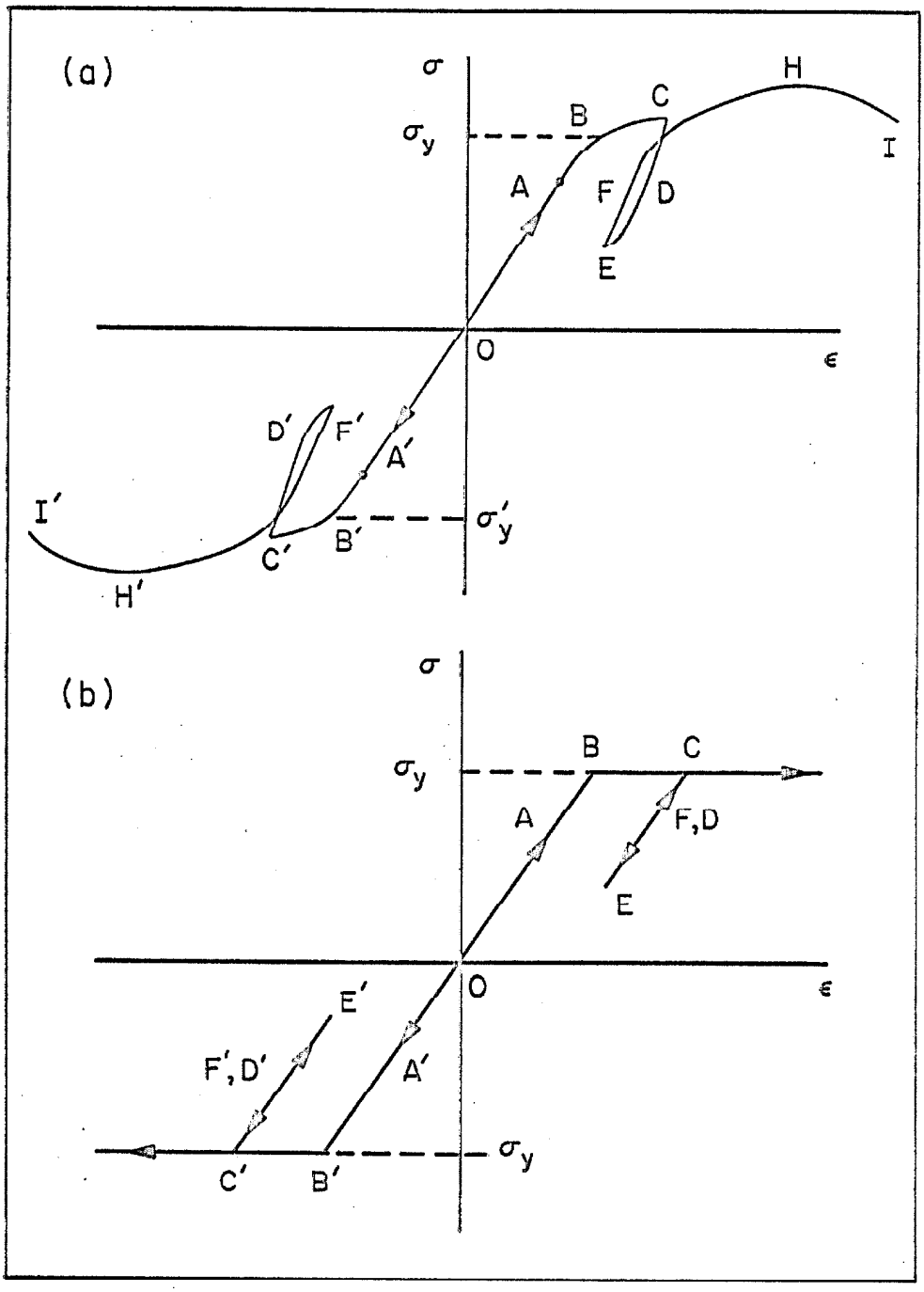


FIG. 2.1 (a) STRESS-STRAIN CURVE FOR AN ELASTO-PLASTIC MATERIAL (b) IDEALIZATION TO AN ELASTIC-PERFECTLY-PLASTIC MATERIAL

For simple compression the behavior is qualitatively similar but may differ quantitatively in case of real materials.

In general, the stress-strain curve shown in Fig. 2.1(a) is influenced by time dependent effects such as creep and strain rate as well as temperature. We idealize the stress-strain curve to that shown in Fig. 2.1(b) under the following assumptions:

1. Deformations are isothermal and time dependent effects are ignored.
2. Work-hardening is neglected.
3. The unloading path (CDE) coincides with the reloading path (EFG) and is parallel to the virgin loading path OA.
4. Behavior under simple tension and simple compression is identical and proportional limit A coincides with yield limit B.

These assumptions are taken to imply that material is elastic-perfectly-plastic. Furthermore, the hysteresis loss during loading and unloading is zero and Bauschinger effect is neglected. These assumptions are similar to those made by Prandtl,[24] following the experimental work of Berliner. The stress-strain curve shown in Fig. 2.1(b) represents the idealized material behavior described above and is used in all of the following analysis.

Complex Loading

Under a complex state of stress, the stress-strain relations for an elasto-plastic material are given by the following relations due to Hill.[22] Let us consider the stress-space defined by the

Cartesian stress tensor $\sigma_{ij}$ and let the yield surface be given by

$$\phi(\sigma_{ij}) = 1 \tag{2.1}$$

The incremental plastic work is given by

$$dw^p = \sigma_{ij} d\epsilon^p_{ij} \tag{2.2}$$

and the incremental strain is the sum of the elastic and the plastic incremental strains

$$d\epsilon'_{ij} = d\epsilon'^{e}_{ij} + d\epsilon^p_{ij} \tag{2.3}$$

with

$$d\epsilon'^{e}_{ij} = \frac{d\sigma'_{ij}}{2G} \tag{2.4}$$

and

$$d\epsilon^p_{ij} = \lambda \frac{\partial \phi}{\partial \sigma_{ij}} \quad \text{if } \phi(\sigma_{ij}) = 1 \text{ and if } d\phi = 0$$

$$= 0 \quad \text{if } \phi(\sigma_{ij}) < 1 , \tag{2.5}$$

$$\text{or if } \phi(\sigma_{ij}) = 1 \text{ and } d\phi < 0$$

Also

$$d\epsilon_{ii} = \frac{(1 - 2\mu) d\sigma_{ii}}{E} \qquad \text{(summation convention)}$$

where

$\sigma_{ij}$ is the Cartesian stress tensor

$\sigma'_{ij}$ is the Cartesian deviatoric stress tensor

$\epsilon_{ij}$ is the Cartesian strain tensor

$\epsilon'_{ij}$ is the Cartesian deviatoric strain tensor

$\lambda$ is a positive scalar quantity

G is the shear modulus

E is the Young's modulus

$\mu$ is the Poisson's ratio

e,p are superscripts denoting elastic and plastic behavior

It may be pointed out here that equation $d\epsilon^p_{ij} = \lambda(\partial\phi/\partial\sigma_{ij})$ implies that incremental plastic strain vector is directed along the normal to the yield surface at a regular point. The condition $dw^p < 0$ denotes that the incremental plastic strain vector is directed along inward normal to the yield surface and is used as the criteria for unloading.

## 2.3 Yielding in Structures in Terms of Generalized Forces and Displacements

During vibration, stresses and strains are set up in the components of a structural system, which vary from point to point and vary with time. While it may be possible to work with stresses and strains, in most structures, it is more convenient to work with forces and displacements, which are obtained by suitable integration over a cross-section with an assumed stress-strain relationship.

Let $\overline{Q}$ represent an n dimensional force vector and $\overline{q}$ an n dimensional displacement vector at a section such that the internal work is of the form

$$W = \langle \overline{Q}, \overline{q} \rangle \qquad (2.6)$$

where $\langle\ \rangle$ is the symbol denoting inner product of two vectors. Then $\bar{Q}$ is called the generalized force vector and $\bar{q}$ the generalized displacement vector. For any system the choice of generalized forces is not unique; but once they are chosen, generalized displacements are determined by the requirement that Eq. 2.6 be satisfied.

Let us consider an n dimensional force-space generated by the generalized forces at a section. The state of force at the section is then represented by a point, say A, with coordinates $Q_1, Q_2, \ldots, Q_n$ or equivalently by the vector $\bar{Q}$ from the origin to the point A. For simplicity, such a point is shown in Fig. 2.2 for a two dimensional force-space. Let us suppose that there are no initial forces at the section, so that we start at the origin, in the force-space. Let us apply the forces gradually. Stresses and strains will develop in the section and so long as the state of stress at any point of the section is such that, in the stress-space, relation between stresses and strains is linear; relation between generalized forces and displacements will be linearly elastic and can be written as

$$\bar{Q} = [K]\,\bar{q} \tag{2.7}$$

where $[K]$ is a constant stiffness matrix.

When generalized forces assume such values that yielding is imminent at one or more points of the cross-section in stress-space (Eqs. 2.5), yielding will also be imminent in force-space. The locus of all such points in force-space is a closed surface $Y'$ and is called the initial yield surface. In the space enclosed by $Y'$,

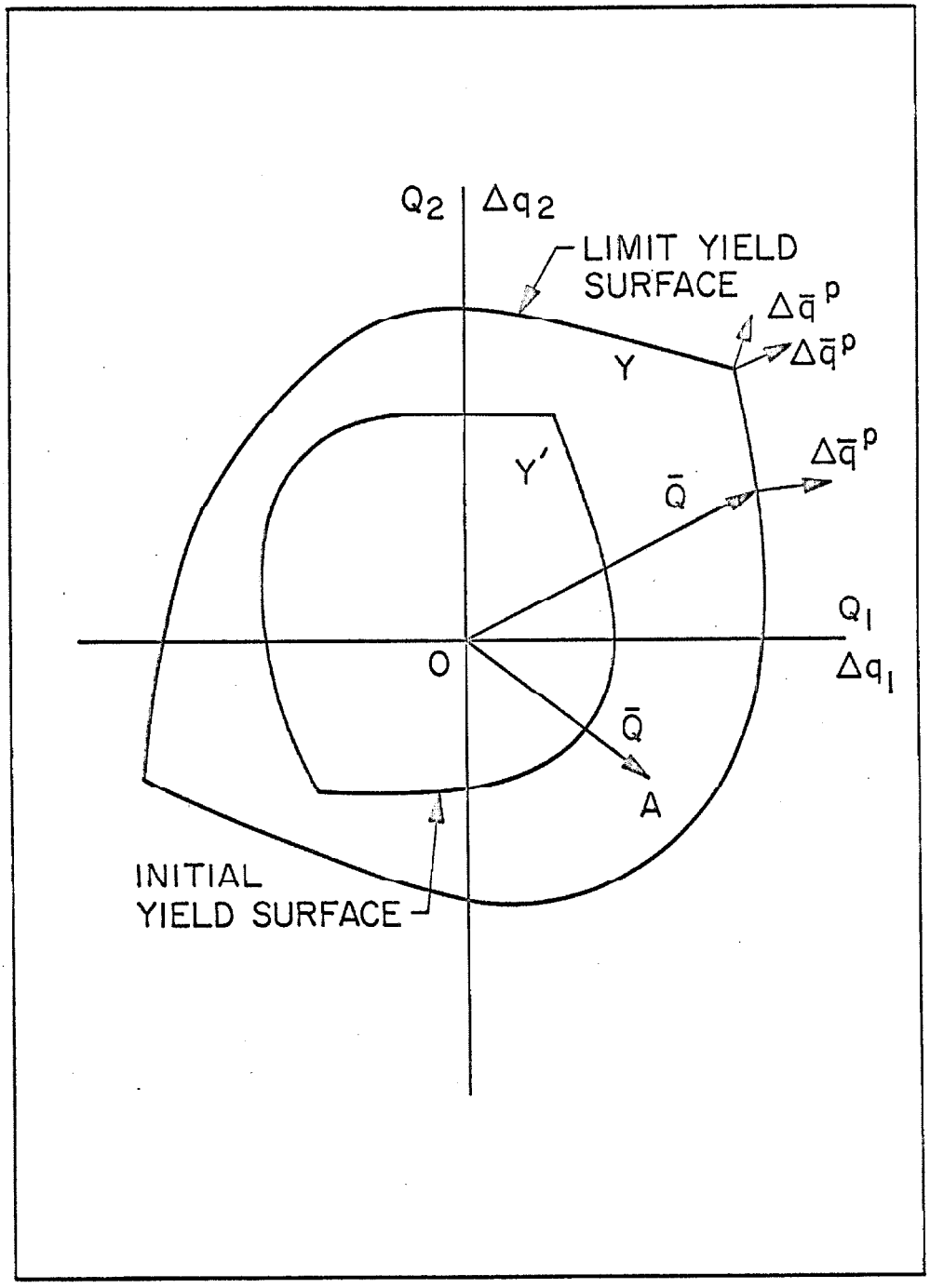


FIG. 2.2 INITIAL AND LIMIT YIELD SURFACES IN TWO DIMENSIONAL FORCE-SPACE

generalized forces and displacements are related by Eq. 2.7. As the yielding continues at one or more points, the section remains partly-elastic and partly-plastic, until yielding is imminent at all points of the section. The section is now fully plastic. The locus of the set of all such points in the force-space is called the limit yield surface Y and can be written as a scalar function of the generalized forces of the form

$$\Phi(\bar{Q}) = 1 \tag{2.8}$$

The limit yield surface is again a closed surface enclosing the origin and Y'. In the space between Y and Y', the section is partly-elastic and partly-plastic. If it is assumed that the relation between generalized forces and displacements remains linearly elastic, and is given by Eq. 2.7, up to Y (hereafter called the yield surface), the yield behavior in terms of generalized forces and displacements becomes analogous to the yield behavior in terms of stresses and strains discussed in Section 2.2. Following this analogy, it is possible to establish parallel algebraic relations in terms of generalized forces and displacements. Assuming that the coordinate axes of the generalized forces $\underline{Q}$ and the displacement increments $\Delta\bar{q}$ coincide, and following the postulates of Drucker[36], it is concluded that the yield surface must be convex and the plastic displacement vector $\Delta\bar{q}^p$ must lie along the outer normal to the yield surface at a regular point. Since the yield surface is a level surface of function $\Phi$, the normal to the surface must be in the direction of the gradient and

$$\Delta\bar{q}^p = \lambda \frac{\partial \Phi}{\partial \bar{Q}} \tag{2.9}$$

where $\lambda$ is a positive scalar.

During yielding the force vector $\bar{Q}$ moves on the yield surface, which remains fixed, since the material is assumed to be non-work-hardening. In plasticity theory, this is called loading and is characterized by the relations $\Phi(\bar{Q}) = 1$ and $d\Phi = 0$. The change from plastic behavior to elastic behavior occurs if $\Phi(\bar{Q}) = 1$ and $d\Phi < 0$. This is called unloading. The work done during yielding is given by

$$dW^p = \langle \bar{Q}, \Delta\bar{q}^p \rangle \tag{2.10}$$

If the yield surface encloses the origin, it follows from Eqs. 2.9 and 2.10 that during loading $\Phi(\bar{Q}) = 1$ and $dW^p \geq 0$. If $\Phi(\bar{Q}) = 1$ and $dW^p < 0$, unloading must occur. These relations provide alternative conditions for loading and unloading and are adopted in this study. The criteria for elastic and inelastic behavior at a section can now be written:

the section is linearly elastic if $\Phi(\bar{Q}) < 1$

or if $\Phi(\bar{Q}) = 1$ and $dW^p < 0$ (2.11)

the section is yielding if $\Phi(\bar{Q}) = 1$ and $dW^p \geq 0$ (2.12)

and

$$\Phi(\bar{Q}) \not> 1 \tag{2.13}$$

Following the theory of plasticity, it is assumed that displacement increments can be decomposed into elastic and plastic parts, so that

$$\Delta\bar{q} = \Delta\bar{q}^e + \Delta\bar{q}^p \tag{2.14}$$

During yielding the tip of the force vector moves on the yield surface and the incremental generalized force vector is related to the incremental displacement vector by the relation

$$\Delta\bar{Q} = [K]\,\Delta\bar{q}^e \tag{2.15}$$

Since the plastic incremental displacement vector $\Delta\bar{q}^p$ is normal to the yield surface and the force vector moves on the yield surface, $\Delta\bar{Q}$ and $\Delta\bar{q}^p$ must be orthogonal and, hence,

$$\langle \Delta\bar{Q}, \Delta\bar{q}^p \rangle = 0 \tag{2.16}$$

or using Eq. 2.15,

$$\langle K\Delta\bar{q}^e, \Delta\bar{q}^p \rangle = 0$$

Substituting for $\Delta\bar{q}^e$ from Eq. 2.14, there results

$$\langle K(\Delta\bar{q} - \Delta\bar{q}^p), \Delta\bar{q}^p \rangle = 0$$

or

$$\langle K\Delta\bar{q}, \Delta\bar{q}^p \rangle - \langle K\Delta\bar{q}^p, \Delta\bar{q}^p \rangle = 0$$

Substituting for $\Delta\bar{q}^p$ from Eq. (2.9) gives

$$\lambda \left\langle K\Delta\bar{q}, \frac{\partial\Phi}{\partial\bar{Q}} \right\rangle - \lambda^2 \left\langle K\frac{\partial\Phi}{\partial\bar{Q}}, \frac{\partial\Phi}{\partial\bar{Q}} \right\rangle = 0$$

Solving for $\lambda$ gives

$$\lambda = \frac{\langle K\Delta\bar{q}, \frac{\partial\Phi}{\partial\bar{Q}}\rangle}{\langle K\frac{\partial\Phi}{\partial\bar{Q}}, \frac{\partial\Phi}{\partial\bar{Q}}\rangle} \tag{2.17}$$

Eq. 2.9 can now be written

$$\Delta\bar{q}^p = \frac{\langle K\Delta\bar{q}, \frac{\partial\Phi}{\partial\bar{Q}}\rangle}{\langle K\frac{\partial\Phi}{\partial\bar{Q}}, \frac{\partial\Phi}{\partial\bar{Q}}\rangle} \frac{\partial\Phi}{\partial\bar{Q}} \tag{2.18}$$

and Eq. 2.14 can be written

$$\Delta\bar{q}^e = \Delta\bar{q} - \frac{\langle K\Delta\bar{q}, \frac{\partial\Phi}{\partial\bar{Q}}\rangle}{\langle K\frac{\partial\Phi}{\partial\bar{Q}}, \frac{\partial\Phi}{\partial\bar{Q}}\rangle} \frac{\partial\Phi}{\partial\bar{Q}} \tag{2.19}$$

Also Eq. 2.15 can be written

$$\Delta\bar{Q} = [K]\left(\Delta\bar{q} - \frac{\langle K\Delta\bar{q}, \frac{\partial\Phi}{\partial\bar{Q}}\rangle}{\langle K\frac{\partial\Phi}{\partial\bar{Q}}, \frac{\partial\Phi}{\partial\bar{Q}}\rangle} \frac{\partial\Phi}{\partial\bar{Q}}\right) \tag{2.20}$$

Dividing Eq. 2.20 by $\Delta t$ and taking limit as $\Delta t \to 0$

$$\dot{\bar{Q}} = [K]\left(\dot{\bar{q}} - \frac{\langle K\dot{\bar{q}}, \frac{\partial\Phi}{\partial\bar{Q}}\rangle}{\langle K\frac{\partial\Phi}{\partial\bar{Q}}, \frac{\partial\Phi}{\partial\bar{Q}}\rangle} \frac{\partial\Phi}{\partial\bar{Q}}\right) \tag{2.21}$$

where $\dot{\bar{Q}}$ denotes $d\bar{Q}/dt$.

Equation 2.21 thus defines the force-displacement relationship at a section when yielding is taking place. We can now write the force-displacement relationship at a section under the most general

condition of loading. From Eq. 2.7, Eqs. 2.11-2.13 and Eq. 2.21, we have

$$\bar{Q} = [K](\bar{q} - \bar{q}_o) \qquad \text{if } \Phi(\bar{Q}) < 1, \quad \text{or if } \Phi(\bar{Q}) = 1 \text{ and } \dot{W}^p < 0 \tag{2.22}$$

and

$$\dot{\bar{Q}} = [K]\left(\dot{\bar{q}} - \frac{\langle K\dot{\bar{q}}, \frac{\partial\Phi}{\partial\bar{Q}}\rangle}{\langle K\frac{\partial\Phi}{\partial\bar{Q}}, \frac{\partial\Phi}{\partial\bar{Q}}\rangle}\frac{\partial\Phi}{\partial\bar{Q}}\right) \text{ if } \Phi(\bar{Q}) = 1 \text{ and } \dot{W}^p \geq 0. \tag{2.23}$$

where $\bar{q}_o$ denotes current position of equilibrium

The force-displacement relations derived above apply at the regular points of the yield surface. In many cases the yield surface is piecewise smooth, consisting of a number of yield surfaces $\Phi_i(\bar{Q})$ which are regular and meet to form singular regimes. At such intersections the normal to the yield surface is not defined uniquely and Eq. 2.9 does not hold. Following Koiter[25] and assuming that loading surfaces act independently, we can write the total plastic displacement as the sum of the contributions from certain of the $\Phi_i(\bar{Q})$, determined by loading criteria (Eqs. 2.11-2.13), with each $\Phi_i(\bar{Q})$ satisfying Eq. 2.8, that is

$$\Delta\bar{q}^p = \sum_{i=1}^{s} g_i\lambda_i \frac{\partial\Phi_i}{\partial\bar{Q}} \tag{2.24}$$

where

$$g_i = 0 \quad \text{for } \Phi_i(\bar{Q}) < 1 \text{ or } \Phi_i(\bar{Q}) = 1 \text{ and } \dot{W}^p < 0$$

$$= 1 \quad \text{for } \Phi_i(\bar{Q}) = 1 \text{ and } \dot{W}^p \geq 0$$

and

$$\Phi_i(\bar{Q}) \not> 1$$

where s is the total number of surfaces at a singular regime.

Following this general idea one can work out consistent schemes, in specific cases,to deal with singular regimes by following through the movement of the force vector, step by step.

A Special Case

In the case of one dimensional force-space, let $Q_i$ be the only generalized force at a section and $q_i$ the corresponding displacement. For this case Eq. 2.8, describing the yield surface, degenerates to

$$\left(\frac{Q_i}{Q_{yi}}\right) = 1 \tag{2.25}$$

where $Q_{yi}$ is the yield limit of $Q_i$. The force-displacement relationship defined by Eqs. 2.22 and 2.23 now simplifies to

$$\begin{aligned} Q_i &= k_i |q_i - q_{oi}| \qquad \text{if } Q_i < |Q_{yi}| \\ &\qquad\qquad \text{or if } Q_i = |Q_{yi}| \text{ and } \dot{W}^p < 0 \\ &= |Q_{yi}| \qquad \text{if } \dot{W}^p \geq 0 \end{aligned} \tag{2.26}$$

The force-displacement relationship defined by Eqs. 2.26 represents an elastic-perfectly-plastic behavior and has been used extensively by a number of investigators[6,10,14,18] to study the response of a large class of structures. A typical force-displacement curve for such a

behavior is shown in Fig. 2.3. The curve AC (shown dotted) represents the transition from elastic to perfectly plastic state. The positions of points A and C and the shape of the curve AC depend on the form of the member. In the elastic-perfectly-plastic force-displacement relationship, defined by Eqs. 2.26, the curve AC is replaced by the extension of OA to B. Effects of this approximation are discussed in Section 3.4 of Chapter III.

It is clear now that in structures where more than one force is present at a section, to assume a force-displacement relationship defined by Eqs. 2.26 amounts to ignoring the effects of interaction between these forces. The main purpose of this study is to investigate the effects of such interaction on the response of structures, by using the more general force-displacement relationship defined by Eqs. 2.22 and 2.23. For purposes of comparison the response of structures with a force-displacement relationship defined by Eqs. 2.26 is called elasto-plastic (denoted by EP). Response with force-displacement relationship defined by Eqs. 2.22 and 2.23 is called elasto-plastic with interaction (denoted by EPI). Elastic response is denoted by E.

## 2.3 Equations of Motion

The equations of motion of a large class of structures can be written in the form

$$[M]\ddot{\overline{X}} + [D]\dot{\overline{X}} + \overline{P}(\overline{X}) = \overline{F}(t) \qquad (2.27)$$

where

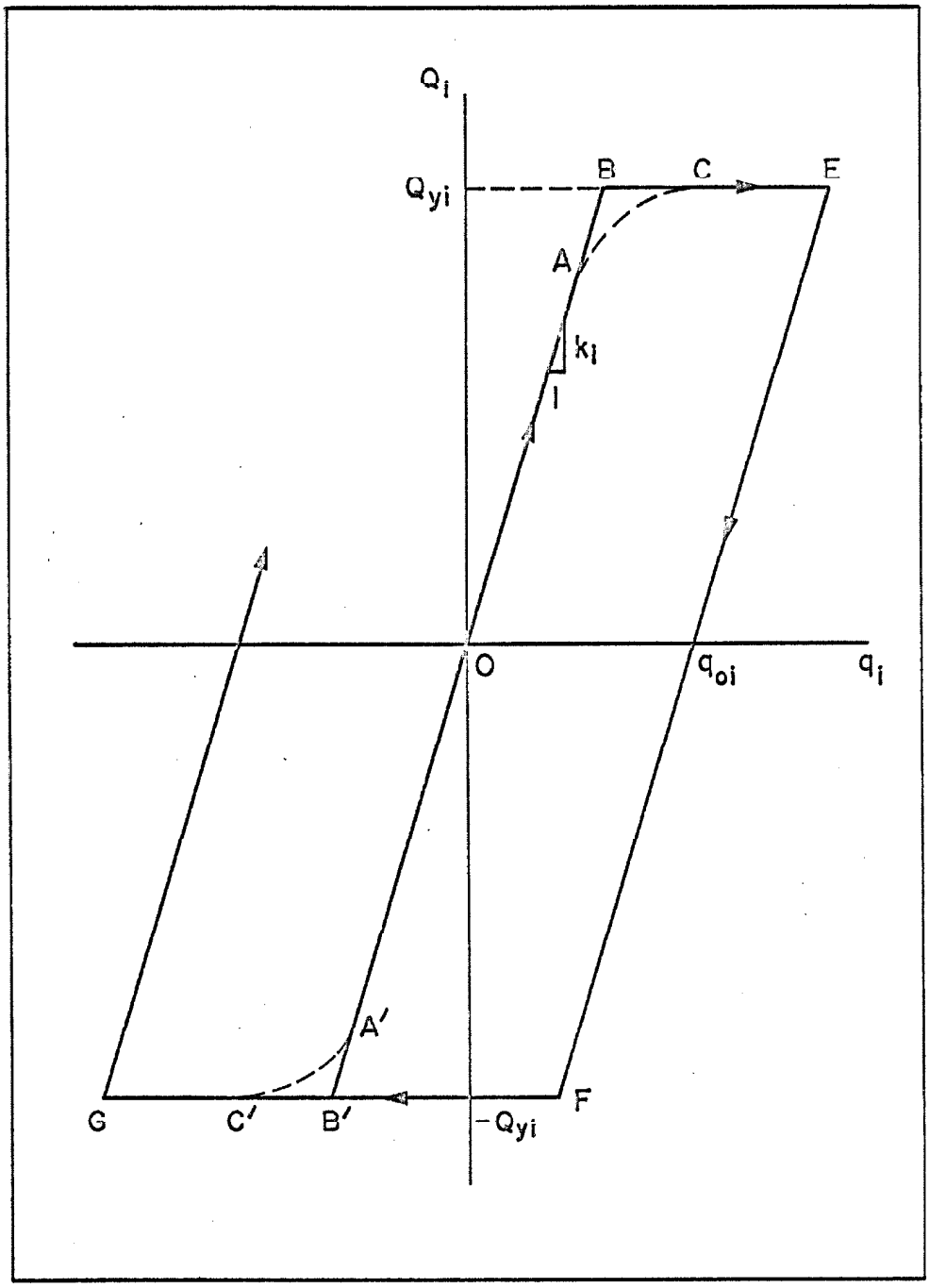


FIG. 2.3 FORCE-DISPLACEMENT CURVE FOR ELASTO-PLASTIC BEHAVIOR

| | |
|---|---|
| $[M]$ | is the mass matrix |
| $[D]$ | is the damping matrix |
| $\bar{X}$ | is the displacement vector defining the motion of the structure |
| $\bar{P}(\bar{X})$ | is a vector valued function of $\bar{X}$ called the restoring-force |
| $\bar{F}(t)$ | is the vector valued forcing function |
| $\dot{\bar{X}}$ | denotes $d\bar{X}/dt$ |

If the force-displacement relationships at various sections of a structure are known, the restoring force function $\bar{P}(\bar{X})$ can be computed and the response of the structure is given by integration of Eq. 2.27. The responses of a large class of structures have been computed [12,13,15,16,19,20] for force-displacement relationships which are either elasto-plastic (Eqs. 2.26), bilinear or general yielding. For the force-displacement relationship defined by Eqs. 2.22 and 2.23, essentially similar procedures can be used to study the response of a structure. It may be noted that in the investigations referred to above, since the force-displacement relation for each pair is defined independently, the response for each pair can be obtained separately. Since Eqs. 2.23 are coupled, this is not possible when a force-displacement relationship defined by these equations is used. We illustrate this now by deriving the equations of motion for a simple frame.

A Simple Frame

Let us consider a single-story frame shown in Fig. 2.4. It consists of a rigid mass supported on four columns, which are

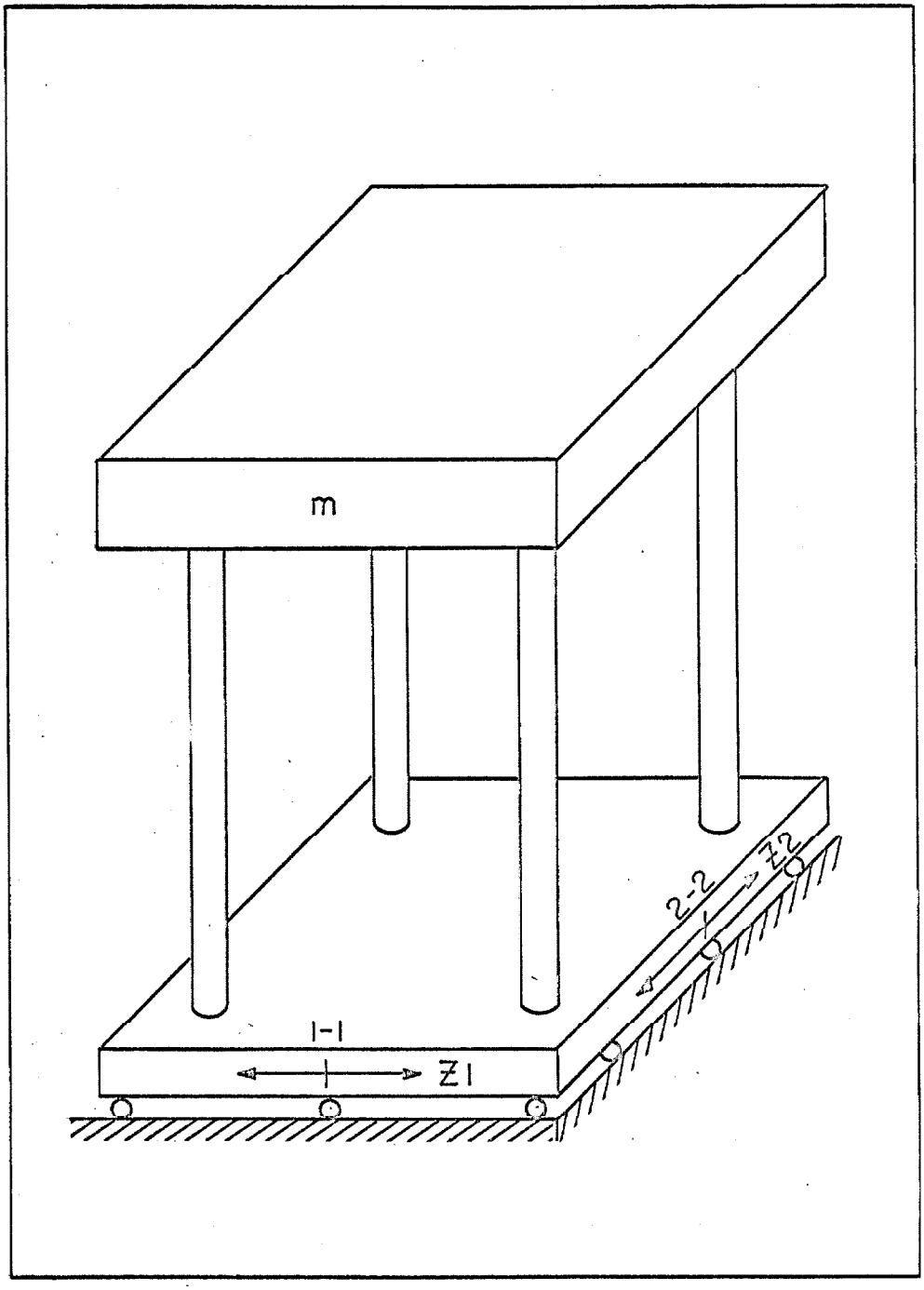


FIG. 2.4 A SIMPLE FRAME

assumed to be uniform and identical. Columns are rigidly clamped at the top and bottom and their principal axes lie in the directions 1-1 and 2-2. The weight of the columns is small compared to m and is neglected. Damping is supposed to be viscous. The base is mounted on ball-bearings and is free to move in the horizontal plane. Let $\bar{z}$ denote the displacement of the base in the horizontal plane and $\bar{q}$ the displacement of the mass center relative to the base. We further assume that the shear and the mass centers of the frame coincide and influence of axial and shear forces on yielding is neglected. Under these simplifying assumptions yielding occurs at the top and bottom sections of the columns with the interacting forces at these sections being the bending moments $L_1$ and $L_2$ in the directions 1-1 and 2-2 respectively. It may also be noted that for this simple case the response of the frame depends only upon the behavior at the top and bottom sections of the columns. When the behavior at these sections is linear, the frame is linear. When yielding occurs at these sections the frame is turned into a mechanism and behaves in a fully plastic fashion. This permits some simplification to be made in writing the equations of motion, if generalized forces and displacements are chosen judiciously.

Let the lateral restoring forces in the directions 1-1 and 2-2 be chosen as the generalized forces $Q_1$ and $Q_2$. These are related to $L_1$ and $L_2$ by

$$Q_1 = \frac{8L_1}{h} \quad , \qquad Q_2 = \frac{8L_2}{h} \tag{2.28}$$

where

| | |
|---|---|
| h | is the height of the frame |
| $L_1, L_2$ | are the bending moments at the top and bottom sections of the columns in the direction 1-1 and 2-2 |

The generalized displacements $q_1$ and $q_2$ are then the lateral displacements due to translation in directions 1-1 and 2-2 and, hence, the internal work is given by

$$W = Q_1 q_1 + Q_2 q_2 \tag{2.29}$$

The equations of motion can now be written in terms of $q_1$ and $q_2$ by making use of Eqs. 2.22, 2.23, and 2.26. Equations for elastic response, elasto-plastic response and elasto-plastic response with interaction are given below in expanded form.

$$\begin{aligned} m\ddot{q}_1 + c_1\dot{q}_1 + Q_1 &= -m\ddot{z}_1 \\ m\ddot{q}_2 + c_2\dot{q}_2 + Q_2 &= -m\ddot{z}_2 \end{aligned} \tag{2.30}$$

where

For elastic response:

$$\begin{aligned} Q_1 &= k_1 q_1 \\ Q_2 &= k_2 q_2 \end{aligned} \tag{2.31}$$

For elasto-plastic response:

$$
\begin{aligned}
Q_1 &= k_1(q_1 - q_{o1}) && \text{if } Q_1 < |Q_{y1}| \ , \\
& && \text{or if } Q_1 = |Q_{y1}| \text{ and } \dot{W}_1^p < 0 \\
&= |Q_{y1}| && \text{if } \dot{W}_1^p \geq 0 \\
Q_2 &= k_2(q_2 - q_{o2}) && \text{if } Q_2 < |Q_{y2}| \ , \\
& && \text{or if } Q_2 = |Q_{y2}| \text{ and } \dot{W}_2^p < 0 \ . \\
&= |Q_{y2}| && \text{if } \dot{W}_2^p \geq 0
\end{aligned}
\tag{2.32}
$$

For elasto-plastic response with interaction:

$$Q_1 = k_1(q_1 - q_{o1})$$

and

$$Q_2 = k_2(q_2 - q_{o2}) \tag{2.33}$$

$$\text{if } \Phi(Q_1, Q_2) < 1 \ ,$$

$$\text{or if } \Phi(Q_1, Q_2) = 1 \text{ and } \dot{W}^p < 0$$

and

$$\dot{Q}_1 = k_1 k_2 \frac{\left\{\left(\frac{\partial \Phi}{\partial Q_2}\right)^2 \dot{q}_1 - \frac{\partial \Phi}{\partial Q_1} \cdot \frac{\partial \Phi}{\partial Q_2} \dot{q}_2\right\}}{\left\{k_1\left(\frac{\partial \Phi}{\partial Q_1}\right)^2 + k_2\left(\frac{\partial \Phi}{\partial Q_2}\right)^2\right\}}$$

$$\dot{Q}_2 = k_1 k_2 \frac{\left\{-\frac{\partial \Phi}{\partial Q_1}\frac{\partial \Phi}{\partial Q_2} \dot{q}_1 + \left(\frac{\partial \Phi}{\partial Q_1}\right)^2 \dot{q}_2\right\}}{\left\{k_1\left(\frac{\partial \Phi}{\partial Q_1}\right)^2 + k_2\left(\frac{\partial \Phi}{\partial Q_2}\right)^2\right\}} \tag{2.34}$$

$$\text{if } \Phi(Q_1, Q_2) = 1 \text{ and } \dot{W}^p \geq 0$$

We now put these equations into dimensionless form by making the following changes in variables. Let

$$\omega_1^2 = \frac{k_1}{m} \quad ; \quad \omega_2^2 = \frac{k_2}{m}$$

$$u_1 = \frac{q_1}{q_{y1}} \quad ; \quad u_2 = \frac{q_2}{q_{y2}}$$

$$u_{o1} = \frac{q_{o1}}{q_{y1}} \quad ; \quad u_{o2} = \frac{q_{o2}}{q_{y2}}$$

$$c_1 = 2mw_1\xi_1 \quad ; \quad c_2 = 2mw_2\xi_2 \qquad (2.35)$$

$$a_{y1} = \frac{Q_{y1}}{m} \quad ; \quad a_{y2} = \frac{Q_{y2}}{m}$$

$$p_1 = \frac{Q_1}{Q_{y1}} \quad ; \quad p_2 = \frac{Q_2}{Q_{y2}}$$

$$\tau = \omega_1 t \quad ; \quad \zeta = \frac{\omega_1}{\omega_2}$$

Substituting Eqs. 2.35 in Eqs. 2.30 through 2.34 and denoting $du/d\tau$ by $\dot{u}$, we get

$$\begin{aligned} \ddot{u}_1 + 2\xi_1\dot{u}_1 + p_1 &= -\ddot{z}_1\left(\frac{\tau}{\omega_1}\right)/a_{y1} \\ \zeta^2\ddot{u}_2 + 2\xi_2\zeta\dot{u}_2 + p_2 &= -\ddot{z}_2\left(\frac{\tau}{\omega_2\zeta}\right)/a_{y2} \end{aligned} \qquad (2.36)$$

where

For elastic response:

$$p_1 = u_1$$
$$p_2 = u_2 \tag{2.37}$$

For elasto-plastic response:

$$\begin{aligned} p_1 &= (u_1 - u_{o1}) && \text{if } p_1 < |1| \ , \\ & && \text{or if } p_1 = |1| \text{ and } \dot{W}_1^p < 0 \\ &= |1| && \text{if } \dot{W}_1^p \geq 0 \\ p_2 &= (u_2 - u_{o2}) && \text{if } p_2 < |1| \ , \\ & && \text{or if } p_2 = |1| \text{ and } \dot{W}_2^p < 0 \\ &= |1| && \text{if } \dot{W}_2^p \geq 0 \end{aligned} \tag{2.38}$$

For elasto-plastic response with interaction:

$$p_1 = (u_1 - u_{o1})$$
$$p_2 = (u_2 - u_{o2})$$
$$\text{if } \Phi(p_1, p_2) < 1$$
$$\text{or if } \Phi(p_1, p_2) = 1 \text{ and } \dot{W}^p < 0$$
$$\dot{p}_1 = k_2 \frac{\left\{\left(\frac{\partial \Phi}{\partial p_2}\right)^2 \dot{u}_1 - \frac{\partial \Phi}{\partial p_1} \frac{\partial \Phi}{\partial p_2} \frac{q_{y2}}{q_{y1}} \dot{u}_2\right\}}{\left\{k_1 \left(\frac{\partial \Phi}{\partial p_1}\right)^2 + k_2 \left(\frac{\partial \Phi}{\partial p_2}\right)^2\right\}} \tag{2.39}$$

$$\dot{p}_2 = k_1 \frac{\left\{ -\frac{\partial \Phi}{\partial p_1} \frac{\partial \Phi}{\partial p_2} \frac{q_{y1}}{q_{y2}} \dot{u}_1 + \left(\frac{\partial \Phi}{\partial p_1}\right)^2 \dot{u}_2 \right\}}{\left\{ k_1 \left(\frac{\partial \Phi}{\partial p_1}\right)^2 + k_2 \left(\frac{\partial \Phi}{\partial p_2}\right)^2 \right\}}$$

$$\text{if } \Phi(p_1, p_2) = 1 \text{ and } \dot{W}^p \geq 0$$

It may be observed that for elastic and elasto-plastic response the equations of motion are uncoupled in the directions 1-1 and 2-2 and can be integrated independently. For elasto-plastic response with interaction, the equations of motion are coupled and this can not be done.

Equations of Energy Input and Energy Loss

In many problems of structural dynamics a study of the energy input and energy dissipation by damping and hysteresis provides valuable insight into the overall behavior of the system. In earthquake engineering such studies have been successfully used to explain the response of structures during earthquakes[5] and to establish simple design criteria.[7,9] Expressions for energy input and energy loss by damping and hysteresis are derived below for the simple frame.

Equations of motion of the frame can be written as

$$m\ddot{q}_i + c_i\dot{q}_i + Q_i = -m\ddot{z}_i(t) \qquad (2.40)$$

where $i = 1, 2$ and $Q_i$ is defined for each case by Eqs. 2.31 through 2.34. Equation 2.40 is the same as the equation of motion of a frame

with an immovable base, whose mass is excited by the force $-m\ddot{z}_i(t)$. As the frame moves through an increment of deflection $dq_i$, energy is supplied to the frame by the force and

$$dEI_i = - m\ddot{z}_i(t)\, dq_i \tag{2.41}$$

where $EI_i(t)$ is the energy input to the frame in time $t$ along $i$-$i$. From Eq. 2.40 it follows that

$$EI_i(t) = \int_o^{q_i} -m\ddot{z}_i(t)\, dq_i = m\int_o^{q_i} \ddot{q}_i\, dq_i + c_i\int_o^{q_i} \dot{q}_i\, dq_i + \int_o^{q_i} Q_i\, dq_i \tag{2.42}$$

where it is assumed that the frame starts from rest. Setting $\ddot{q}_i = d\dot{q}_i/dt$ and $dq_i = \dot{q}_i\, dt$, Eq. 2.42 can be written as

$$EI_i(t) = m\int_o^{\dot{q}_i} \dot{q}_i\, d\dot{q}_i + c_i\int_o^t \dot{q}_i^2\, dt + \int_o^t Q_i\dot{q}_i\, dt$$

$$= \frac{1}{2}m\dot{q}_i^2(t) + c_i\int_o^t \dot{q}_i^2\, dt + \int_o^t Q_i\, q_i\, dt \tag{2.43}$$

The first term on the right-hand side of Eq. 2.43 represents the kinetic energy of the frame at time $t$. The second term represents the energy dissipated by viscous damping and the third term is the sum of the potential energy at time $t$ and the energy dissipated by hysteresis. We can lump together the kinetic energy and the potential energy and call it the residual energy at time $t$. The energy input to the frame during time $t$ can now be written as

$$EI_i(t) = RE_i(t) + DE_i(t) + HE_i(t) \tag{2.44}$$

where

$RE_i(t)$ is the residual energy at time t in direction i-i

$DE_i(t)$ is the energy loss due to damping during time t, in direction i-i

and

$HE_i(t)$ is the energy loss due to hysteresis during time t, in direction i-i

The terms in Eq. 2.44 are given by the following equations

$$RE_i(t) = \frac{1}{2} m \dot{q}_i^2 + \frac{1}{2} k_i q_i^2 \tag{2.45}$$

$$DE_i(t) = c_i \int_o^t \dot{q}_i^2 \, dt \tag{2.46}$$

For elastic response:

$$HE_i(t) = 0$$

For elasto-plastic response:

$$\begin{aligned} HE_i(t) &= \int_o^t Q_i \dot{q}_i \, dt \qquad \text{if } Q_i = |Q_{yi}| \text{ and } \dot{W}_i^p \geq 0 \\ &= 0 \qquad\qquad\quad \text{if } Q_i < |Q_{yi}| \ , \\ &\qquad\quad \text{or if } Q_i = |Q_{yi}| \text{ and } \dot{W}_i^p < 0 \end{aligned} \tag{2.47}$$

For elasto-plastic response with interaction:

$$\begin{aligned} HE_i(t) &= \int_o^t Q_i \dot{q}_i^p \, dt \qquad \text{if } \Phi(Q_1, Q_2) = 1 \text{ and } \dot{W}^p \geq 0 \\ &= 0 \qquad\qquad\quad \text{if } \Phi(Q_1, Q_2) < 1 \ , \\ &\qquad\quad \text{or if } \Phi(Q_1, Q_2) = 1 \text{ and } \dot{W}^p < 0 \end{aligned} \tag{2.48}$$

By the change of variables defined by Eqs. 2.35, these expressions can be rewritten in the dimensionless form

$$\frac{RE_i(\tau)}{\frac{1}{2} Q_{yi} q_{yi}} = \dot{u}_i^2 + u_i^2 \tag{2.49}$$

and

$$\frac{DE_i(\tau)}{\frac{1}{2} Q_{yi} q_{yi}} = 4\xi_i \int_o^\tau \dot{u}_i^2 \, d\tau \tag{2.50}$$

For elastic response:

$$\frac{HE_i(\tau)}{\frac{1}{2} Q_{yi} q_{yi}} = 0$$

For elasto-plastic response:

$$\begin{aligned} \frac{HE_i(\tau)}{\frac{1}{2} Q_{yi} q_{yi}} &= 2\int_o^\tau p_i \dot{u}_i \, d\tau \qquad \text{if } p_i = |1| \text{ and } \dot{W}_i^p \geq 0 \\ &= 0 \qquad \text{if } p_i < |1| \\ &\qquad \text{or if } p_i = |1| \text{ and } \dot{W}_i^p < 0 \end{aligned} \tag{2.51}$$

For elasto-plastic response with interaction:

$$\begin{aligned} \frac{HE_i(\tau)}{\frac{1}{2} Q_{yi} q_{yi}} &= 2\int_o^\tau p_i \dot{u}_i^p \, d\tau \qquad \text{if } \Phi(p_1, p_2) = 1 \text{ and } \dot{W}^p \geq 0 \\ &= 0 \qquad \text{if } \Phi(p_1, p_2) < 1 \\ &\qquad \text{or if } \Phi(p_1, p_2) = 1 \text{ and } \dot{W}^p < 0 \end{aligned} \tag{2.52}$$

where

$\frac{1}{2} Q_{yi} q_{yi}$ is the elastic energy capacity of the frame in direction i-i

It may be remarked here that the foregoing energy analysis is for a structure whose mass is acted upon by the force $-m\ddot{z}(t)$, rather than for a structure whose base is excited by the acceleration $\ddot{z}(t)$. Therefore, the kinetic energy terms in the previous equations represent the energy of motion relative to the base rather than that due to absolute motion. As it is the relative displacements and velocities that are of primary importance in practice, an energy equation expressed in terms of relative motion is more meaningful than one expressed in terms of absolute velocities and displacements[16].

# CHAPTER III

# YIELD SURFACE IN GENERALIZED FORCE-SPACE

## 3.1 Introduction

In this chapter a general approach for determining the equation of yield surface in generalized force-space is discussed. The problem is posed and treated in general terms and references are given to earlier work. For the special case of bending about the principal axes of a section, yield curves are derived for various structural shapes. The chapter is concluded with a discussion of some of the assumptions made in deriving the general theory of yielding.

The notation used in this chapter is the same as in the preceeding chapters with the following additions.

| Symbol | Explanation or Definition |
|---|---|
| $a, b, a_1, b_1$ | dimensions of elliptical sections |
| $f(x_1, x_2)$ | a scalar function of $x_1$ and $x_2$ |
| $k$ | constant in von Mises yield criteria |
| $x_1, x_2$ | coordinates in the plane of a section |
| $B, H, B_1, H_1$ | dimensions of rectangular sections |
| $N$ | axial force at a section |
| $\beta_1, \beta_2, \beta$ | section parameters |
| $\nu, \nu_1$ | parameters |
| $\Gamma_1, \Gamma_2, \Gamma_3, \Gamma_4$ | dimensional constants |
| $\chi$ | a scalar function of $x_1$ |
| $\Lambda$ | a scalar function |
| $\bar{\Omega}$ | a vector valued function |

## 3.2 Equation of the Yield Surface

### Statement of the Problem

The equation of the yield surface in the generalized force-space is a relation between the forces acting at a section when it is fully plastic. More precisely, the problem can be stated as the determination of a stress distribution, which satisfies the criteria of yielding ($\phi(\sigma_{ij}) = 1$ and $\dot{w}^p \geq 0$) at each point of the section, except possibly along a line, meets Hill's criterion of maximum plastic work and is such that the generalized forces at the section are given by

$$\bar{Q} = \int\int_A \bar{\Omega}(\sigma_{ij}, x_1, x_2)\, dA \tag{3.1}$$

where

$\bar{\Omega}$ is a vector valued function

$x_i$ $i = 1, 2$, are coordinates of point in the plane of the section

Let us consider a generalized space in terms of force-ratios $p_i = Q_i/Q_{yi}$. Then the yield surface must intersect each of the coordinate axes of this space in such a way that $\bar{p} = \pm 1$. In the previous chapter it was concluded, on the basis of Drucker's postulates, that the yield surface must be convex. Hence, the lowest bound to the yield surface must be a closed surface formed by the intersection of planes joining the set of points $\bar{p} = \pm 1$. In view of the assumptions made in Section 2.2 of the preceeding chapter (neglecting the Bauchinger effect), it is clear that the yield surface must be

symmetrical about the coordinate axes. Hence, the uppermost bound to the yield surface must be formed by planes normal to the coordinate axes at $p = \pm 1$. These surfaces are shown in Fig. 3.1 for a two-dimensional space.

To determine the equation of the yield surface in terms of generalized forces Sadowsky[26] proposed, in 1943, a heuristic maximum effort principle for ideally plastic bodies. The principle states that "among all statically determined possible stress distributions (satisfying all three equations of equilibrium, the condition of plasticity and boundary conditions), the actual distribution in plastic flow requires a maximum value of the external effort necessary to maintain the flow." Prager[27] applied this principle to a uniform prismatic bar of arbitrary section, under combined torsion and tension. Handelman[28] used it for a bar under combined bending and torsion. In 1947, Hill[29] pointed out that Sadowsky's principle does not lead to correct results, in general, and introduced the principle of maximum plastic work. He applied this principle to determine the stress distribution in a prismatic bar of arbitrary uniform cross section, plastically deformed by bending couples, twisting couple and axial force applied at the ends (Fig. 3.2). The surface of the bar is stress free and the elastic strains are neglected. Using von Mises criterion of yielding ($\sigma'_{ij}\sigma'_{ij} = k^2$) and representing the stresses in terms of a stress function $f(x_1, x_2)$, he obtained

$$\sigma_{13} = - k \frac{\partial f}{\partial x_2} \quad ; \quad \sigma_{23} = k \frac{\partial f}{\partial x_1}$$

and (3.2)

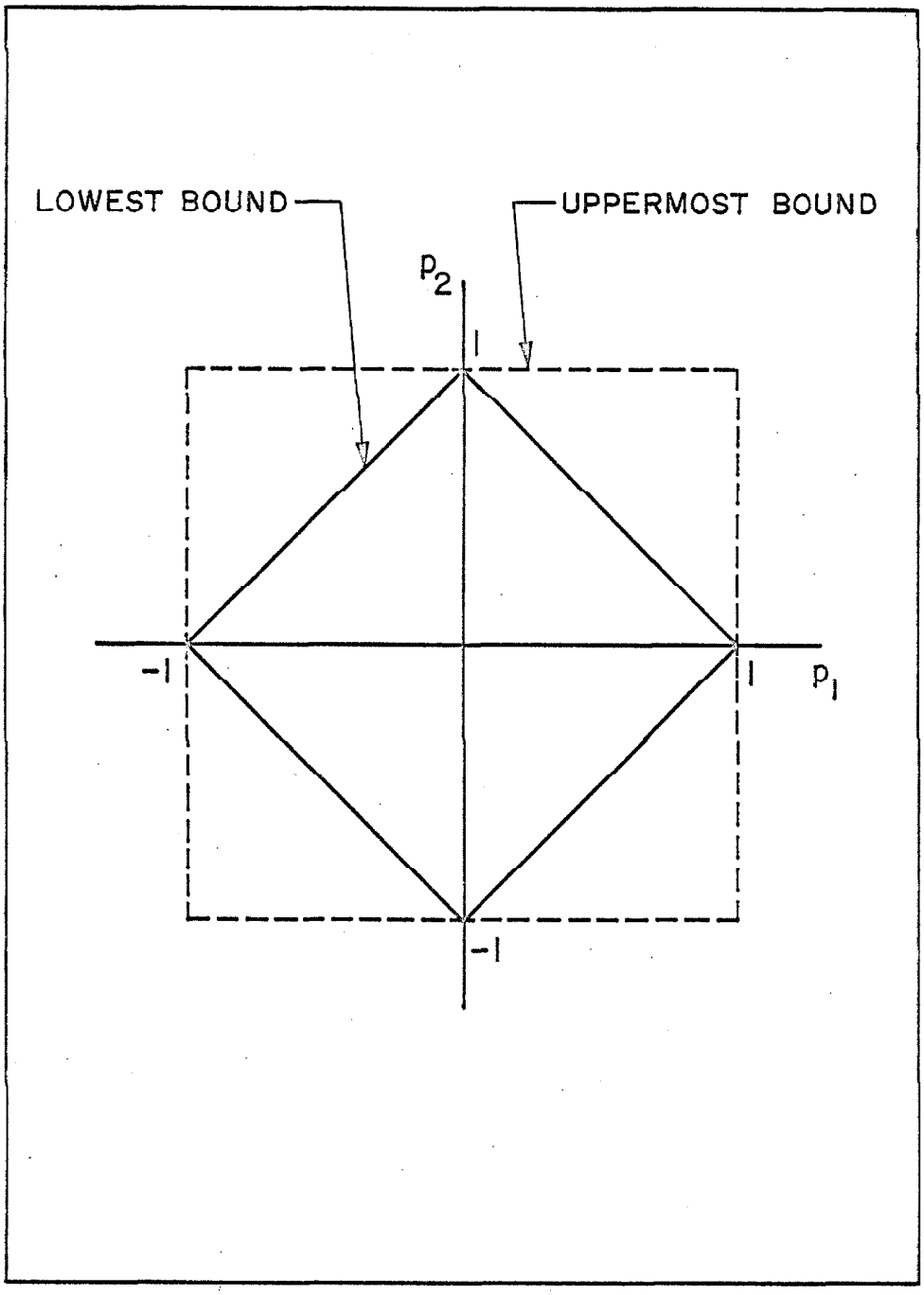


FIG. 3.1 UPPERMOST AND LOWEST BOUNDS ON YIELD CURVES IN TWO DIMENSIONAL FORCE-SPACE

$$\sigma_{33} = \sqrt{3}\, k \left(1 - \frac{\partial f}{\partial x_1} - \frac{\partial f}{\partial x_2}\right)^{\frac{1}{2}}$$

Using the principle of maximum work he found that the stress function must satisfy the following differential equation

$$\frac{\partial}{\partial x_1}\left\{\frac{(\Gamma_1 x_1 + \Gamma_2 x_2 + \Gamma_3)\frac{\partial f}{\partial x_1}}{\left(1 - \frac{\partial f}{\partial x_1} - \frac{\partial f}{\partial x_2}\right)^{\frac{1}{2}}}\right\} + \frac{\partial}{\partial x_2}\left\{\frac{(\Gamma_1 x_1 + \Gamma_2 x_2 + \Gamma_3)\frac{\partial f}{\partial x_2}}{\left(1 - \frac{\partial f}{\partial x_1} - \frac{\partial f}{\partial x_2}\right)^{\frac{1}{2}}}\right\} + \frac{2\Gamma_4}{\sqrt{3}} = 0$$

with $f = 0$ on the boundary,

where

$\Gamma_1, \Gamma_2, \Gamma_3, \Gamma_4$ are dimensional constants related to the rates of bending, extension and torsion

The generalized forces generated by the stress distribution are given by

$$N = \sqrt{3}\, k \iint_A \left(1 - \frac{\partial f}{\partial x_1} - \frac{\partial f}{\partial x_2}\right)^{\frac{1}{2}} dA$$

$$L_1 = \sqrt{3}\, k \iint_A x_1 \left(1 - \frac{\partial f}{\partial x_1} - \frac{\partial f}{\partial x_2}\right)^{\frac{1}{2}} dA \qquad (3.4)$$

$$L_2 = \sqrt{3}\, k \iint_A x_2 \left(1 - \frac{\partial f}{\partial x_1} - \frac{\partial f}{\partial x_2}\right)^{\frac{1}{2}} dA$$

and

$$L_3 = 2k \iint_A f\, dA$$

where

$N$ is the axial force

$L_1, L_2, L_3$ are bending and twisting couples along axes 1, 2, and 3 respectively

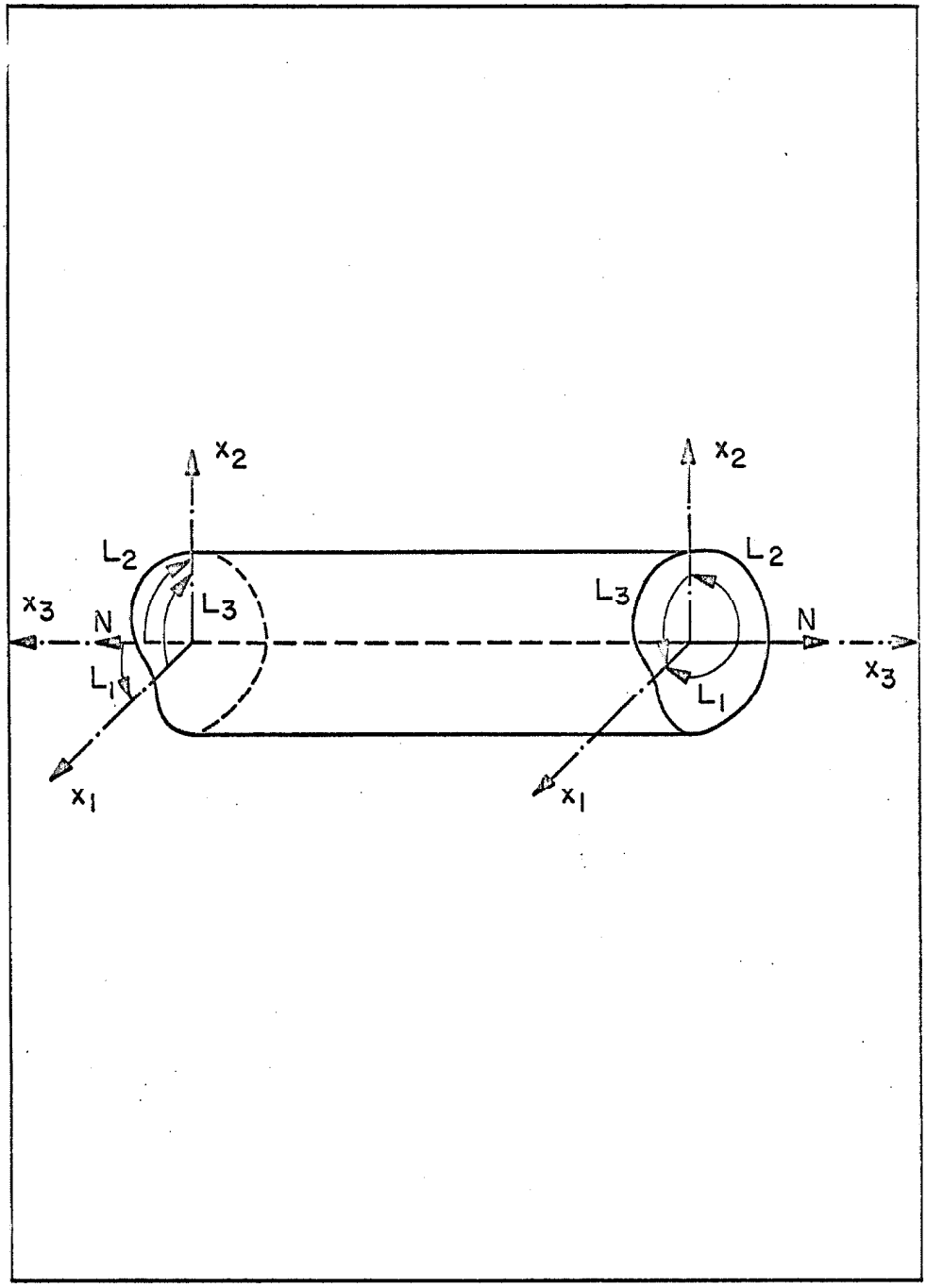


FIG. 3.2 A UNIFORM BAR WITH AN AXIAL FORCE, BENDING MOMENTS AND A TORSIONAL MOMENT APPLIED TO ITS ENDS

An analytic solution of the above equations is not possible even for simple sections. For any given section, however, these equations can be solved numerically and an equation for the yield surface can be obtained in terms of generalized forces through Eqs. 3.4. Imegwu[30,31] and Steele[32] have solved such problems for combined bending and torsion by numerical integration of Eqs. 3.3 and 3.4. In formulating Eqs. 3.2 and 3.3, the material is assumed to be rigid plastic. For an actual material with a finite rigidity Hill and Siebel showed theoretically[33] and experimentally[34] that actual loads approach the rigid-plastic yield level values asymptotically, approaching within a few per cent of computed yield values when the plastic deformations are of the order of the elastic deformations. From this it seems that for all practical purposes the rigid-plastic approximation can be justified in obtaining the equation of the yield surface.

Upper and Lower Bounds

In the plastic analysis of structures the technique of obtaining approximations to the exact solutions, from above and below, has been very successful. An elegant theory of limit analysis based on upper and lower bound limit theorems has been developed; and where acceptable bounds can be found, it is of great practical significance. Several investigators[2,32,35] have used this approach to obtain lower and upper bound approximations to the yield surface in terms of generalized forces. Siebel[35] has obtained such approximations for bending and torsion of circular bars and has found good

correlation between experimental and analytical results. Hodge[2] has used this approach to obtain yield curves for bending and shear, bending and torsion, and bending, bending and torsion for several structural shapes. He has also given solutions for a number of static load problems using linearized interaction curves. In the next section we use this approach to obtain the yield curves for the case of bending about the principal axes of a section.

## 3.3 Yield Curves for Bending About the Principal Axes of a Section

The case of a prismatic bar acted upon at its ends by bending couples in the plane of the principal axes provides a simple example in which it is possible to deduce an exact yield curve. In this case it is possible to obtain the maximum of the lower bound solutions--which is, therefore, the exact solution. At any point of the section we have only tensile or compressive axial stresses and the yield criterion (Eq. 2.1) in stress space, reduces to the simple relation

$$\sigma_{33} = \pm\sigma_y \tag{3.5}$$

where

$\sigma_{33}$ is the stress normal to the section

$\sigma_y$ is the uniaxial yield stress

The generalized forces at the section are the bending moments along the principal axes which are given by

$$Q_1 = \iint_A x_1 \sigma_{33} \, dA$$

$$Q_2 = \iint_A x_2 \sigma_{33} \, dA \tag{3.6}$$

To satisfy equilibrium the stress distribution should be such that the axial force

$$N = \iint_A \sigma_{33} \, dA = 0 \tag{3.7}$$

Solid Rectangular Sections

Let us consider a rectangular section shown in Fig. 3.3a. Let $x_2 = \chi(x_1)$ be the equation of the curve separating tensile and compressive zones. The stress field at the section is then completely defined by this curve and Eqs. 3.6 define a family of curves in the generalized force-space $(Q_1, Q_2)$ in terms of the parametric function $\chi(x_1)$. The highest lower bound, which must be the exact yield curve, can therefore be found if we can find a function $\chi(x_1)$ which satisfies Eq. 3.7 and is such that given $Q_1, Q_2$ is maximized. For such $\chi(x_1)$, Eqs. 3.6 define the exact yield curve. This is an isoperimetric problem in calculus of variation and is easily solved. Let us first consider the case when $|\chi(\pm B)| \leq H$. The axial force at the section is given by

$$N = \int_{-B}^{B} \left\{ \int_{-H}^{\chi(x_1)} \sigma_y \, dx_2 + \int_{\chi(x_1)}^{H} (-\sigma_y) \, dx_2 \right\} dx_1$$

$$= 2\sigma_y \int_{-B}^{B} \chi(x_1) \, dx_1 \tag{3.8}$$

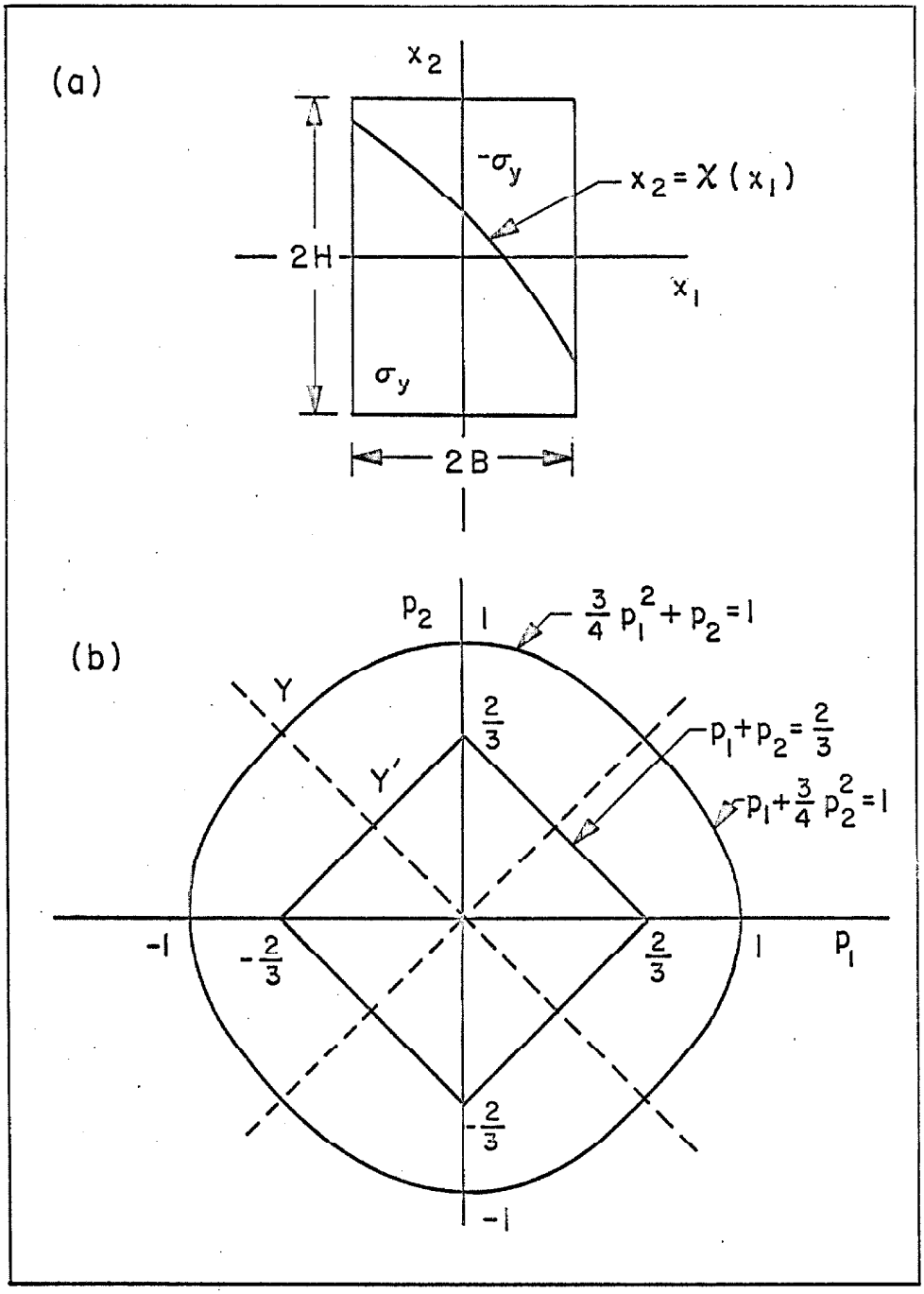


FIG. 3.3 (a) A SOLID RECTANGULAR SECTION (b) INITIAL AND LIMIT YIELD CURVES FOR SOLID RECTANGULAR SECTIONS

The moments for bending along $x_1$ and $x_2$ are given by

$$Q_1 = \int_{-B}^{B} \left\{ \int_{-H}^{\chi(x_1)} x_1(\sigma_y)\, dx_2 + \int_{\chi(x_1)}^{H} x_1(-\sigma_y)\, dx_2 \right\} dx_1$$

$$= -2\sigma_y \int_{-B}^{B} x_1 \chi(x_1)\, dx_1 \qquad (3.9)$$

and

$$Q_2 = -\int_{-B}^{B} \left\{ \int_{-H}^{\chi(x_1)} x_2(\sigma_y)\, dx_2 + \int_{\chi(x_1)}^{H} x_2(-\sigma_y)\, dx_2 \right\} dx_1$$

$$= \sigma_y \int_{-B}^{B} (H^2 - \chi^2(x_1))\, dx_1 \qquad (3.10)$$

It is necessary to find a function $\chi(x_1)$, such that $Q_2$, defined by Eq. (3.10), attains a maximum value and integral constraints on N and $Q_1$ (Eqs. 3.8 and 3.9) are satisfied. Let us define a function

$$\Lambda(x_1, \chi) = H^2 - \chi^2(x_1) - \nu\, x_1 \chi(x_1) - \nu_1 \chi(x_1) \qquad (3.11)$$

where

$\nu, \nu_1$ are constants

Then a necessary condition, for $Q_2$ to be a maximum, is that $\chi(x_1)$ satisfies the Euler equation

$$\frac{d}{dx_1}\left(\frac{\partial \Lambda}{\partial \chi'}\right) = \frac{\partial \Lambda}{\partial \chi}$$

where

$\chi'$ denotes $\frac{d\chi}{dx_1}$

Substituting for $\Lambda(x_1, \chi)$ from Eq. 3.11 yields

$$\chi(x_1) = -\nu x_1 - \nu_1 \tag{3.12}$$

To satisfy Eq. 3.7 it is necessary to have

$$N = 2\sigma_y \int_{-B}^{B} (-\nu x_1 - \nu_1)\, dx_1 = 0$$

so that

$$\nu_1 = 0$$

Hence

$$\chi(x_1) = -\nu x_1 \tag{3.13}$$

Substituting for $\chi(x_1)$ from Eq. 3.13 into Eqs. 3.9 and 3.10, gives

$$\begin{aligned} Q_1 &= \frac{4\sigma_y}{3} B^3 \nu \\ Q_2 &= 2\sigma_y (H^2 B - \frac{B^3}{3} \nu^2) \end{aligned} \tag{3.14}$$

Equations 3.14 represent the yield curve in the parametric form. For the rectangular section, the yield moments are given by

$$\begin{aligned} Q_{y1} &= 2B^2 H \sigma_y \\ Q_{y2} &= 2H^2 B \sigma_y \end{aligned} \tag{3.15}$$

Dividing Eqs. 3.14 by $Q_{y1}$ and $Q_{y2}$ respectively there is obtained

$$p_1 = \frac{2}{3}\frac{B}{H}\nu$$

$$p_2 = 1 - \frac{1}{3}\frac{B^2}{H^2}\nu^2 \qquad (3.16)$$

Eliminating $\nu$ between $p_1$ and $p_2$ gives

$$\frac{3}{4}p_1^2 + p_2 = 1$$

This is the equation of the yield curve in p-space, when $|\chi(\pm B)| \leq H$ or from Eq. 3.13, when $|\nu| \leq \frac{H}{B}$. This corresponds to $|p_1| \leq \frac{2}{3}$. By symmetry, the equation of the yield curve, when $|p_1| \geq \frac{2}{3}$, must be given by

$$\frac{3}{4}p_2^2 + p_1 = 1$$

The yield curve is completely defined by the equations

$$\frac{3}{4}p_1^2 + p_2 = 1 \quad \text{when} \quad |p_1| \leq \frac{2}{3}$$

and (3.17)

$$\frac{3}{4}p_2^2 + p_1 = 1 \quad \text{when} \quad |p_1| \geq \frac{2}{3}$$

Initial Yield Curve

In the previous chapter we defined the initial yield curve Y' as the locus of all points in force-space, where yielding is imminent at one or more points of a section. In bending of rectangular sections, yielding becomes imminent first at one of the corners when the flexural stress reaches a value $\pm\sigma_y$. The equation for Y' is therefore given by

$$\left|\frac{Q_1 B}{I_1}\right| + \left|\frac{Q_2 H}{I_2}\right| = \sigma_y \qquad (3.18)$$

where

$I_1, I_2$ are the moments of inertia of the section about $x_2$ and $x_1$ axes respectively

Substituting for $I_1$ and $I_2$ in Eq. 3.18 and using Eq. 3.15

$$\left|\frac{3p_1}{2}\right| + \left|\frac{3p_2}{2}\right| = 1 \qquad (3.19)$$

Thus Y' is a closed curve formed by a set of straight lines intercepting the coordinate axes at $|p| = 2/3$. Both Y and Y' are shown in Fig. 3.3b. It may be noted that Eqs. 3.17 and 3.19 do not contain section parameters and therefore hold for all solid rectangular sections.

Hollow Rectangular Sections

The equation of the yield curve for a hollow rectangular section can be directly written in parametric form, using Eqs. 3.16. Figure 3.4a shows the dimensions of a hollow rectangular section. Let $B_2 = \beta_1 B_1$ and $H_2 = \beta_2 H_1$. The yield moments for the section are given by

$$Q_{y1} = 2(1 - \beta_1^2\beta_2)B_1^2 H_1 \sigma_y$$

and (3.20)

$$Q_{y2} = 2(1 - \beta_2^2\beta_1)H_1^2 B_1 \sigma_y$$

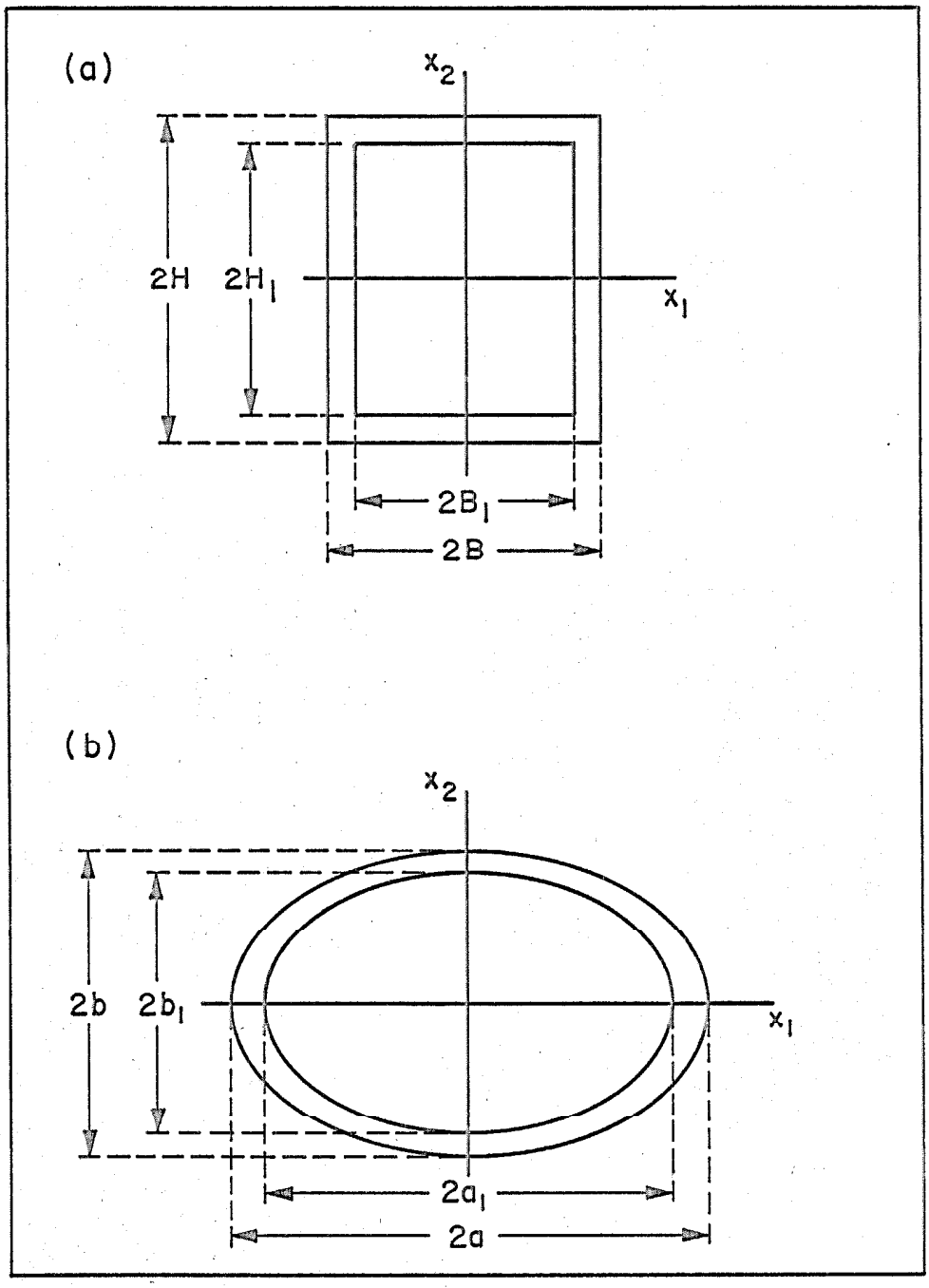


FIG. 3.4 (a) A HOLLOW RECTANGULAR SECTION
(b) A HOLLOW ELLIPTICAL SECTION

and the yield curve is given by the following parametric equations.

For $|\nu| \leq \frac{\beta_1}{\beta_2}\frac{B_1}{H_1}$ and also $\leq \frac{B_1}{H_1}$

$$p_1 = \frac{2}{3}\frac{(1-\beta_1^3)}{(1-\beta_1^2\beta_2)}\frac{B_1}{H_1}\nu$$

$$p_2 = 1 - \frac{1}{3}\frac{(1-\beta_1^3)}{(1-\beta_1\beta_2^2)}\left(\frac{B_1}{H_1}\right)^2\nu^2 \qquad (3.21)$$

For $\frac{B_1}{H_1} \leq |\nu| \leq \frac{\beta_1}{\beta_2}\frac{B_1}{H_1}$

$$p_1 = \frac{1}{(1-\beta_1^2\beta_2)}\left\{1 - \frac{1}{3}\left(\frac{H_1}{B_1}\right)^2\frac{1}{\nu^2} - \frac{2}{3}\left(\frac{B_1}{H_1}\right)\beta_1^3\nu\right\}$$

$$p_2 = \frac{1}{(1-\beta_1\beta_2^2)}\left\{\frac{2}{3}\left(\frac{H_1}{B_1}\right)\frac{1}{\nu} - \beta_2^2\beta_1 + \frac{1}{3}\beta_1^3\left(\frac{B_1}{H_1}\right)^2\nu^2\right\} \qquad (3.22)$$

or if $\frac{\beta_1}{\beta_2}\frac{B_1}{H_1} \leq |\nu| \leq \frac{B_1}{H_1}$

$$p_1 = \frac{1}{(1-\beta_1^2\beta_2)}\left\{\frac{2}{3}\left(\frac{B_1}{H_1}\right)\nu - \beta_1^2\beta_2 + \frac{1}{3}\left(\frac{H_1}{B_1}\right)^2\beta_2^3\frac{1}{\nu^2}\right\}$$

$$p_2 = \frac{1}{(1-\beta_1\beta_2^2)}\left\{1 - \frac{1}{3}\left(\frac{B_1}{H_1}\right)^2\nu^2 - \frac{2}{3}\left(\frac{H_1}{B_1}\right)\beta_2^3\frac{1}{\nu}\right\} \qquad (3.23)$$

For $|\nu| \geq \frac{\beta_1}{\beta_2}\frac{B_1}{H_1}$ and also $\geq \frac{B_1}{H_1}$

$$p_2 = \frac{2}{3} \frac{(1 - \beta_2^3)}{(1 - \beta_1 \beta_2^2)} \frac{H_1}{B_1} \frac{1}{\nu}$$

$$p_1 = 1 - \frac{1}{3} \frac{(1 - \beta_2^3)}{(1 - \beta_2 \beta_1^2)} \left(\frac{H_1}{B_1}\right)^2 \frac{1}{\nu^2} \qquad (3.24)$$

For any rectangular section Eqs. 3.21, 3.24 and one of the Eqs. 3.22 or 3.23 apply, depending upon the ratio $\beta_1/\beta_2$. In the particular case $\beta_1 = \beta_2$, Eqs. 3.23 and 3.23 drop out and Eqs. 3.21 and 3.24 reduce to Eqs. 3.16. Thus the yield curve is again given by Eqs. 3.17. This case includes hollow square sections of uniform thickness. For the general case, the equation of the Y' curve is given by

$$\left| \frac{3}{2} \frac{(1 - \beta_1^2 \beta_2)}{(1 - \beta_1^3 \beta_2)} p_1 \right| + \left| \frac{3}{2} \frac{(1 - \beta_1 \beta_2^2)}{(1 - \beta_1 \beta_2^3)} p_2 \right| = 1 \qquad (3.25)$$

This is again a closed curve formed by a set of straight lines intersecting the coordinate axes at $|p_1| = \frac{2}{3} \frac{(1 - \beta_2 \beta_1^3)}{(1 - \beta_1^2 \beta_2)}$ and $|p_2| = \frac{2}{3} \frac{(1 - \beta_1 \beta_2^3)}{(1 - \beta_1 \beta_2^2)}$. A similar approach can be used to obtain the yield curve directly from Eqs. 3.16, for idealized I-sections. It may be noted that for such sections the yield curve is, in general, a piecewise smooth curve with corners.

Solid Elliptical Sections

The yield curve for solid elliptical section has been worked out in Appendix II along the same lines as for the rectangular section, and is given by

$$p_1^2 + p_2^2 = 1 \tag{3.26}$$

The equation of the Y' curve is given by

$$p_1^2 + p_2^2 = \left(\frac{3\pi}{16}\right)^2 \tag{3.27}$$

Since both Eqs. (3.26) and (3.27) are independent of section parameters, they hold for all solid elliptical sections and, in particular, for circular sections. Both the Y and Y' curves are shown in Fig. 3.5.

Hollow Elliptical Sections

For the hollow elliptical section shown in Fig. 3.4b, the yield curve is given by the parametric equations

$$p_1 = \left\{ \frac{a^3 b}{(b^2 + a^2\nu^2)^{\frac{1}{2}}} - \frac{a_1^3 b_1}{(b_1^2 + a_1^2\nu^2)^{\frac{1}{2}}} \right\} \frac{\nu}{a^2 b - a_1^2 b_1}$$

$$p_2 = \left\{ \frac{b^3 a}{(b^2 + a^2\nu^2)^{\frac{1}{2}}} - \frac{b_1^3 a_1}{(b_1^2 + a_1^2\nu^2)^{\frac{1}{2}}} \right\} \frac{1}{(b^2 a - b_1^2 a_1)} \tag{3.28}$$

The equation of the Y' curve is given by

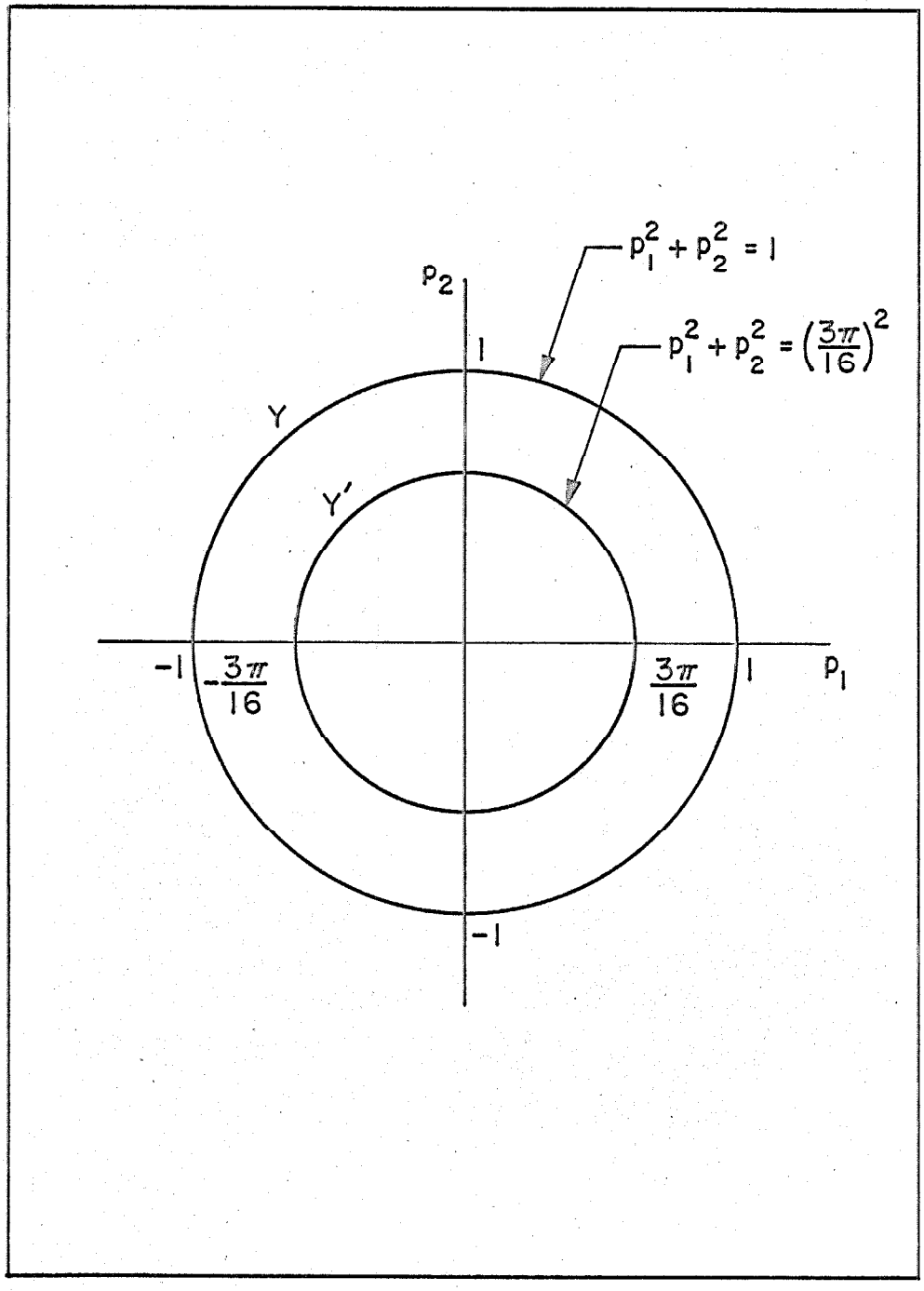


FIG. 3.5 INITIAL AND LIMIT YIELD CURVES FOR SOLID ELLIPTICAL SECTIONS

$$\left\{\frac{16a(a^2b - a_1^2b_1)}{3\pi(a^3b - a_1^3b_1)}\right\}^2 p_1^2 + \left\{\frac{16b(b^2a - b_1^2a_1)}{3\pi(b^3a - b_1^3a)}\right\}^2 p_2^2 = 1 \qquad (3.29)$$

For the special case of $a_1 = \beta a$, $b_1 = \beta b$, there is obtained

$$p_1 = \frac{a\nu}{(b^2 + a^2\nu^2)^{\frac{1}{2}}}$$

$$p_2 = \frac{b}{(b^2 + a^2\nu^2)^{\frac{1}{2}}}$$

and the yield curve is again given by Eq. 3.26. The Y' curve is given by

$$p_1^2 + p_2^2 = \left\{\frac{3\pi}{16}\frac{(1 - \beta^4)}{(1 - \beta^3)}\right\}^2 \qquad (3.30)$$

This particular case includes the hollow circular tubes of uniform thickness.

## 3.4 A Discussion of Some of the Assumptions

### Transition From Elastic to Perfectly Plastic State

In Chapter II, while developing the theory of yielding at a section, it was assumed that the section remains linearly elastic up to Y, thus ignoring the partly-elastic and partly-plastic behavior between Y and Y'. According to the theory of plasticity, as the loading is continued beyond the initial yield surface Y' new yield surfaces are formed which for elastic-perfectly-plastic material

approach the limit yield surface Y. These new yield surfaces, which are functions of the history of loading, may be thought of as arising from the original surface by translation, by expansion, by the combination of a number of independent loading surfaces, or by any consistent procedure.[38] The general behavior from Y' to Y is similar to the phenomenon of work-hardening and is discussed next, in this section.

In Section 3.3, equations for Y and Y' for various sections were derived. Using these equations it is possible to draw some conclusions about the effects of neglecting the partly-elastic partly-plastic region, in terms of section parameters. The ratio of the volume enclosed between Y and Y' to the volume enclosed by Y may be regarded as a relative measure of the effect of neglecting the partly plastic region. Let $R_e$ and $R_r$ denote this ratio for elliptical and rectangular sections. Then, from Eqs. 3.17, 3.18, 3.25, 3.26 and 3.30 (with $\beta_1 = \beta_2$), it can be shown that

$$R_e = 1 - \left\{\frac{3\pi}{16}\,\frac{(1-\beta^4)}{(1-\beta^3)}\right\}^2$$

$$R_r = 1 - 0.3\left\{\frac{(1-\beta^4)}{(1-\beta^3)}\right\}^2 \qquad (3.31)$$

$R_e$ and $R_r$ are plotted in Fig. 3.6 as functions of $\beta$, which determines the thickness of the section. $\beta = 0$ corresponds to a solid section and it is seen that except for thin hollow sections for which $\beta \to 1$, this simplification may lead to a significant departure

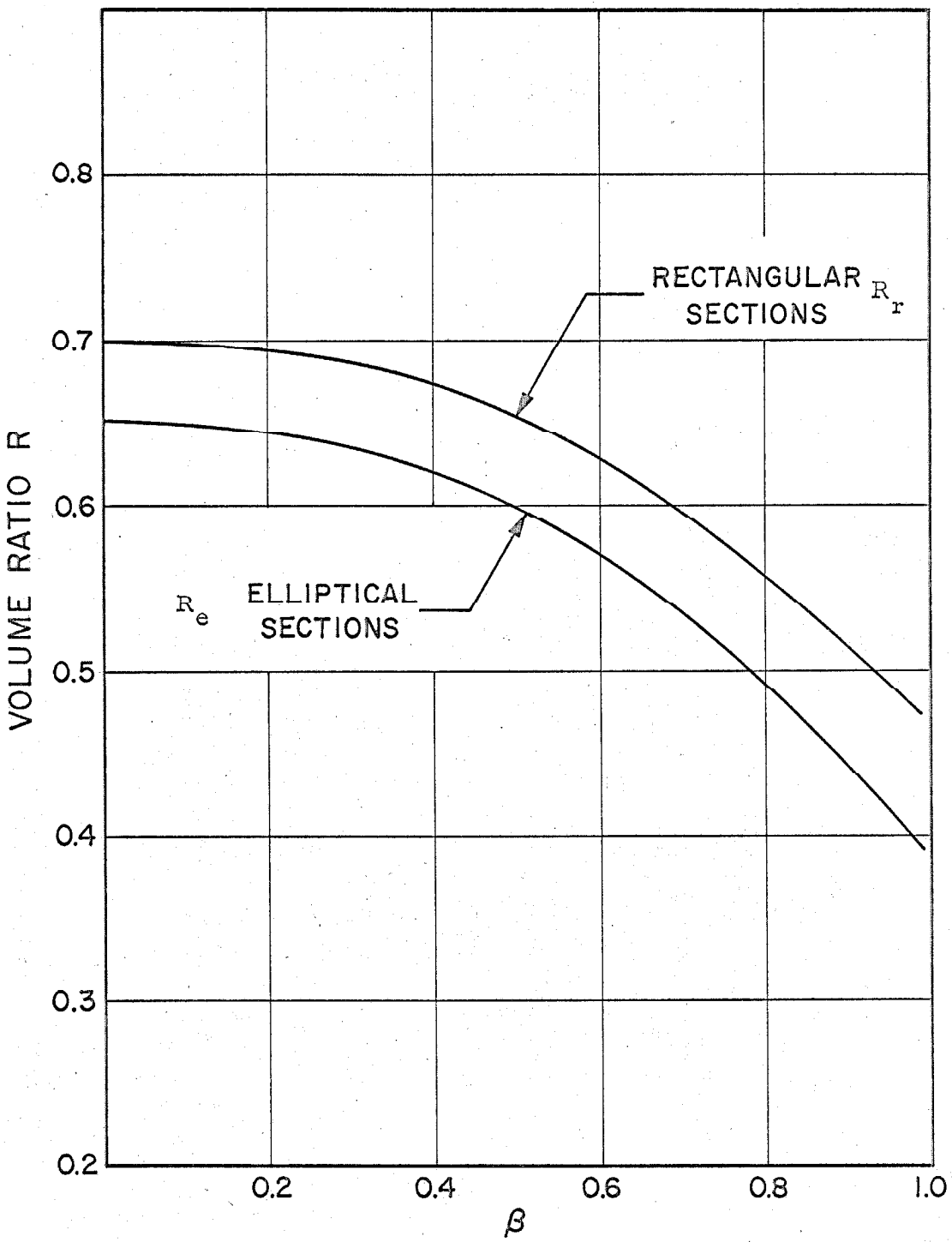


FIG. 3.6 RATIO OF THE AREA ENCLOSED BETWEEN Y AND Y' TO THE AREA ENCLOSED BY Y, FOR ELLIPTICAL AND RECTANGULAR SECTIONS

from actual behavior. It seems that it would be more realistic to use an intermediate yield surface depending on the value of $\beta$. This also indicates that in view of this approximation, one may as well use simple approximate yield surfaces and where singular regimes may present problems, replace the exact yield surfaces by smooth approximations.

It was pointed out in Section 2.2 that ignoring the effects of the region between Y and Y' is analogous to neglecting the effect of curved transition in the elasto-plastic force-displacement relationship shown in Fig. 2.3. Recently, Iwan[37] has studied the effect of rounding on steady-state response of a simple oscillator, using a distributed-element model to represent a general yielding behavior. His results indicate that rounding causes a significant change in the steady-state amplitude as compared with a sharp-cornered elasto-plastic approximation depending on the level of excitation. Generalization of distributed-element model to higher dimensions may lead to some understanding of the consequences of this assumption.

Work-hardening

The theory of yielding has been developed under the assumption that the behavior is not work-hardening. Real structures do exhibit work-hardening during yielding and in studying the response of structures it is usually taken into account by assuming a bilinear or general yielding[16] type of force-displacement relationship. It is possible to introduce work-hardening in the present theory by

following the corresponding formulation in continuum mechanics. If this is done, the new surfaces (called loading surfaces) which grow out of the initial yield surface Y', do not terminate on a limit yield surface Y, but continue to change as plastic deformation occurs. Shield and Ziegler[40] have shown that the behavior of a work-hardening material can be described by the initial yield condition, the flow rule associated with initial and subsequent loading surfaces and a hardening law that specifies the construction of subsequent loading surfaces. The last of these requirements is still in an uncertain state of development. In a step-by-step integration procedure, if a consistent scheme can be devised to construct the yield surface after each incremental plastic displacement the theory developed in the previous chapter can be extended, at least conceptually, to work-hardening materials. However, considering that loading may produce corners[39] as the yield surface deforms, it seems that it would be very difficult to develop a numerical procedure for solving problems.

Deterioration of Material During Repeated Loading

In developing the theory of yielding an implicit assumption was made that the material does not deteriorate during yielding. It is known that deterioration does occur[21] in real materials but the current state of knowledge of this phenomenon is very limited. Recently, Popov[22] carried out tests on ASTM A36 beams with alternating cycles of end deflections producing strains 4 to 18 times the yield strains. He found remarkably stable hysteresis loops that show little deterioration in five cycles. Hanson[21] carried out an

extensive experimental study of the post-elastic static and dynamic behavior of a single-story frame with steel columns. In this study the frame was subjected to repeated cyclic loading with deflections up to two times the yield deflection and it was found that dynamic hysteresis curves are stable and close to static curves. The results of these tests are reassuring but are clearly inadequate for many problems of structural dynamics. During earthquakes, if plastic deformations are permitted, structures must undergo large plastic strains and large number of load reversals.[22] There is a clear need for more work in this area and this must be kept in mind when interpreting the results of inelastic behavior under dynamic loads.

## 3.5 Summary and Conclusions

The general problem of determining the equation of the yield surface, in terms of forces acting at a section, has been discussed. The equations of the yield surface, and the initial yield surface, have been derived for bending about the principal axes of a section. Some of the assumptions made in deriving the theory of yielding have been discussed. Based on this work the following conclusions can be drawn.

1. The approximate expressions for the yield surface can be easily obtained, under general condition of loading, by the use of upper and lower bound theorems.

2. The effect of assuming elastic behavior, during transition from elastic to plastic state, may lead to significant errors for many

structural sections. In such cases, it may be more realistic to use as the yield surface one lying between the initial and the limit yield surfaces. The choice of such a surface should be guided by the aim of getting the best fit between experimental and analytical results.

3. In view of the approximations involved in the assumption discussed in 2 above, the need to determine exact equations of the yield surface is not critical and use of approximate methods is justified. In cases where singular regimes may present problems exact yield surfaces may be replaced by smooth approximations.

4. The theory of yielding developed in this study can be extended, conceptually, to include work-hardening. However, it will be very difficult to develop procedures to solve any real problems.

5. An understanding of the deterioration in the yield strength of materials under repeated loading is important for inelastic design under dynamic loads. The current state of knowledge about this is meager and there is need for extensive work, both experimental and theoretical.

# CHAPTER IV

# THE RESPONSE OF STRUCTURES TO SINUSOIDAL EXCITATION

## 4.1 Introduction

The study of the response of dynamic systems to sinusoidal excitation is of interest for two reasons: 1) To understand the behavior of systems whose exciting forces are sinusoidal; 2) In the case of systems, whose exciting forces are not sinusoidal, the analytic simplicity of sinusoidal functions permits analytical solutions to a large class of problems. In many nonlinear systems, if an analytical solution can be found for sinusoidal excitation, it gives considerable insight into the dynamic characteristics of the system which may be helpful in interpreting the response to other types of excitations. Such solutions are also useful in checking the numerical accuracy and correctness of computer programs used to solve an actual problem. In the case of linear systems, if response to sinusoidal excitation is known, response to other types of excitations can be obtained by the use of Fourier analysis.

In this chapter the dynamic response of the simple frame, described in Section 2.3 of Chapter II, is investigated for sinusoidal base excitation. The response is obtained for elastic behavior, elasto-plastic behavior, and elasto-plastic behavior with interaction. To explain the special features of the effect of interaction, various aspects of the response, for each of the three cases, are shown. The steady-state response of the frame is investigated in detail and curves of energy input per cycle and steady-state amplitude are

presented for elasto-plastic response with and without interaction. The chapter is concluded with a discussion of the implications of the effects of interaction.

The notation used in this chapter is the same as in the previous chapters with some exceptions, which are defined. The additional symbols introduced in this chapter are defined here and also inside the text, wherever they first appear.

| Symbol | Explanation or Definition |
|---|---|
| $a_1, a_2$ | acceleration-amplitudes of base excitation in the directions 1-1 and 2-2 |
| $b_1, b_2$ | steady-state displacement-ratio-amplitudes in the directions 1-1 and 2-2 |
| $b'$ | steady state displacement-ratio-amplitude in the direction 1'-1' |
| $d_1, d_2$ | steady-state force-ratio-amplitudes in the directions 1-1 and 2-2 |
| p | subscript denoting peak response |
| $r_1, r_2$ | ratios of excitation-acceleration-amplitudes and yield accelerations in the directions 1-1 and 2-2 |
| $u'$ | displacement-ratio in the direction 1'-1' |
| $HE^*$ | total energy loss due to hysteresis per cycle |
| $TE^*$ | total energy input per cycle |
| $\alpha_1, \alpha_2$ | frequencies of excitation in the directions 1-1 and 2-2 |
| $\beta$ | phase angle |
| $\delta_1, \delta_2$ | phase angles |
| $\eta_1, \eta_2$ | ratios of excitation frequencies and natural frequencies in the directions 1-1 and 2-2 |

| Symbols | Explanation or definition |
|---|---|
| $\kappa$ | phase angle |
| $\rho$ | phase angle |

## 4.2 Response of the Simple Frame to Sinusoidal Base Excitation

### Equations of Motion

Let us consider the vibration of the frame described in Section 2.3 of Chapter II to sinusoidal base excitation acting simultaneously along its principal directions 1-1 and 2-2. Let

$$\ddot{z}_1(t) = a_1 \sin(\alpha_1 t + \beta)$$
$$\ddot{z}_2(t) = a_2 \sin(\alpha_2 t + \beta + \rho) \tag{4.1}$$

where

| | |
|---|---|
| $a_1, a_2$ | are the acceleration-amplitudes of base excitation along the directions 1-1 and 2-2 |
| $\alpha_1, \alpha_2$ | are the frequencies of excitation along the directions 1-1 and 2-2 |
| $\beta, \rho$ | are the phase angles |

The equations of motion of the frame are then given by Eqs. 2.30 through 2.34, with forcing functions $\ddot{z}_1(t)$ and $\ddot{z}_2(t)$ defined by Eqs. 4.1. Setting $\tau = \omega_1 t$ and defining

$$r_1 = \frac{a_1}{a_{y1}} \quad ; \quad r_2 = \frac{a_2}{a_{y2}}$$
$$\eta_1 = \frac{\alpha_1}{\omega_1} \quad ; \quad \eta_2 = \frac{\alpha_2}{\omega_2} \tag{4.2}$$

and

$$\zeta = \frac{\omega_1}{\omega_2}$$

Eqs. 4.1 can be written as

$$\frac{\ddot{z}_1\left(\frac{\tau}{\omega_1}\right)}{a_{y1}} = r_1 \sin(\eta_1 \tau + \beta)$$

$$\frac{\ddot{z}_2\left(\frac{\tau}{\omega_2 \zeta}\right)}{a_{y2}} = r_2 \sin\left(\frac{\eta_2}{\zeta}\tau + \beta + \rho\right) \qquad (4.3)$$

The equations of motion of the frame are now given, in dimensionless form, by Eqs. 2.36 through 2.39, with forcing function defined by Eqs. 4.3. The expressions for the energy input and the energy loss are given by Eqs. 2.49 through 2.52.

Integration of the Equations of Motion

The elastic and the elasto-plastic response of the frame is given by Eqs. 2.36 with restoring force vector $\bar{p}$ defined by Eqs. 2.37 and 2.38 respectively. These equations represent a system of two uncoupled second-order differential equations which can be integrated independently. The response of the frame in these cases is, therefore, independent in the directions 1-1 and 2-2. When the effects of interaction on yielding are considered, the equations of motion are given by Eqs. 2.36, 2.38 and 2.39. These equations form a system of coupled differential equations and must be integrated simultaneously. In this case, therefore, the response in the direction

1-1 depends on the response in the direction 2-2. This interdependence characterizes the basic difference between elasto-plastic response and elasto-plastic response with interaction.

For elastic response, the equations of motion are linear and it is possible to obtain closed form analytic solutions.[41] For elasto-plastic response, the equations of motion are piece-wise linear, and it is again possible to obtain analytic solutions for each part. By following through the transition from one part to another it is possible to write the response in analytic form.[42] For elasto-plastic response with interaction, the equations of motion are non-linear and it has not been possible to derive an analytic solution. In this case, therefore, one has to use a numerical scheme of integration. In this study, the third order Runge-Kutta scheme of integration has been used. Integrals for the energy input and the energy loss have also been computed numerically. The details of numerical computations are given in Appendix III.

Some Features of the Effects of Interaction

For $r_1 = r_2 = r = 0.5$, $\eta_1^2 = \eta_2^2 = \eta^2 = 0.8$, $\xi_1 = \xi_2 = \xi = 0.0$, $\rho = 30^\circ$ and circular yield curve response of the frame was obtained by numerical integration of the equations of motion, for elastic, elasto-plastic and elasto-plastic behavior with interation. In Figs. 4.1 through 4.7, various aspects of the response are plotted and some of the special features of the effects of interaction are discussed below with reference to these figures.

Figures 4.1, 4.2 and 4.3 show the variation of displacement

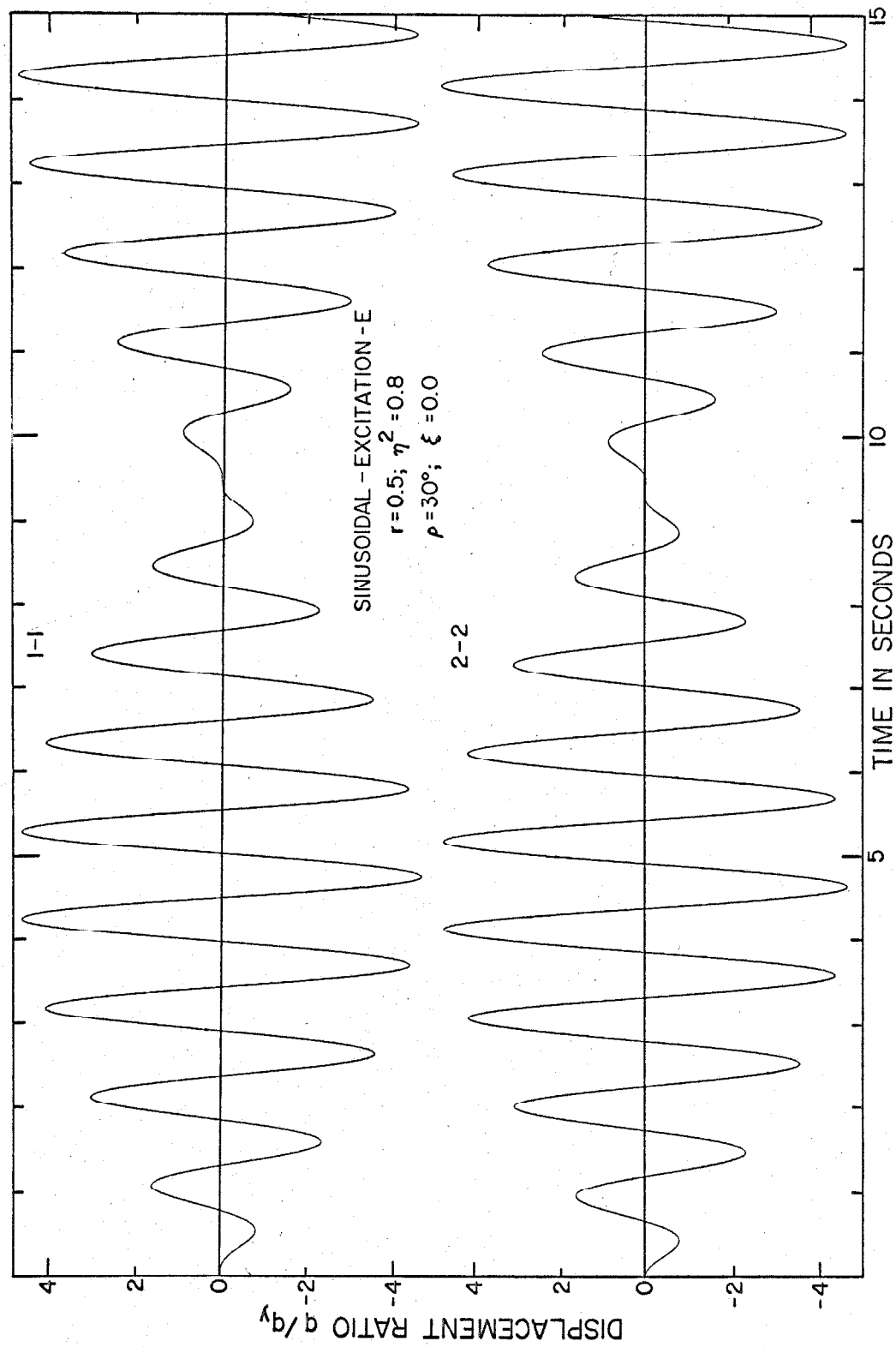


FIG. 4.1 DISPLACEMENT-TIME RESPONSE FOR ELASTIC BEHAVIOR

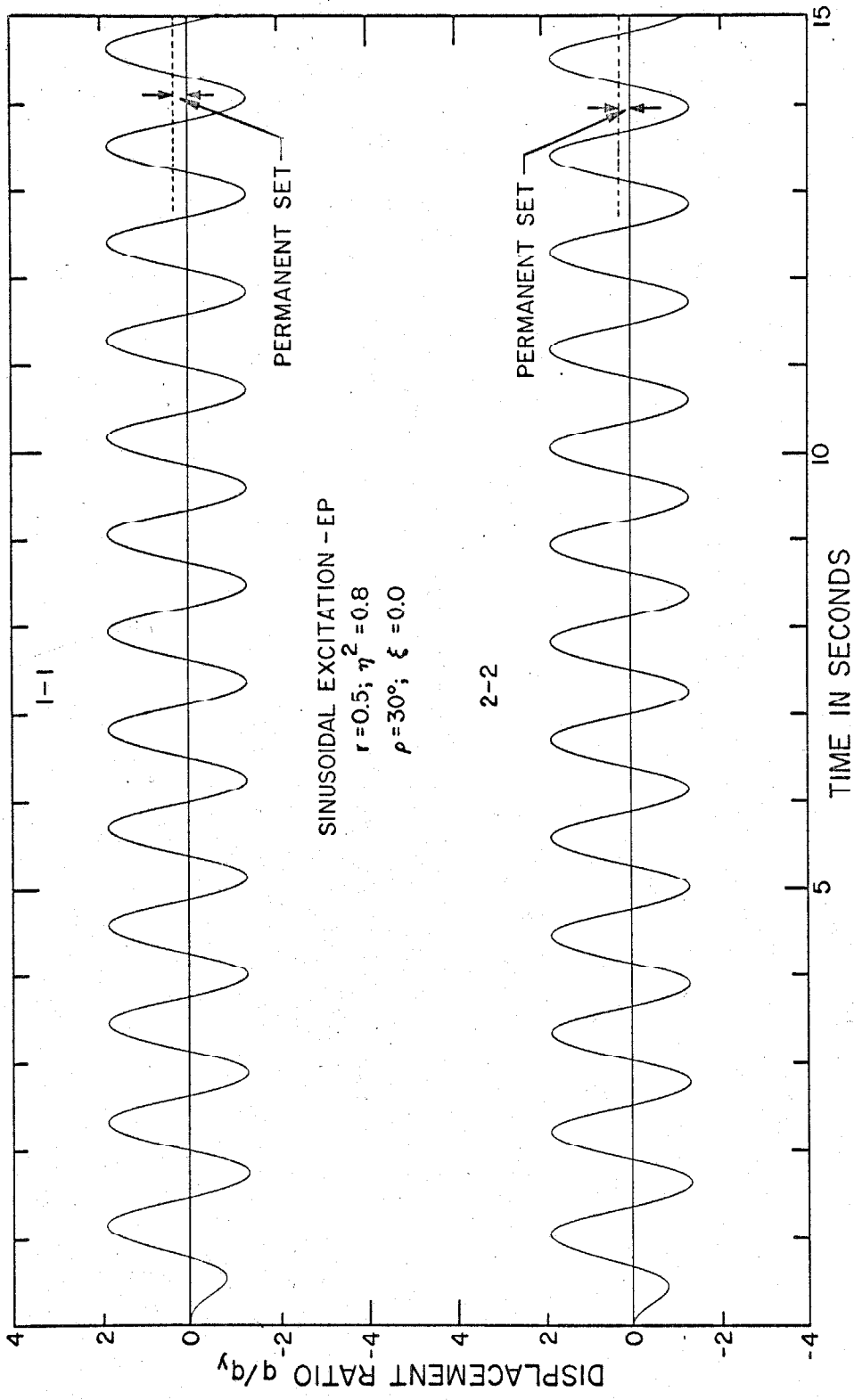


FIG. 4.2 DISPLACEMENT-TIME RESPONSE FOR ELASTO-PLASTIC BEHAVIOR

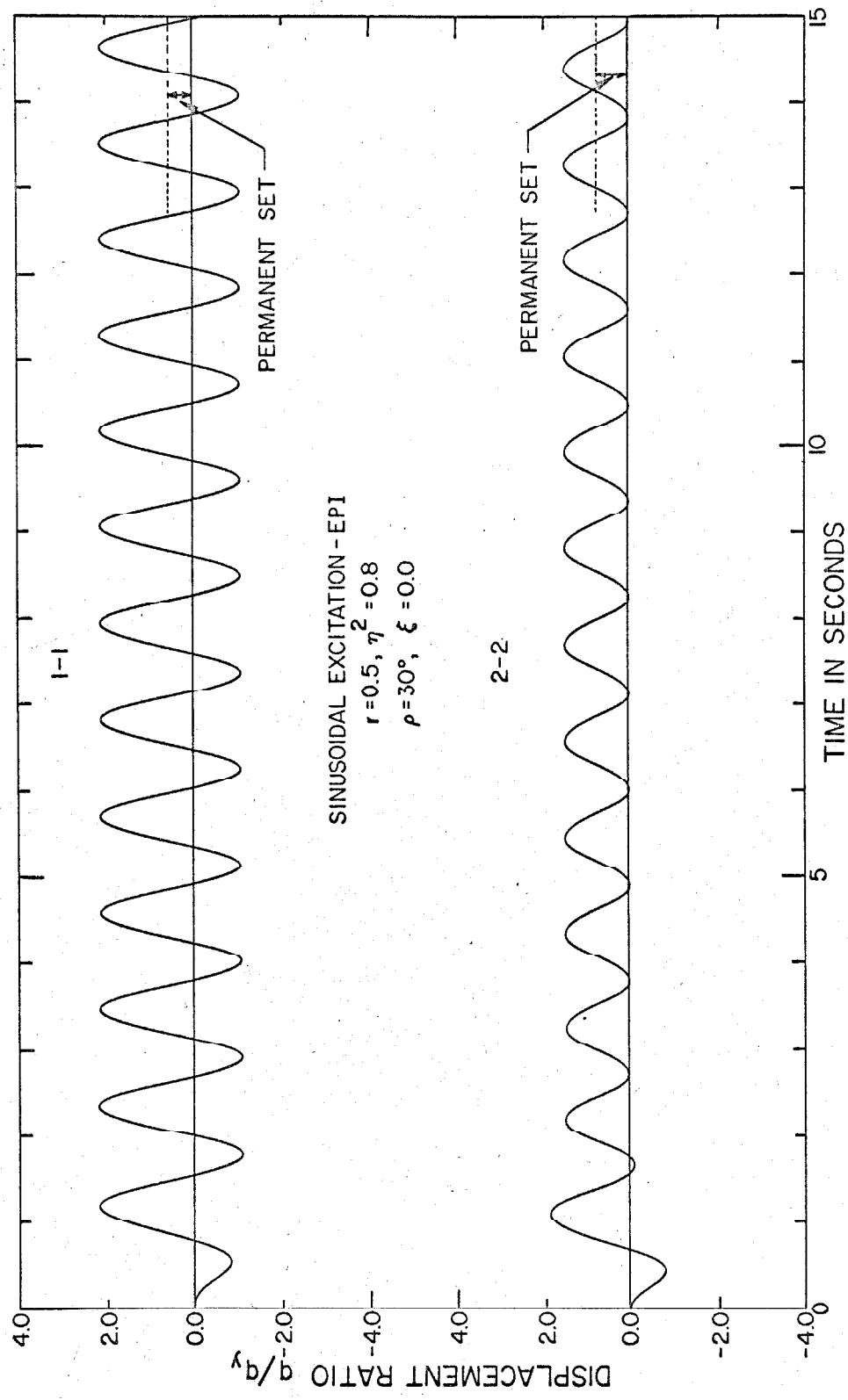


FIG. 4.3 DISPLACEMENT-TIME RESPONSE FOR ELASTO-PLASTIC BEHAVIOR WITH INTERACTION

ratio $q/q_y$ with time, along the principal directions 1-1 and 2-2. In the elastic case, Fig. 4.1, since there is no damping in the system, the transient part of the response persists and response looks like a modulated sine wave. Since the excitation on the two directions is identical, except for the phase difference, the response in directions 1-1 and 2-2 is also identical and differs only in phase. In the elasto-plastic case, Fig. 4.2, the transient part of the response dies out in about four cycles and the frame goes into steady-state oscillations about a new position of equilibrium, which is shown as the permanent set in Fig. 4.2. The response is again identical in the two directions but for the phase difference. It is seen that the amplitude of oscillation for the elasto-plastic case is much smaller than the maximum amplitude in the elastic case. A comparison of Figs. 4.1 and 4.2 shows clearly the effectiveness of hysteretic energy loss during yielding, in limiting the response of the frame. When interaction is considered, Fig. 4.3, the general nature of the response is similar to the elasto-plastic case, with two significant differences. The permanent set and the amplitudes of oscillation are not equal in the two directions. This indicates that interaction causes a redistribution of energy in two directions, so that the amplitude in one direction (1-1) is increased and the amplitude in the other direction (2-2) is decreased.

Figures 4.4 and 4.5 show the force-displacement response of the frame, with and without interaction. In both cases, the transient part dies out in a few cycles and the response settles down to stable steady-state hysteresis loops. It is seen that the shape of the hysteresis loops is quite different in the two cases. For the elasto-

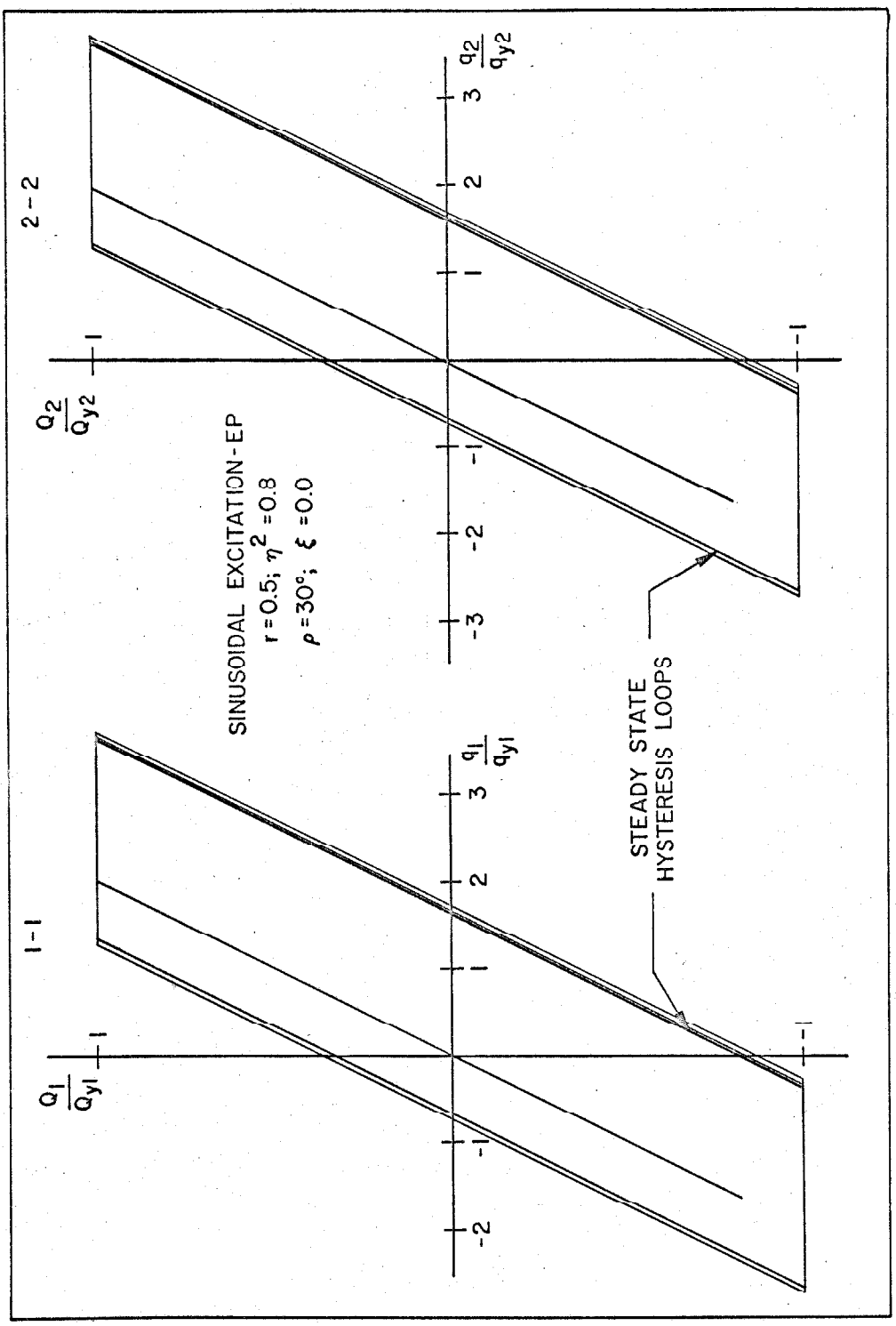


FIG. 4.4 FORCE-DISPLACEMENT RESPONSE FOR ELASTO-PLASTIC BEHAVIOR

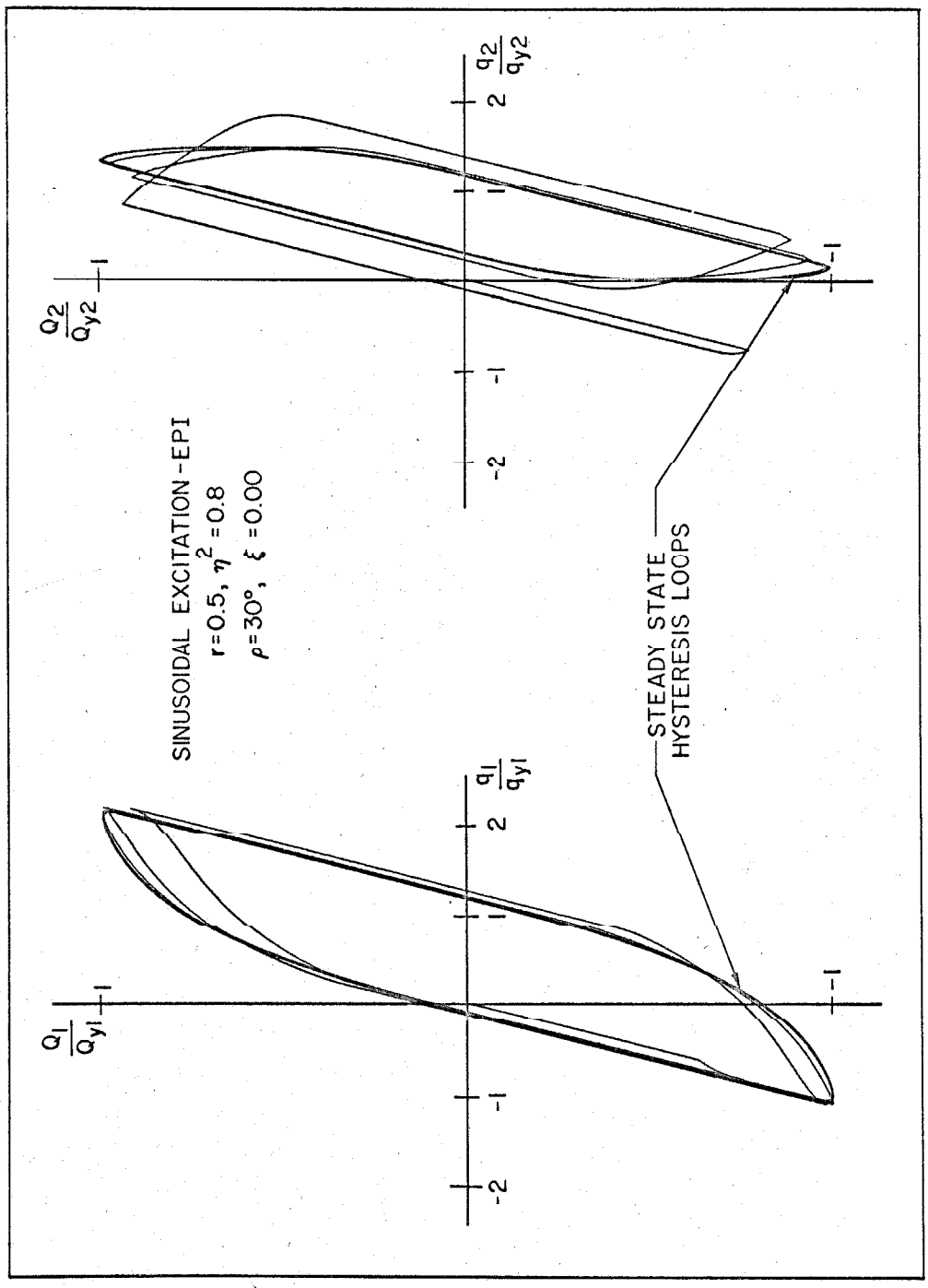


FIG. 4.5 FORCE-DISPLACEMENT RESPONSE FOR ELASTO-PLASTIC BEHAVIOR WITH INTERACTION

plastic case, the restoring force remains constant during yielding and the shape of the loop is completely specified by the maximum amplitude. When interaction is considered, the yield level changes, in general, during yielding and the shape of the hysteresis loop depends on the response in both directions. Hence it is clear that if interaction is considered, the force-displacement relationship cannot be specified independently for each force-displacement pair.

Figure 4.6 shows the locus of the mass-center of the frame in the horizontal plane. The mass center starts at the origin, drifts around during the transient response, and ultimately goes into a steady-state elliptical orbit about a new equilibrium position. On the same figure the motion of the base of the frame is also shown. It is also an ellipse with its principal axes inclined to the principal axes of the frame. It is clear that the steady-state locus of the mass-center for elastic (with damping) and elasto-plastic behavior will also be elliptical, with the same orientation and shape as the locus of the base but of different size. When interaction is considered, the locus is an ellipse of different shape and its principal axes are inclined to the principal axes of the locus of the base.

Figure 4.7 shows the response of the frame in force-space for a circular yield curve. The frame is elastic (denoted by E) when the tip of the force vector $\bar{Q}$, lies inside the circle and plastic (denoted by P) when it lies on the circle. The steady-state (thick lines) and the transient response (thin lines) are indicated on the figure. This figure is presented to indicate the nature of the response in force-space.

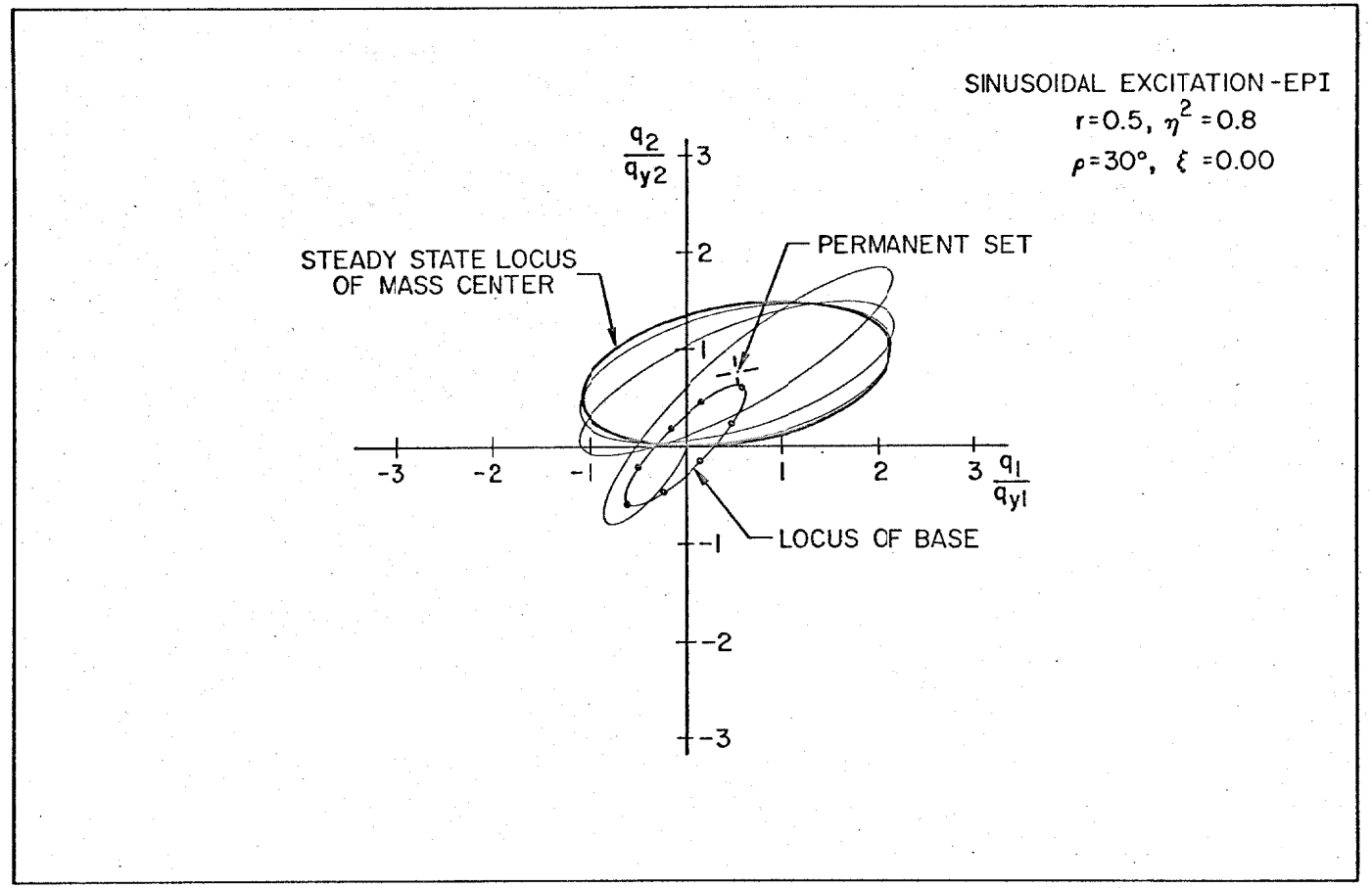


FIG 4.6 DISPLACEMENT RESPONSE IN THE HORIZONTAL PLANE FOR ELASTO-PLASTIC BEHAVIOR WITH INTERACTION AND LOCUS OF BASE MOTION

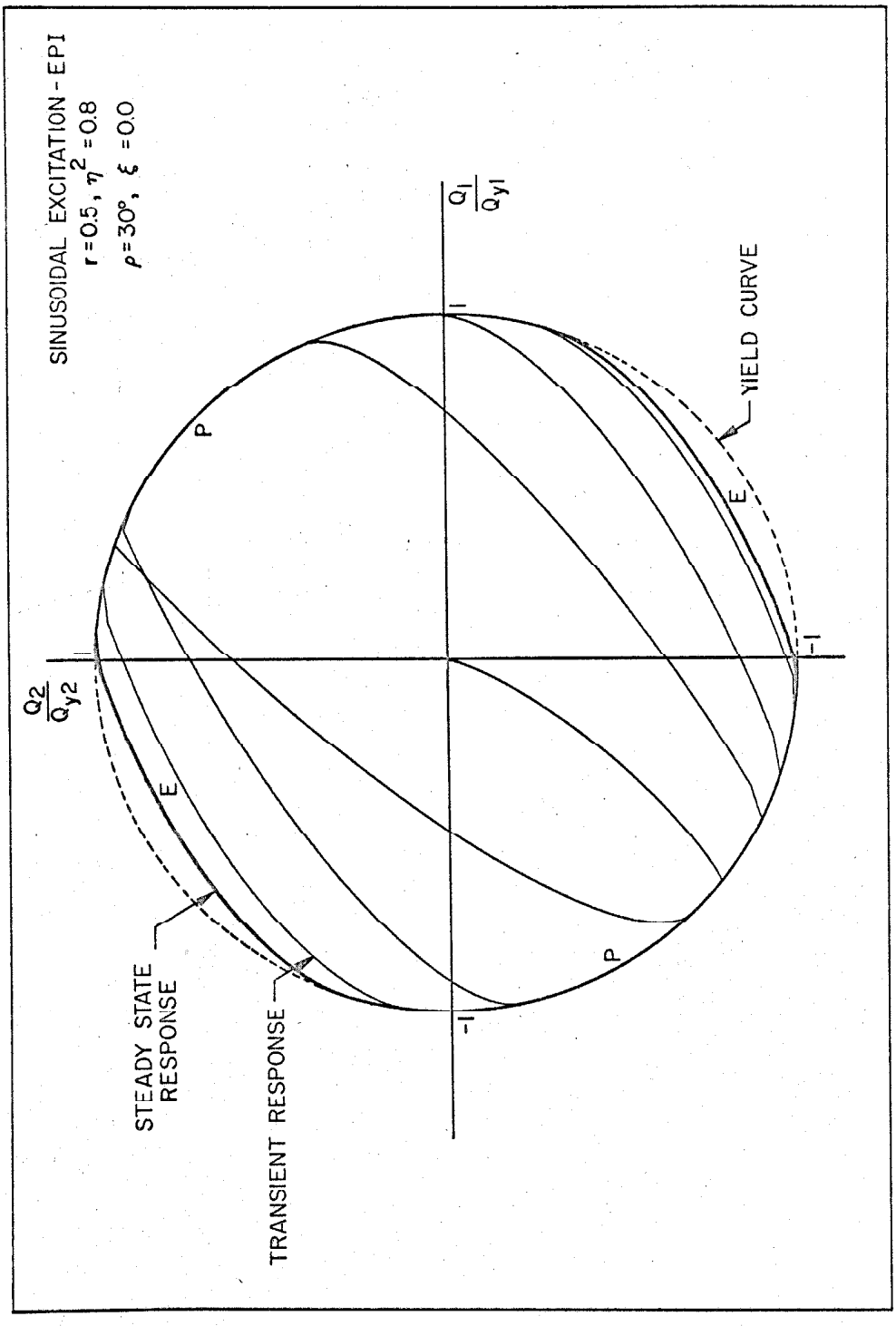


FIG. 4.7 RESPONSE IN THE FORCE-SPACE FOR ELASTO-PLASTIC BEHAVIOR WITH INTERACTION

## 4.3 Steady-state Response of the Simple Frame to Sinusoidal Base Excitation

In the preceding section it was shown that the response of the frame to sinusoidal excitation consists of a transient part, which dies out in a few cycles due to energy dissipation by damping, yielding, or both; and a steady-state part which persists. During steady-state oscillations the energy input per cycle equals the energy dissipated per cycle and a steady response is maintained. The steady-state response of elastic systems has been studied in detail and is available in most text books on vibration.[41] The steady-state response of elasto-plastic systems has also been investigated[42] and some of the approximate methods such as the method of slowly varying parameters,[43] and the method of equivalent linearization[42] have been very successfully used in such investigations. In this section, the expressions for the steady-state response are quoted for elastic and elasto-plastic behavior and analytical and numerical results are obtained for elasto-plastic behavior with interaction. A number of curves are presented for each of these cases and effects of interaction are discussed.

The system of Eqs. 2.36 through 2.39 and 4.3 represent the equations of motion of the frame for sinusoidal excitation. These equations involve a large number of parameters describing the frame and the excitation so that an extensive study would have to be carried out to study the influence of each of these parameters. To limit the size of this investigation, it was decided to study the response of the frame under the following restrictions:

$$\omega_1 = \omega_2 = \omega$$

$$Q_{y1} = Q_{y2} = Q_y$$

$$\xi_1 = \xi_2 = \xi \qquad (4.4)$$

$$a_1 = a_2 = a$$

and

$$\alpha_1 = \alpha_2 = \alpha$$

It is seen that these restrictions confine this study to the class of structures which have identical properties along the two principal directions and are subjected to sinusoidal excitation which is also identical, except for the phase difference in the two directions. These restrictions, Eqs. 4.4, still leave us free to choose from a large number of structural shapes, each with its characteristic yield curve. We restrict this study further to the structures for which the yield curve is given by

$$p_1^2 + p_2^2 = 1 \qquad (4.5)$$

It may be remarked here that the simple frame, Fig. 2.4, with columns of circular section will satisfy all these restrictions.

Under the restrictions imposed by Eqs. 4.4 and 4.5, the equations of motion are considerably simplified and can be written For elastic response:

$$\ddot{u}_1 + 2\xi\dot{u}_1 + u_1 = - r \sin(\eta\tau + \beta)$$

$$\ddot{u}_2 + 2\xi\dot{u}_2 + u_2 = - r \sin(\eta\tau + \beta + \rho) \qquad (4.6)$$

For elasto-plastic response:

$$\ddot{u}_1 + 2\xi\dot{u}_1 + u_1 - u_{o1} = - r \sin(\eta\tau + \beta)$$

$$\text{if } p_1 < |1|,$$

$$\text{or if } p_1 = |1| \text{ and } \dot{W}_1^p < 0$$

$$\ddot{u}_2 + 2\xi\dot{u}_2 + u_2 - u_{o2} = - r \sin(\eta\tau + \beta + \rho)$$

$$\text{if } p_2 < |1|$$

$$\text{or if } p_2 = |1| \text{ and } \dot{W}_2^p < 0$$

and (4.7)

$$\ddot{u}_1 + 2\xi\dot{u}_1 + |1| = - r \sin(\eta\tau + \beta)$$

$$\text{if } \dot{W}_1^p \geq 0$$

$$\ddot{u}_2 + 2\xi\dot{u}_2 + |1| = - r \sin(\eta\tau + \beta + \rho)$$

$$\text{if } \dot{W}_2^p \geq 0$$

For elasto-plastic response with interaction:

$$\ddot{u}_1 + 2\xi\dot{u}_1 + u_1 - u_{o1} = - r \sin(\eta\tau + \beta)$$

$$\ddot{u}_2 + 2\xi\dot{u}_2 + u_2 - u_{o2} = - r \sin(\eta\tau + \beta + \rho) \qquad (4.8)$$

$$\text{if } p_1^2 + p_2^2 < 1$$

$$\text{or if } p_1^2 + p_2^2 = 1 \text{ and } \dot{W}^p < 0$$

and

$$\ddot{u}_1 + 2\xi\dot{u}_1 + p_1 = - r \sin(\eta\tau + \beta)$$

$$\ddot{u}_2 + 2\xi\dot{u}_2 + p_2 = - r \sin(\eta\tau + \beta + \rho) \tag{4.9}$$

$$\dot{p}_1 = p_2^2\dot{u}_1 - p_1 p_2 \dot{u}_2$$

$$\dot{p}_2 = -p_1 p_2 \dot{u}_1 + p_1^2 \dot{u}_2$$

$$\text{if } p_1^2 + p_2^2 = 1 \text{ and } \dot{W}^p \geq 0$$

Let us consider an undamped system and assume that the steady-state response is of the form

$$u_1 = b_1 \sin \eta\tau + u_{o1}$$

$$u_2 = b_2 \sin(\eta\tau + \kappa) + u_{o2} \tag{4.10}$$

where

$b_1, b_2$ are the steady-state displacement amplitude ratios in direction 1-1 and 2-2

$\kappa$ is the phase difference in the steady-state response along two directions

$u_{o2}, u_{o1}$ are the components of permanent set

Elastic Response

The steady-state elastic response is characterized by the following relations[41]

$$b_1 = b_2 = b = - \frac{r}{1 - \eta^2}$$

$$u_{o1} = u_{o2} = 0 \tag{4.11}$$

$$\kappa = \rho$$

and

$$\beta = 0$$

Elasto-Plastic Response

The steady-state response and the stability of elasto-plastic systems has been investigated by Caughey,[43] using the method of slowly varying parameters. Iwan[42] has investigated such systems in detail, using both exact and approximate methods. Both of these investigations were made for bilinear hysteretic systems for which elastic-perfectly-plastic behavior is a particular case. It is characterized by the following relations. The steady-state amplitude and phase angle are such that

$$b_1 = b_2 = b$$

and (4.12)

$$\kappa = \rho$$

The frequency response equation is given by

$$\eta^2 = \frac{C(b)}{b} \pm \left\{ \left(\frac{r}{b}\right)^2 - \left(\frac{S(b)}{b}\right)^2 \right\}^{\frac{1}{2}} \tag{4.13}$$

where

$$S(b) = -\frac{b}{\pi} \sin^2\nu \qquad \text{if } b > 1$$

$$= 0 \qquad \text{if } b < 1$$

$$C(b) = \frac{b}{\pi}\left(\nu - \frac{\sin 2\nu}{2}\right) \qquad \text{if } b > 1$$

$$= b \qquad \text{if } b < 1$$

and

$$\nu = \cos^{-1}\left(1 - \frac{2}{b}\right)$$

The amplitude and the phase resonance of the system occur at the same frequency[43] and peak amplitude of the response is given by

$$b_p = \frac{4/\pi}{\frac{4}{\pi} - r} \tag{4.14}$$

The frequency at which the peak response occurs is given by

$$\eta_p^2 = \frac{C(b_p)}{b_p} \tag{4.15}$$

where

p is the subscript denoting peak response

The hysteretic energy loss in the system, per cycle, is equal to the area enclosed by the hysteresis loops and is given by

$$HE^* = 8Q_y q_y (b - 1)$$

Dividing by the elastic energy capacity, $\frac{1}{2}Q_y q_y$,

$$\frac{HE^*}{\frac{1}{2}Q_y q_y} = 16(b - 1) \tag{4.16}$$

where

$HE^*$ is the total (both directions) energy loss due to hysteresis per cycle

The frequency response equation 4.13 gives the relationship between the frequency ratio $\eta$ and steady-state amplitude b and is plotted in Fig. 4.8 for $r = 0.5, 0.7, 1.0$ and $4/\pi$. Equation 4.15 represents the locus at peak amplitude and is also plotted in Fig. 4.8. These curves show the typical behavior of a softening system. From

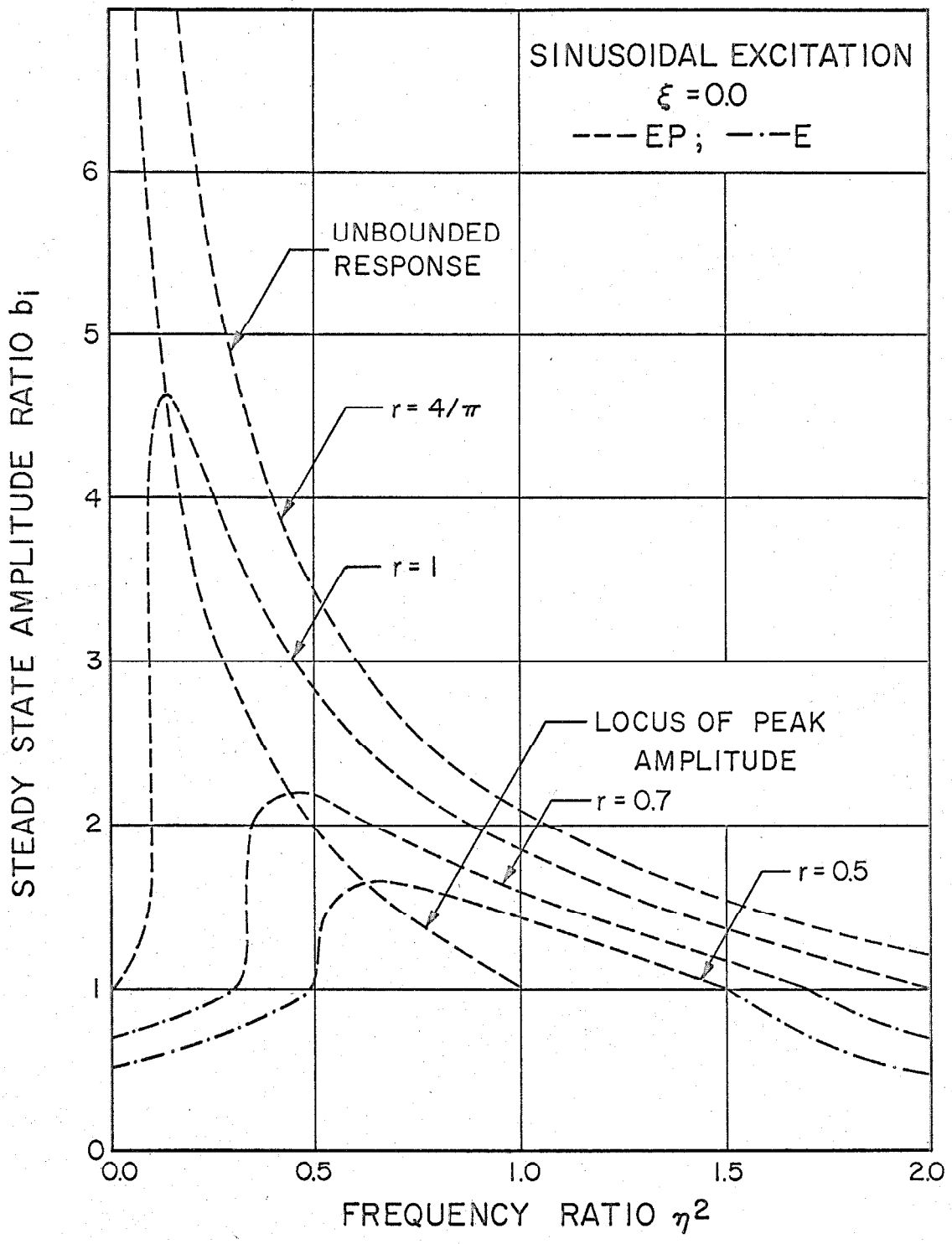


FIG. 4.8 FREQUENCY RESPONSE CURVES

Eq. 4.14 it is seen that if $r = 4/\pi$, $b_p$ becomes infinitely large. This shows that unbounded response occurs if $r \geq 4/\pi$. These curves are compared later with the similar curves for elasto-plastic response with interaction.

Elasto-Plastic Response with Interaction

The equations of motion for elasto-plastic response with interaction are given by Eqs. 4.8 and 4.9. It is clear that the steady-state response must be one of the following types:

1. Elastic, when Eqs. 4.8 hold
2. Plastic, when Eqs. 4.9 hold
3. Partly elastic and partly plastic, when both Eqs. 4.8 and 4.9 hold.

Elastic Response

If the steady-state response is purely elastic, the amplitude and phase angles are given by Eqs. 4.11 so that

$$u_1 = b \sin \eta\tau$$
$$u_2 = b \sin (\eta\tau + \rho) \tag{4.17}$$

and

$$p_1 = u_1$$
$$p_2 = u_2 \tag{4.18}$$

The condition that the frame remains elastic is that

$$p_1^2 + p_2^2 < 1$$

or

$$u_1^2 + u_2^2 < 1$$

Substituting from Eq. 4.17 and simplifying, it can be shown that

$$u_1^2 + u_2^2 = b^2 \left\{1 - \cos \rho \cos (2\eta\tau + \rho)\right\}$$

and

$$\text{Max } (u_1^2 + u_2^2) = b^2(1 + \cos \rho)$$

Hence the steady-state response will be elastic if

$$b < \frac{1}{(1 + \cos \rho)^{\frac{1}{2}}} \tag{4.19}$$

or substituting from Eq. 4.11

$$r < \frac{1 - \eta^2}{(1 + \cos \rho)^{\frac{1}{2}}} \tag{4.20}$$

Plastic Response

If the steady-state response is purely plastic the equations of motion are given by Eqs. 4.9. Let

$$\begin{aligned} p_1 &= d_1 \sin (\eta\tau + \delta_1) \\ p_2 &= d_2 \sin (\eta\tau + \delta_2) \end{aligned} \tag{4.21}$$

For purely plastic response, we have continuous yielding and the following conditions must be satisfied:

$$p_1^2 + p_2^2 = 1 \tag{4.22}$$

and

$$\dot{W}^p \geq 0 \tag{4.23}$$

Differentiating Eq. 4.22 once with respect to $\tau$ gives

$$p_1\dot{p}_1 + p_2\dot{p}_2 = 0$$

Substituting from Eq. 4.21 and simplifying, it can be shown that

$$(d_1^2\cos 2\delta_1 + d_2^2\cos 2\delta_2)\sin 2\eta\tau + (d_1^2\sin 2\delta_1 + d_2^2\cos 2\delta_2)\cos 2\eta\tau = 0$$

Since this condition must hold for all $\tau$, we must have

$$\begin{aligned} \cos 2\delta_1 d_1^2 + \cos 2\delta_2 d_2^2 &= 0 \\ \sin 2\delta_1 d_1^2 + \sin 2\delta_2 d_1^2 &= 0 \end{aligned} \tag{4.24}$$

For non-trivial solutions of $d_1^2$ and $d_2^2$ we must have

$$\begin{vmatrix} \cos 2\delta_1 & \cos 2\delta_2 \\ \sin 2\delta_1 & \sin 2\delta_2 \end{vmatrix} = 0$$

or

$$\sin 2(\delta_2 - \delta_1) = 0$$

This implies that

$$\delta_2 = \delta_1 + \frac{n\pi}{2} \quad , \quad n = 0,1,2,... \tag{4.25}$$

For $n = 0,2,4,...$

$$(d_1^2 + d_2^2)\cos 2\delta_1 = 0$$

so that

$$\delta_1 = \frac{m\pi}{4} \qquad m = 1,3,5,...$$

and

$$p_1 = d_1 \sin\left(\eta\tau + \frac{m\pi}{4}\right)$$
$$p_2 = d_2 \sin\left(\eta\tau + \frac{m\pi}{4}\right) \qquad (4.26)$$

Equations 4.26 do not satisfy Eq. 4.22 and hence even values of $n$ are not admissible. For $n = 1,3,5,\ldots$

$$(d_1^2 - d_2^2) \cos 2\delta_1 = 0$$

which requires that

$$d_1 = d_2 = d$$

and

$$\delta_2 = \delta_1 + \frac{n\pi}{2} \qquad n = 1,3,5,\ldots$$

Since $p_1$ and $p_2$ must satisfy Eq. 4.22 it follows that $d_1 = d_2 = 1$ and

$$p_1 = \sin(\eta\tau + \delta_1)$$
$$p_2 = \cos(\eta\tau + \delta_1) \qquad (4.27)$$

The assumed steady-state response is now defined by Eqs. 4.10 and 4.27 in terms of $b_1$, $b_2$, $\kappa$, $\beta$ and $\delta_1$. These equations must satisfy the equations of motion 4.9. Substituting Eqs. 4.10 and 4.27 into the first two of Eqs. 4.9 and simplifying, it can be shown that

$$\left\{-b_1\eta^2 + \cos\delta_1 + r\cos\beta\right\}\sin\eta\tau + \left\{\sin\delta_1 + r\sin\beta\right\}\cos\eta\tau = 0$$

$$\left\{-b_2\eta^2\cos\kappa - \sin\delta_1 + r\cos(\beta + p)\right\}\sin\eta\tau +$$

$$+ \left\{-b_2\eta^2\sin\kappa + \cos\delta_1 + r\sin(\beta + \rho)\right\}\cos\eta\tau = 0$$

To satisfy these equations for all $\tau$, the coefficients of $\cos \eta\tau$ and $\sin \eta\tau$ must vanish, so that

$$\begin{aligned} -b_1\eta^2 + \cos \delta_1 + r \cos \beta &= 0 \\ \sin \delta_1 + r \sin \beta &= 0 \\ -b_2\eta^2 \cos \kappa - \sin \delta_1 + r \cos (\beta + \rho) &= 0 \\ -b_2\eta^2 \sin \kappa + \cos \delta_1 + r \sin (\beta + \rho) &= 0 \end{aligned} \tag{4.28}$$

It is also neccssary to satisfy the last two of Eqs. 4.9. It can be shown that only one of these is independent in view of Eq. 4.22. Substituting Eqs. 4.10 and 4.27 into the first of these equations and simplifying it can be shown that

$$\begin{aligned} b_1 \cos \delta_1 - b_2 \sin (\delta_1 - \rho) + (b_1 - b_2 \sin \rho) \cos (2\eta\tau + \delta_1) \\ + b_2 \cos \rho \sin (2\eta\tau + \delta_1) = 2 \end{aligned} \tag{4.29}$$

It is not possible to satisfy Eq. 4.29 for all $\tau$, except for $\rho = \pi/2$, as will be shown later. For this special case, Eqs. 4.28 and 4.29 provide a set of transcendental equations which can be solved for the unknown variables $b_1$, $b_2$, $\kappa$, $\beta$ and $\delta_1$. For other values of $\rho$, it is not possible to do so.

Condition for Continued Yielding

It was shown that for continued yielding we must satisfy Eq. 4.22 and 4.23. For $p_1$ and $p_2$ defined by Eq. 4.27, Eq. 4.22 is identially satisfied. Hence, it is necessary to look only into the

Eq. 4.23. $\dot{W}^P$ can be written as

$$\dot{W}^P = Q_y q_y (p_1 \dot{u}_1 + p_2 \dot{u}_2)$$

Substituting from Eqs. 4.10 and 4.27 and simplifying, it can be shown that

$$\dot{W}^P = \frac{Q_y q_y}{2} \left\{ b_1 \sin \delta_1 + b_2 \cos (\rho - \delta_1) + R \sin (2\eta\tau + \mu) \right\}$$

where

$$R = (b_1^2 + b_2^2 - 2b_1 b_2 \sin \rho)^{\frac{1}{2}}$$

and

$$\tan \mu = \frac{b_1 \sin \delta_1 + b_2 \sin (\delta_1 + \rho)}{b_1 \cos \delta_1 - b_2 \sin (\delta_1 + \rho)}$$

From Eq. 4.30 it is clear that $\dot{W}^P \geq 0$, for all $\tau$, if and only if

$$b_1 \sin \delta_1 + b_2 \cos (\rho - \delta_1) \geq R \geq 0$$

Substituting for R and simplifying, it can be shown that the necessary conditions for continued yielding are

$$b_1 \sin \delta_1 + b_2 \cos (\rho - \delta_1) \geq 0$$

and (4.30)

$$b_1 \cos \delta_1 - b_2 \sin (\rho - \delta_1) \geq 0$$

Partly-Elastic and Partly-Plastic Response

If the conditions of continued yielding, Eqs. 4.30, are not satisfied the steady-state response is partly-elastic and partly-plastic. For this case, the equations of motion are given by Eqs. 4.8 for the elastic part and Eqs. 4.9 for the plastic part. This is the exact

counterpart of the elasto-plastic case (EP), for which results of approximate analysis were quoted earlier in this section. In view of the difficulties encountered in obtaining analytic solutions for perfectly-plastic response, there seems to be no hope that such approximate methods can be used for partly-elastic and partly-plastic response.

Steady-State Response for Special Values of Phase Angle $\rho$.

Phase Angle $\rho = 0$.

When $\rho = 0$, the set of equations 4.8 and 4.9 are identical in directions 1-1 and 2-2 and therefore, the response is also identical both in phase and amplitude. The locus of the mass center lies along a straight line inclined at $45^{\circ}$ to the axes 1-1 and 2-2, and the problem can be reduced to a one dimensional problem by considering the motion along this direction. Let us define a new coordinate system with the axes 1'-1' and 2'-2' inclined to the axes 1-1 and 2-2 at $45^{\circ}$ as shown in Fig. 4.9(a). Let $u'$ denote the displacement ratio in the direction 1'-1'. Then the equations of motion of the frame reduce to

$$\ddot{u}' + 2\xi\dot{u}' + p' = r\sqrt{2}\,\sin(\eta\tau + \beta)$$

where

$$\begin{aligned} p' &= u' - u'_o \qquad \text{if } |p'| < 1 \\ &\qquad\qquad \text{or if } |p'| = 1 \text{ and } \dot{W}^{p'} < 0 \\ p' &= |1| \qquad\quad \text{if } \dot{W}^{p'} \geq 0 \ . \end{aligned} \tag{4.31}$$

Equations 4.31 are of the same form as equations of motion for

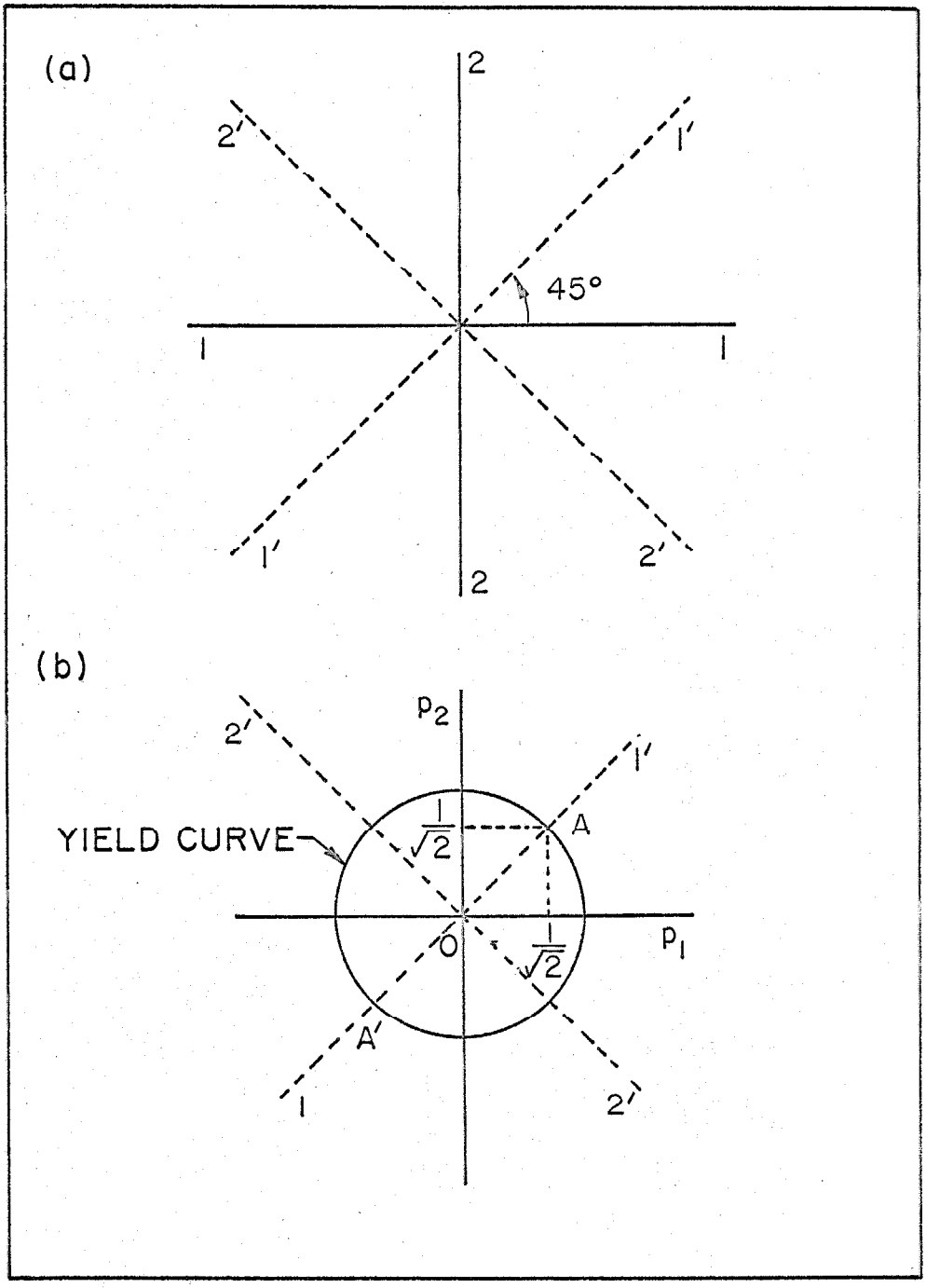


FIG. 4.9 RESPONSE FOR PHASE ANGLE $\rho = 0^{\circ}$

elasto-plastic response and can be solved by the approximate methods used for such systems. Knowing the response in the direction 1'-1' the response in the directions 1-1 and 2-2 is given by $u_1 = u_2 = u'/\sqrt{2}$.

It is instructive to look at this case as a two dimensional problem, and see how the interaction comes into play. Consider the response in the force-space shown in Fig. 4.9(b). The force vector starts at the origin and in view of the symmetry moves along the straight line 1'-1' until it hits the yield surface at A. The system now goes into the plastic state and again due to symmetry, the tip of the force vector stays at A so that the restoring force ratios are given by $p_1 = p_2 = 1/\sqrt{2}$. On unloading the force vector again moves along 1'-1' and the response remains elastic, until it hits A', where yielding is initiated and $p_1 = p_2 = -1/\sqrt{2}$. For this case, the equations of motion reduce to

$$\ddot{u}_i + 2\xi\dot{u}_i + p_i = r \sin \eta\tau$$

where $i = 1, 2$, and

$$\begin{aligned} p_i &= u_i - u_{oi} \qquad \text{if } |\bar{p}| < 1 \\ &\qquad\qquad \text{or if } |\bar{p}| = 1 \text{ and } \dot{W}^p < 0 \\ &= \left| \frac{1}{\sqrt{2}} \right| \qquad \text{if } \dot{W}^p \geq 0 \end{aligned} \tag{4.32}$$

Equations 4.32 are again of the same form as the equations of motion for elasto-plastic response and can be solved by approximate methods used for such systems. It can be shown by setting $u' = \sqrt{2}\, u_i$ that

Eq. 4.32 becomes identical with Eq. 4.31. It may be pointed out here that for elasto-plastic response without interaction, the equations of motion are given by Eqs. 4.7, which are the same as Eqs. 4.32, except that in the former $p = |1|$ during yielding. This shows that the response obtained from Eqs. 4.7 and Eqs. 4.32 will be different.

The frequency response curves, showing the amplitude ratio $b'$ against frequency ratio $\eta^2$, are shown in Fig. 4.10 both for the elasto-plastic response (EP) and the elasto-plastic response with interaction (EPI). The loci of peak amplitude are also plotted on the same figure. Figure 4.11 shows the plot of the ratio of energy per cycle to the elastic energy capacity of the system against frequency ratio $\eta^2$. These curves show the following changes in the response due to the effect of interaction on yielding:

1. For the elasto-plastic response with interaction, the locus of peak amplitude is shifted further to the left of the locus of peak amplitude for the elasto-plastic response. Since a shift to the left, in the locus of peak amplitude, is a characteristic of soft systems, this indicates that interaction has the effect of making the system softer.
2. For the elasto-plastic response with interaction, the unbounded response occurs for $r = 2\sqrt{2}/\pi$, whereas for the elasto-plastic response it occurs for $r = 4/\pi$.
3. The curves for the steady-state amplitude ratio $b'$ are significantly different in the two cases. Interaction has the effect of increasing the amplitude for low values of

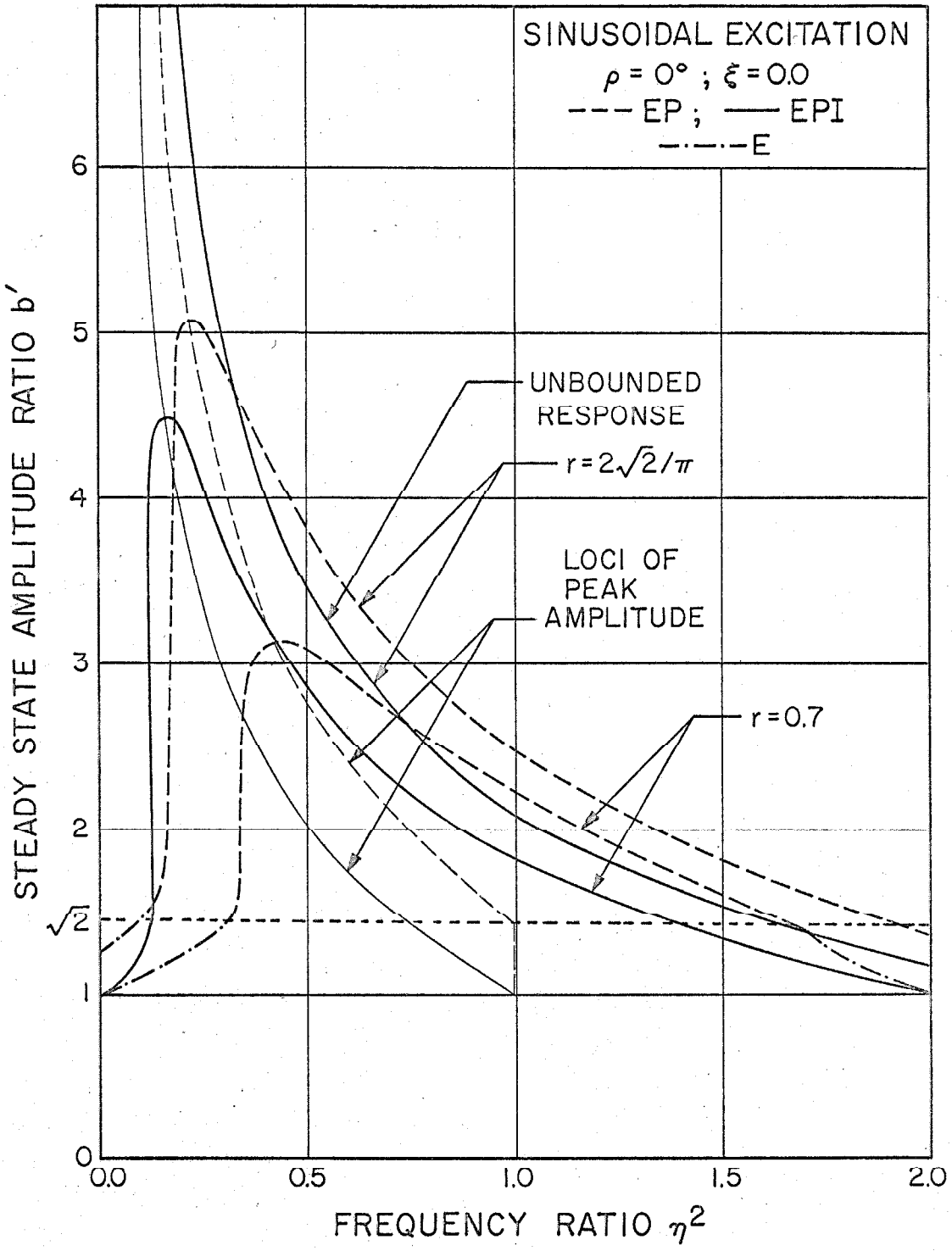


FIG. 4.10 FREQUENCY RESPONSE CURVES

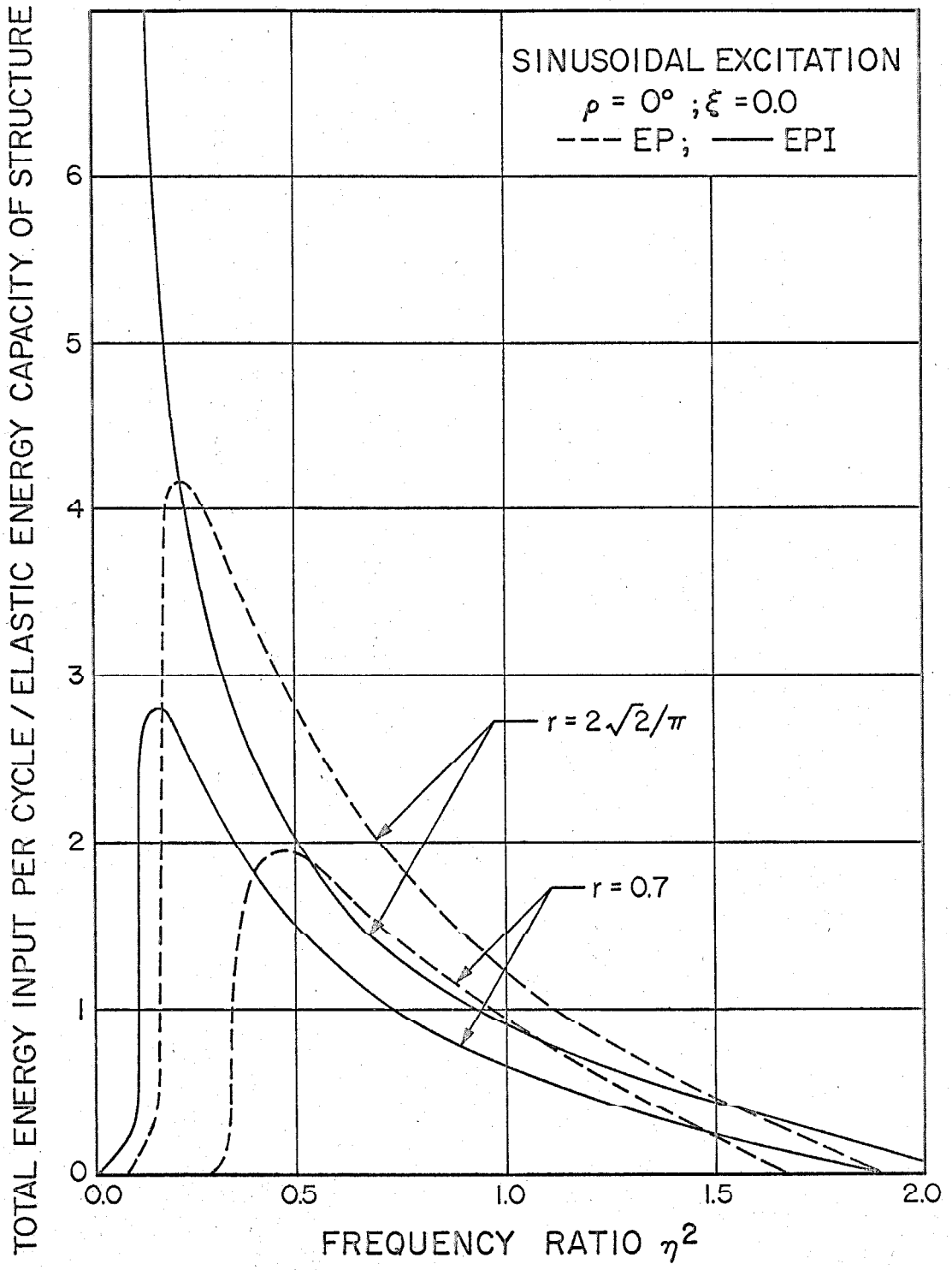


FIG. 4.11 TOTAL ENERGY INPUT PER CYCLE

frequency ratio $\eta^2$ and decreasing the amplitude for higher values of $\eta^2$, depending upon the value of r.

4. From Fig. 4.10 it is seen that for elasto-plastic response the behavior is plastic if $b' > 1/\sqrt{2}$. For elasto-plastic response with interaction yielding occurs if $b' > 1$. This indicates that interaction has the effect of causing yielding at lower force levels. Since yielding produces permanent displacements in the structure, this is significant where permanent displacements are to be avoided.

5. The ratio of energy input per cycle to the elastic energy capacity of the system is also significantly different in the two cases. It is seen that over most of the frequency range, the energy input is decreased.

For $\rho = 0$, the basic cause of these changes in the response is very simple. From Eqs. 4.31 and 4.32 it is clear that interaction has the effect of reducing the yield level by the factor $1/\sqrt{2}$.

Phase angle $\rho = \pi/2$

In the beginning of this section it was assumed that the response of the frame is given by Eqs. 4.10 and 4.27, in terms of $b_1$, $b_2$, $\kappa$, $\beta$ and $\delta_1$. It was also found that for the perfectly plastic case, these parameters must satisfy Eqs. 4.28 and 4.29. Substituting $\rho = \pi/2$ in Eqs 4.28 gives

$$
\begin{aligned}
&-b_1\eta^2 + \cos\delta_1 + r\cos\beta = 0 \\
&\sin\delta_1 + r\sin\beta = 0 \\
&-b_2\eta^2\cos\kappa - \sin\delta_1 - r\sin\beta = 0 \\
&-b_2\eta^2\sin\kappa + \cos\delta_1 + r\cos\beta = 0
\end{aligned}
\tag{4.33}
$$

From Eqs. 4.33 it can be shown that

$$
\begin{aligned}
\kappa &= \pi/2 \\
b_1 &= b_2 = b
\end{aligned}
\tag{4.34}
$$

and

$$r^2 + b^2\eta^4 - 2rb\eta^2\cos\beta = 1 \tag{4.35}$$

Substituting $\rho = \pi/2$ and $b_1 = b_2 = b$ in Eq. 4.29 gives

$$2 - 2b\cos\delta_1 = 0 \tag{4.36}$$

Thus it is seen that in this case it is possible to satisfy Eq. 4.29 for all $\tau$, and Eqs. 4.33 along with Eq. 4.36 satisfy all the equations of motion. Equation 4.36 and the last of Eqs. 4.33 gives

$$\cos\beta = \frac{b^2\eta^2 - 1}{br} \tag{4.37}$$

Substituting for $\cos\beta$ in Eq. 4.35 gives

$$r^2 + b^2\eta^4 - 2\eta^2(b^2\eta^2 - 1) = 1 \tag{4.38}$$

This is the frequency response equation.

Peak Response

Equation 4.38 can be rewritten as

$$b^2 = \frac{1}{\eta^4}(r^2 - 1 + 2\eta^2) \tag{4.39}$$

so

$$\frac{db^2}{d\eta} = -\frac{4(r^2-1)}{\eta^5} - \frac{4}{\eta^3}$$

For peak response, $db^2/d\eta = 0$, hence

$$\frac{4(r^2-1)}{\eta^5} - \frac{4}{\eta^3} = 0$$

This gives

$$\eta_p = (1 - r^2)^{\frac{1}{2}} \tag{4.40}$$

and from Eq. 4.39

$$b_p = \frac{1}{(1 - r^2)^{\frac{1}{2}}} \tag{4.41}$$

where

p is the subscript denoting peak response

Combining Eqs. 4.40 and 4.41 gives

$$b_p = \frac{1}{\eta_p} \tag{4.42}$$

This is the locus of peak amplitude. Substituting Eq. 4.42 and Eq. 4.37 gives $\beta = \pi/2$. This shows that phase and amplitude resonance occur at the same frequency. Also, from Eq. 4.41, it is seen that unbounded response occurs for $r \geq 1$.

For $\rho = \pi/2$, it is seen from Eq. 4.19 that for elastic response $b < 1$, and the response is given by Eq. 4.11. For $b = 1$, Eqs. 4.11 and 4.38 are identical and give

$$\eta^2 = 1 \pm r \tag{4.43}$$

For $b > 1$, yielding must occur. Substituting Eqs. 4.34 and 4.36 in Eqs. 4.30 it is seen that for $\rho = \pi/2$, the conditions for continued yield are satisfied. Thus for $\rho = \pi/2$, the response is elastic if $b \leq 1$ and is perfectly plastic if $b > 1$.

Energy input per cycle and energy loss per cycle are given by Eqs. 2.44 and 2.52. Substituting from Eqs. 4.10 and integrating from 0 to $2\pi$, it can be shown that

$$\begin{aligned} TE^* / \tfrac{1}{2} Q_y q_y &= 4\pi r b \sin \beta \\ HE^* / \tfrac{1}{2} Q_y q_y &= 4\pi b \sin \delta_1 \end{aligned} \tag{4.44}$$

where

$TE^*$ is the total energy input (both directions) per cycle

$HE^*$ is the hysteretic energy loss (both directions) per cycle

From Eqs. 4.33 it is seen that $r \sin \beta = -\sin \delta_1$. Hence, $|TE^*| = |HE^*|$, which is a necessary condition for steady-state response. From Eqs. 4.40 it is seen that maximum energy input occurs when $\beta = \pi/2$, which corresponds to the peak amplitude.

The frequency response curves and loci of peak amplitude are plotted in Fig. 4.12, both for the elasto-plastic response and elasto-

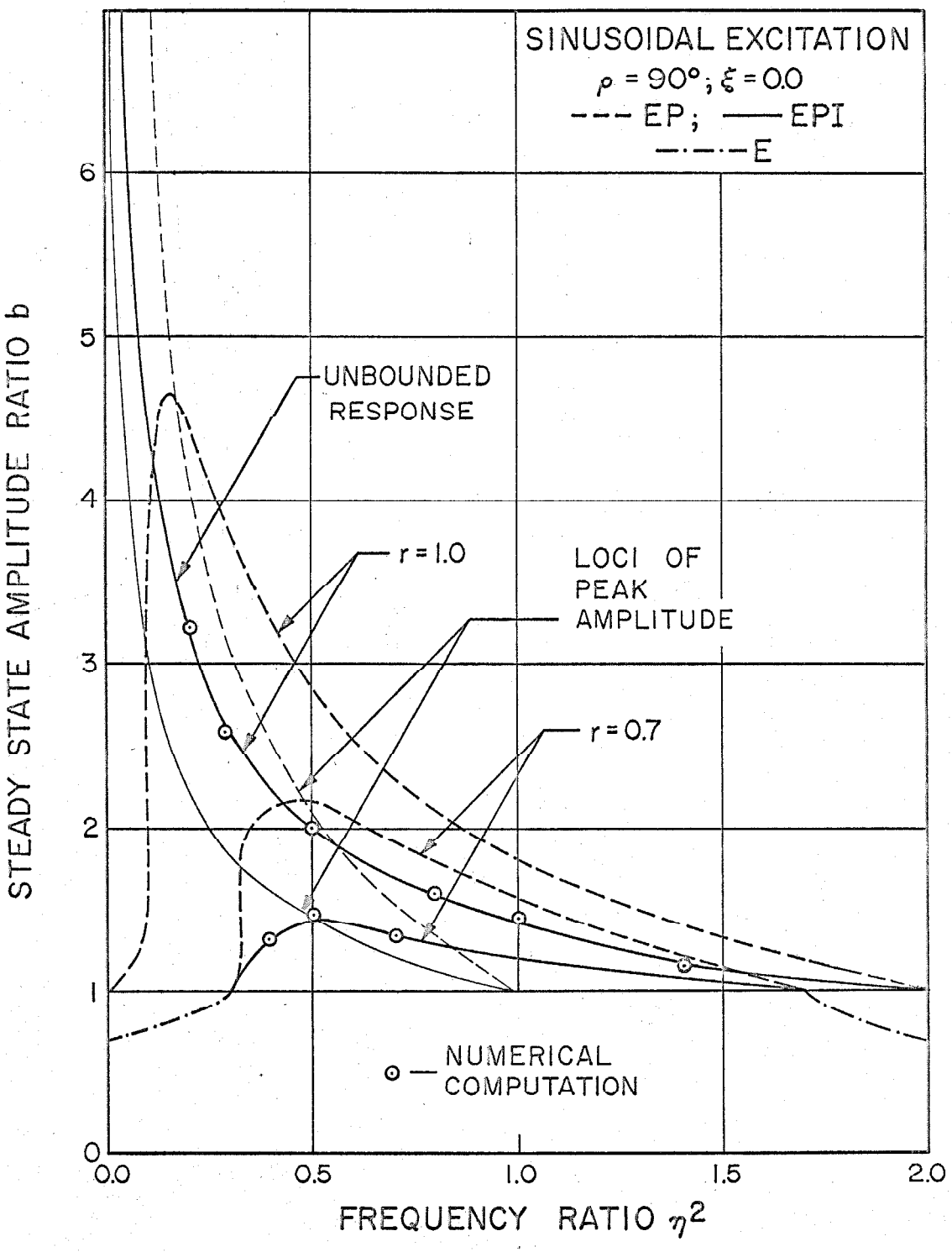


FIG. 4.12 FREQUENCY RESPONSE CURVES

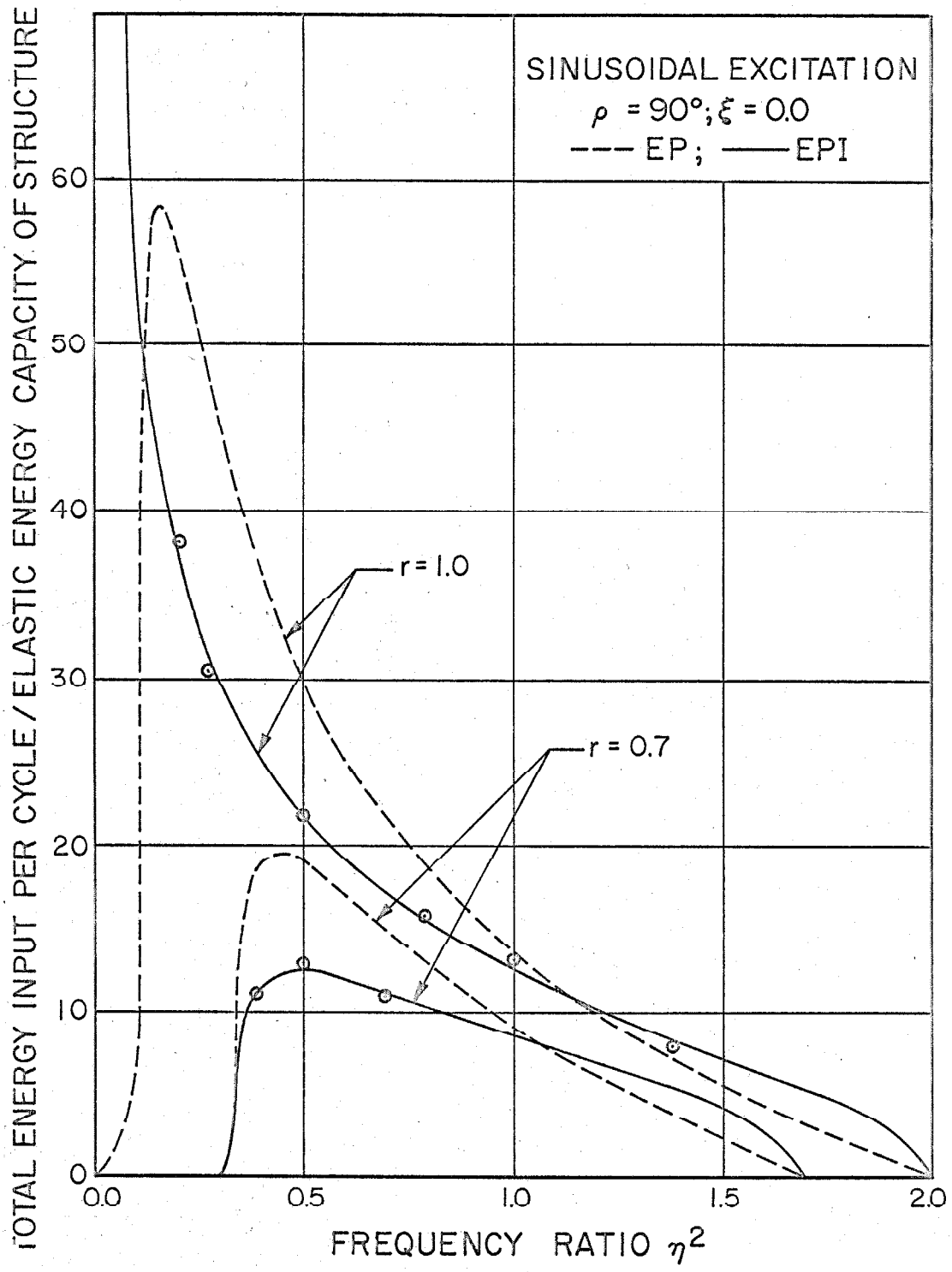


FIG. 4.13 ENERGY INPUT PER CYCLE

plastic response with interaction. Curves for the ratio of energy input per cycle to the elastic energy capacity of the system are plotted in Fig. 4.13. The general nature of these curves is the same as the curves for $\rho = 0$. In this case, the interaction has the effect of causing continuous yielding for $b > 1$. It can be shown that for $r < 0.95$, the steady-state amplitude for the elasto-plastic response with interaction is always less than the steady-state amplitude for the elasto-plastic response and for $r > 0.95$ the same is true except for the small values of $\eta^2$ depending on $r$. This indicates the effectiveness of interaction in reducing the response.

Check on Numerical Integration and Computer Program

For $\rho = \pi/2$, we have obtained the exact solution for the steady-state response. This makes it possible to check the accuracy of the numerical integration and the correctness of the computer program. For this purpose, the response for a number of cases was obtained by numerical integration and is shown by isolated points in Figs. 4.12 and 4.13. Maximum differences were found to be less than 2 per cent in amplitude and 4 per cent in energy computation. This agreement is considered to be satisfactory.

Phase angles $0 < \rho < \pi/2$

For $\rho = 0$ and $\pi/2$, it has been possible to obtain analytical solutions for steady-state response and to examine the effects of interaction. As shown earlier it is not possible to determine an analytic solution for other values of the phase angle. To study how

the response changes as the phase angle is changed from 0 to $\pi/2$, the response was obtained by numerical computation for $r = 0.5$, $\eta^2 = 0.9$ and $\rho = 0^\circ, 10^\circ, 45^\circ, 60^\circ, 80^\circ$ and $90^\circ$. Figure 4.14 shows the locus of the mass center for each of the above values of phase angle. The locus of the base is also shown on each plot. It is seen that the locus changes gradually from a straight line for $\rho = 0$ to a circle for $\rho = \pi/2$. In general, the locus is an ellipse, with its principal axes inclined to the principal axes of the locus of the base.

Figure 4.15 shows the variation of total energy input and maximum amplitude, along with their components, with the phase angle $\rho$. From this figure it is clearly seen that although the excitation is the same in two directions, but for the phase difference, the energy input and steady-state amplitude of oscillation are different. This is due to the redistribution of energy caused by the interaction. It is also seen from Fig. 4.15 that the energy input does not change much with phase angle, but maximum steady-state amplitude decreases uniformly as the phase angle increases from 0 to $\pi/2$. Since the yielding occurs at a fixed level for $\rho = 0$ and continuously for $\rho = \pi/2$, it indicates that ability of the system to remove energy, by hysteresis, at low yield levels reduces the amplitude of response.

Effect of Damping

In the cases so far considered the damping has been zero. To see how damping affects the response both with and without interaction,

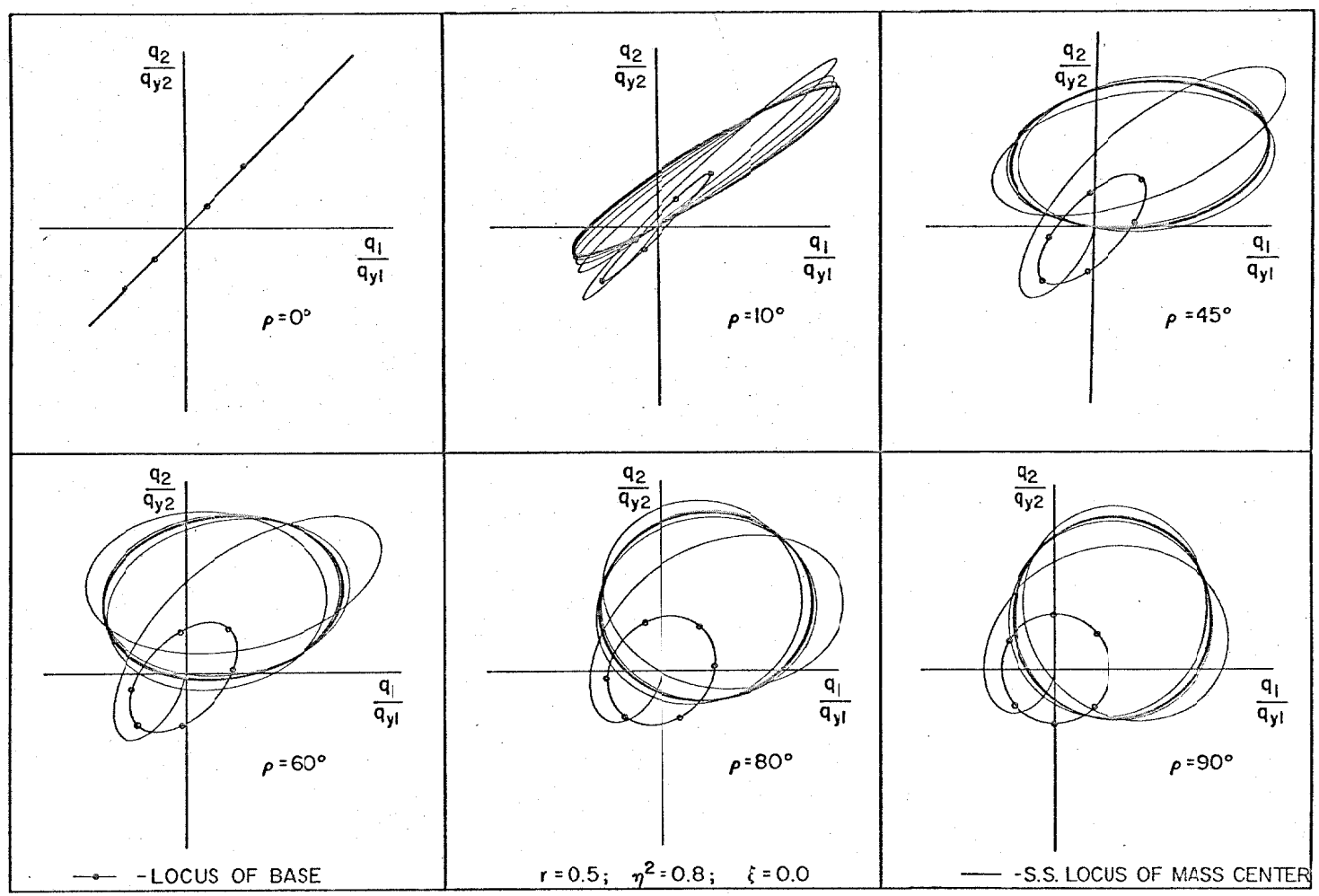


FIG. 4.14 RESPONSE TO SINUSOIDAL EXCITATION IN THE HORIZONTAL PLANE FOR DIFFERENT VALUES OF PHASE ANGLE

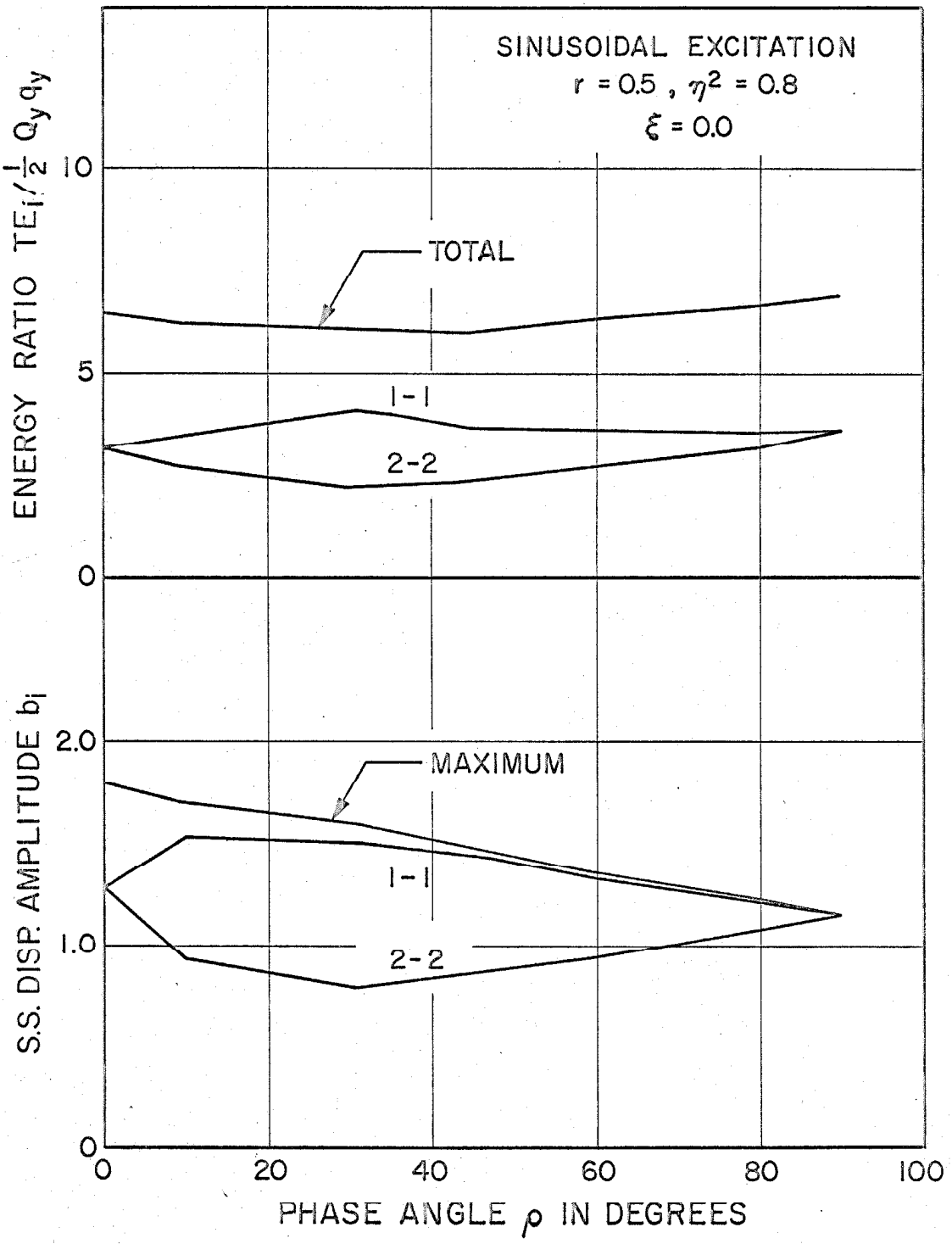


FIG. 4.15 EFFECT OF PHASE ANGLE ON THE RESPONSE

the response was obtained by numerical integration for $r = 1.0$, $\eta^2 = 0.8$, $\rho = 90^o$ and $\xi = 0.0$, 0.02, 0.05 and 0.1. The variation of energy input and steady-state amplitude with damping is shown in Fig. 4.16. It is seen that damping has the effect of increasing the energy input slightly in both cases but more so in the elasto-plastic case. The steady-state amplitude is decreased in both cases as damping increases and the damping is more effective when there is no interaction.

The Shape of the Yield Curve

So far the effects of interaction have been discussed with reference to the circular yield curve defined by Eq. 4.5. In Section 3.2 of Chapter III, it was shown that it is possible to define lowest and uppermost bounds of the yield surfaces and for two-dimensional force-space these are shown in Fig. 3.1. It may be noted that the uppermost bound represents the elasto-plastic behavior without interaction and we have already discussed the response for such behavior along with the response for the circular yield curve. The response for the lowest bound has been computed, by numerical integration, for $r = 0.5$, $\rho = 90^o$ and $\xi = 0.0$. Curves showing the variation of steady-state amplitude and energy input per cycle with frequency ratio $\eta^2$, are plotted in Figs. 4.17 and 4.18. These figures show that the response is quite sensitive to the shape of the yield curve. The lowest yield curve permits more interaction as compared to the circular yield curve and this is reflected by the fact that peak amplitude is shifted further to the left and the steady-state

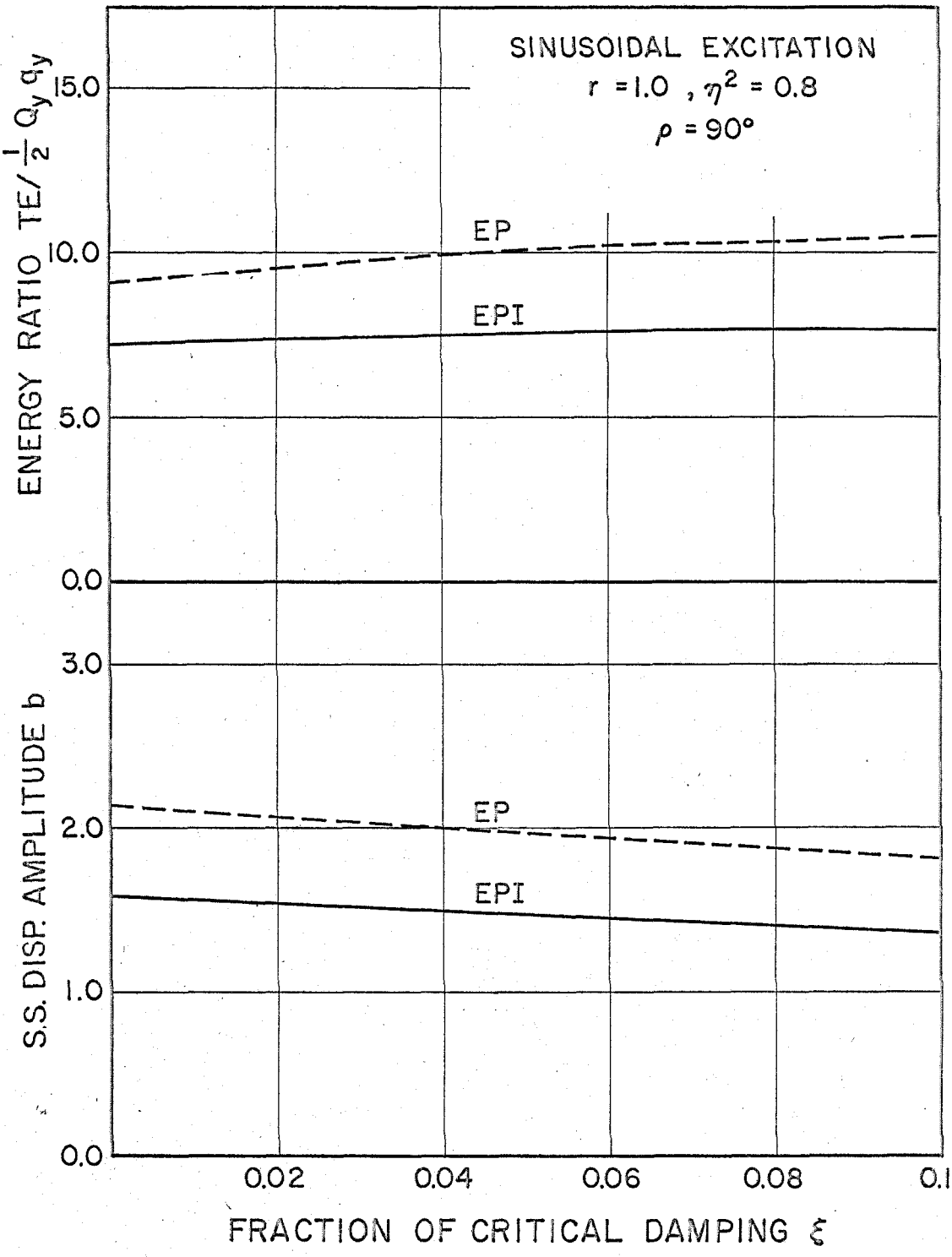


FIG. 4.16 EFFECT OF DAMPING ON THE RESPONSE

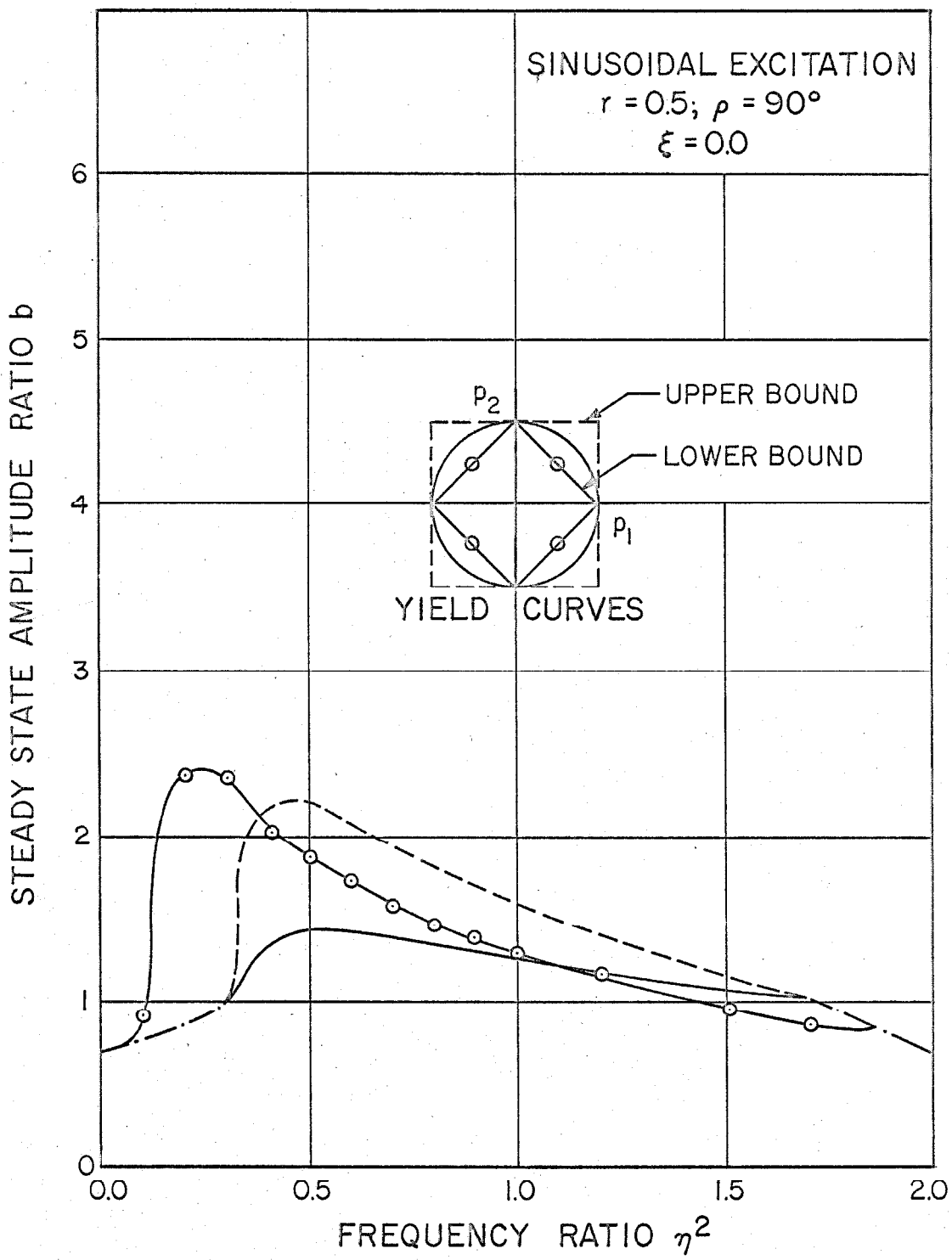


FIG. 4.17 EFFECT OF THE SHAPE OF YIELD CURVE ON STEADY-STATE AMPLITUDE

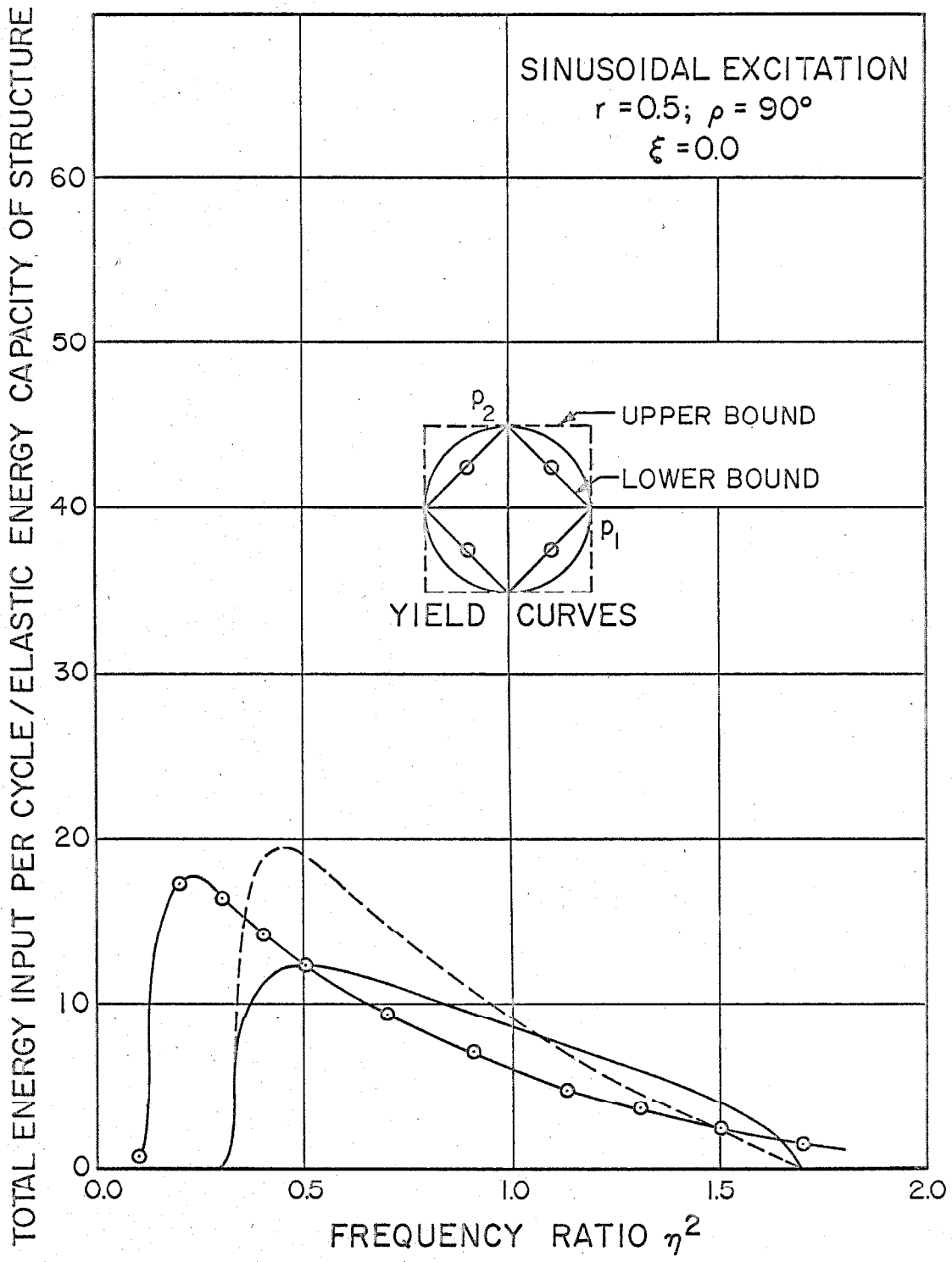


FIG. 4.18 EFFECT OF THE SHAPE OF YIELD CURVE ON THE TOTAL ENERGY INPUT PER CYCLE

amplitude and energy input are increased for low values of $\eta^2$. It is also seen that for circular and uppermost yield curve, yielding occurs for $b > 1$, where as for the lowest yield curve, yielding starts at lower values of b. Since yielding causes permanent set this fact is of significance, where permanent set cannot be permitted.

## 4.4 Summary and Conclusions

The dynamic response of a simple frame subjected to sinusoidal base excitation acting simultaneously along its principal directions has been presented. To limit the size of the study, the discussion has been restricted to frames which have identical properties along the two principal directions and a circular yield curve. The excitation has also been assumed to be identical along the two directions, but for a phase difference. Using the equations of motion derived in Chapter II, the response of the frame has been obtained for inelastic interaction between bending moments acting along the principal directions of a section. For purposes of comparison, the response has also been obtained for elastic and elasto-plastic behavior and the changes introduced in the response due to interaction have been discussed. For steady-state response, the problem of getting analytical solutions has been investigated and it has been possible to get an exact solution when the phase angle $\rho$ is equal to $90^{\circ}$. Using analytical results for this case, the accuracy of the numerical computations and correctness of the computer program have been checked. On the basis of these results, the following

conclusions can be drawn about the effects of interaction and their implications:

1. Interaction causes yielding, and hence energy dissipation by hysteresis, at force levels lower than the fixed yield level for elasto-plastic behavior. This has the effect of reducing the steady-state amplitude and energy input per cycle over most of the frequency range. This ability to limit the response, in general, is a significant feature of the effect of interaction.

2. Due to the coupling introduced by interaction, a redistribution of energy takes place along the principal directions. This transfer of energy causes an increase in the amplitude of response in one direction and a decrease in the other. If interaction is not included in the analysis, this phenomenon will not be anticipated.

3. Since interaction permits plastic deformations at yield levels lower than the fixed yield level for elasto-plastic behavior, it causes permanent displacements at lower force levels. This is of significance in problems where permanent displacements cannot be tolerated. For structures subjected to recurring loads, occurrence of plastic deformations at low force levels introduces also the possibilities of fatigue failure and cumulative damage.

4. In interpreting the results of the dynamic tests of structures, in the post-elastic range, interaction between forces present at a section may be significant. In the test set up used by Hanson,[21] the axial force and the shear force were also present along with the bending moment at any section. By using the general theory of yield-

ing developed in Chapter II, it is possible to derive a theoretical force-displacement relationship incorporating the effects of interaction between these forces. Hanson[21] has reported that the yield in the frame was initiated earlier than predicted by the theoretical force-displacement relationship and has attributed this, in part, to the effect of axial force which was not included in the analysis.

5. The theory of yielding derived in Chapter II is based on the assumption that the section remains elastic up to the yield surface, thus ignoring the effect of partly-elastic partly-plastic region. It has been shown in Section 4.3 that the response to sinusoidal excitation is very sensitive to the shape of the yield surface. In view of this, it seems that ignoring partly-elastic partly-plastic region may introduce significant errors in the estimates of the response. As pointed out in Section 3.4 of Chapter III, a simple way to get a more realistic response may be to use an intermediate yield surface lying between the initial and limit yield surfaces. The choice of such a surface can be made by getting the best fit between the analytical and the experimental results.

6. The discussion in this chapter has been restricted to a special class of frames and excitation. This leaves a number of parameters unstudied and these may be responsible for some other significant effects of interaction. Further study is, therefore, needed to investigate the influence of these parameters.

# CHAPTER V

# THE RESPONSE OF STRUCTURES TO EARTHQUAKE-TYPE EXCITATION

## 5.1 Introduction

The motivation to pursue this study came, originally, while considering the inelastic response of structures subjected to simultaneous base excitation by the horizontal components of an earthquake. For such an excitation, if a structure is assumed to undergo only a planar motion, its response can be obtained by considering the equations of motion along two mutually perpendicular directions. It is clear that for linearly elastic behavior, the response of the structure can be obtained by the superposition of response along the two directions. However, if the response is inelastic, such a superposition is not possible, and as shown in Chapter II, interaction between forces acting at a section comes into play in determining the behavior of the structure. In section 2.3 of Chapter II, the equations of motion of a simple frame were derived for elastic, elasto-plastic and interactive elasto-plastic behavior. In this chapter, these equations are used to study the response of the frame to the Taft earthquake and to an ensemble of artificial earthquakes. The calculated response is presented through a series of curves having various parameters representing the characteristics of the frame. Effect of interaction on the response of the frame is discussed in detail, and use of these curves for inelastic design of structures is indicated.

The notation used in this chapter is the same as in the preceeding chapters with the following additions.

| Symbol | Explanation or Definition |
|---|---|
| $T_1$, $T_2$ | natural periods of the structure in the directions 1-1 and 2-2 |
| $\hat{\ddot{z}}_1$, $\hat{\ddot{z}}_2$ | r.m.s. values of the horizontal component of ground acceleration during an earthquake, in the directions 1-1 and 2-2 |
| $\hat{\ddot{z}}$ | r.m.s. value of the ground acceleration vector during an earthquake |
| $\gamma_1, \gamma_2$ | acceleration ratios $\hat{\ddot{z}}/a_{y1}$, $\hat{\ddot{z}}/a_{y2}$ |
| $\mu_1$, $\mu_2$ | ductility ratios $q_{max\,1}/q_{y1}$, $q_{max\,2}/q_{y2}$ |
| $\mu^*$ | ratio of the maximum radial displacement during an earthquake to the yield displacement |
| $\Omega$ | ratio of hysteretic energy loss during an earthquake to the elastic energy capacity of the structure |

## 5.2 Response of the Frame to Earthquake Type Excitation

### Equations of Motion

Let $\ddot{z}_1(t)$ and $\ddot{z}_2(t)$ denote the horizontal components of ground acceleration during an earthquake. Let $\hat{\ddot{z}}_1$ and $\hat{\ddot{z}}_2$ denote the r.m.s. of each of these components and let

$$\hat{\ddot{z}} = (\hat{\ddot{z}}_1^2 + \hat{\ddot{z}}_2^2)^{\frac{1}{2}} \tag{5.1}$$

$\hat{\ddot{z}}$ is then the r.m.s. value of the vector representing ground acceleration during the earthquake. It is independent of the direction

in which the two components are recorded and is in a way an absolute measure of the strength of the earthquake. Let

$$\ddot{z}_1(t) = \hat{\ddot{z}}\, g_1(t)$$
$$\ddot{z}_2(t) = \hat{\ddot{z}}\, g_2(t) \qquad (5.2)$$

where

$g_1(t), g_2(t)$ are the dimensionless time records of ground motion in the directions 1-1 and 2-2 respectively

Also let

$$\gamma_1 = \frac{\hat{\ddot{z}}}{a_{y1}}$$
$$\gamma_2 = \frac{\hat{\ddot{z}}}{a_{y2}} \qquad (5.3)$$

where

$a_{y1}, a_{y2}$ are the yield accelerations in the directions 1-1 and 2-2 respectively

$\gamma_1, \gamma_2$ are the acceleration ratios in the direction 1-1 and 2-2 respectively

Setting $\tau = \omega_1 t$ and substituting for $\hat{\ddot{z}}$ from Eq. 5.3 in Eq. 5.2, gives

$$\frac{\ddot{z}_1\left(\frac{\tau}{\omega_1}\right)}{a_{y1}} = \gamma_1 g_1\left(\frac{\tau}{\omega_1}\right) \qquad (5.4)$$

$$\frac{\ddot{z}_2\left(\frac{\tau}{\omega_2\zeta}\right)}{a_{y2}} = \gamma_2 g_2\left(\frac{\tau}{\omega_2\zeta}\right)$$

where

$\zeta$ denotes the ratio $\omega_1/\omega_2$

The equations of motion of the frame for earthquake type excitation are now given, in dimensionless form, by Eqs. 2.36 through 2.39, with the forcing function defined by Eq. 5.4. The expressions for energy input and energy loss are given by Eqs. 2.44 and 2.49 through 2.51. If the ground acceleration record of the horizontal components of an earthquake is digitized at identical time intervals for each component, the response can be obtained by numerical integration of these equations. In this study a third order Runge-Kutta scheme of integration has been used. Integrals for energy input and energy loss have also been computed numerically. Details of numerical computation are given in Appendix III.

For circular yield curve with $T_1 = 1.0$, $T_2 = 0.5$, $\gamma_1 = 0.5$, $\gamma_2 = 0.3$, $\xi = 0.02$ and horizontal components of the Taft earthquake record, response of the frame has been computed for elastic, elasto-plastic and elasto-plastic behavior with interaction, by numerical integration of Eqs. 2.36 through 2.39. Various aspects of the response are shown in Figs. 5.2 through 5.11. These figures are used below to explain, qualitatively, some of the features of the effect of interaction.

Figures 5.2 through 5.7 show the displacement-time response of the frame for elastic, elasto-plastic and elasto-plastic behavior

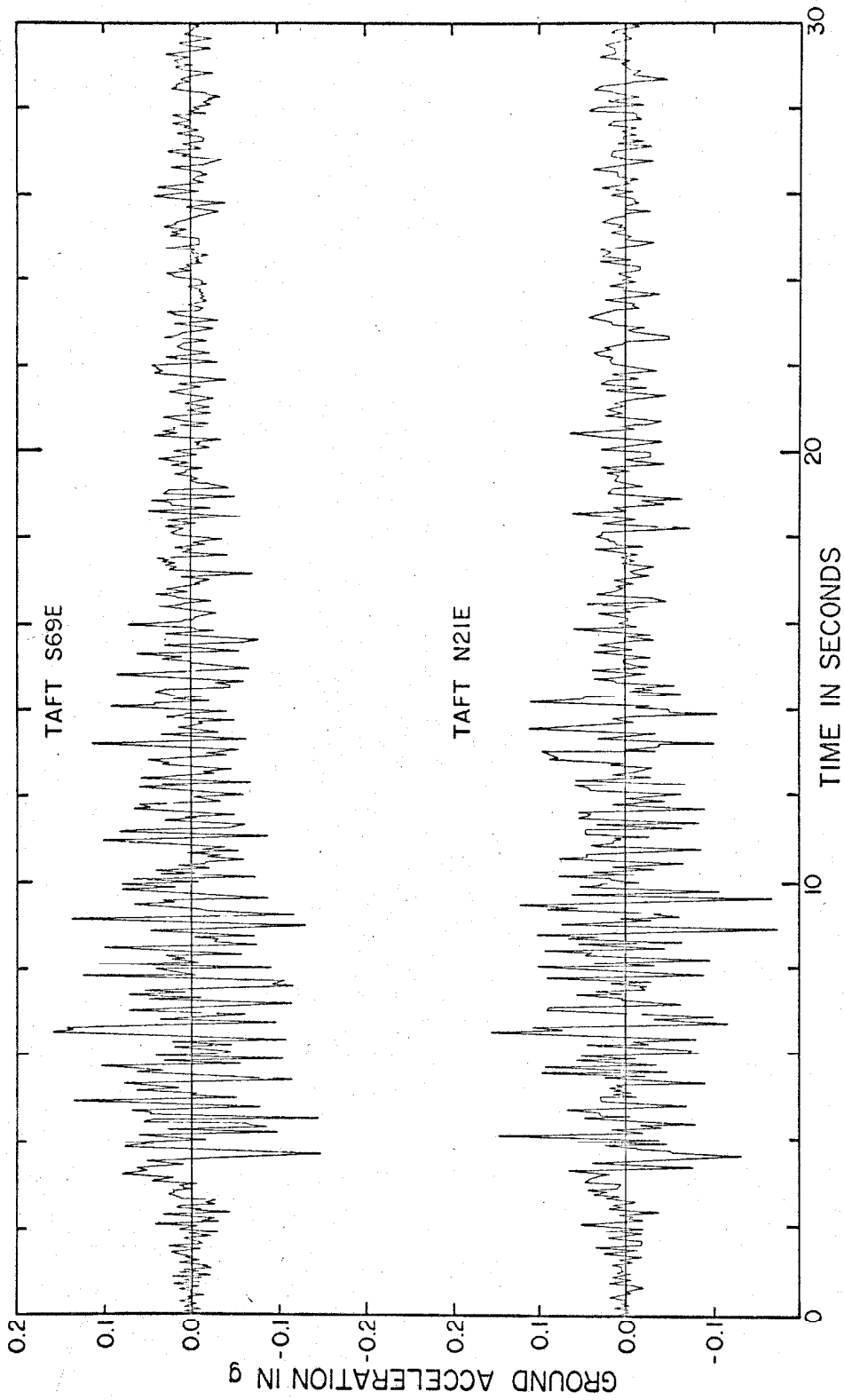


FIG. 5.1 HORIZONTAL COMPONENTS OF GROUND ACCELERATION RECORDED AT TAFT, CALIFORNIA DURING THE EARTHQUAKE OF JULY 21, 1952

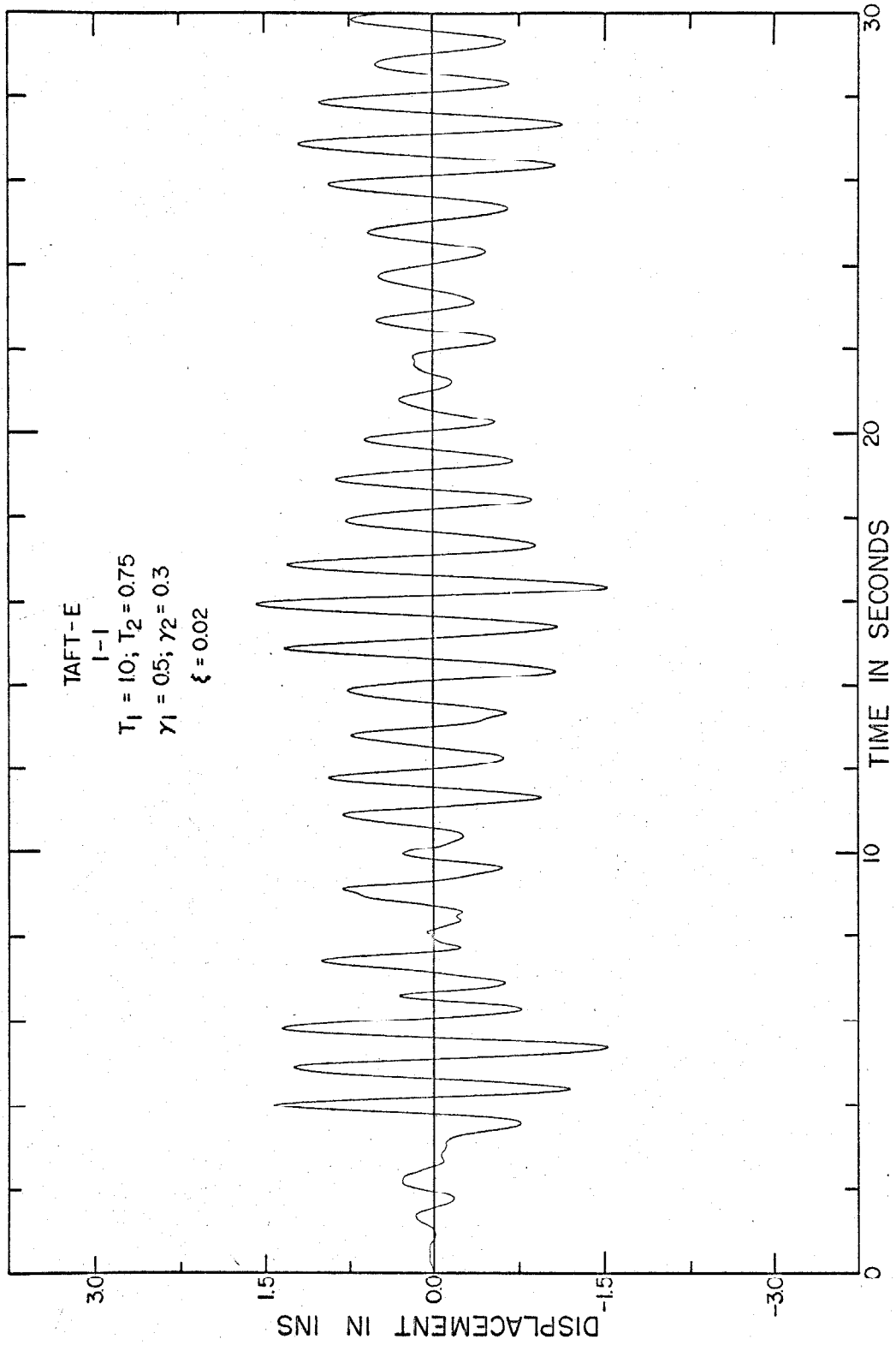


FIG. 5.2 DISPLACEMENT-TIME RESPONSE FOR ELASTIC BEHAVIOR

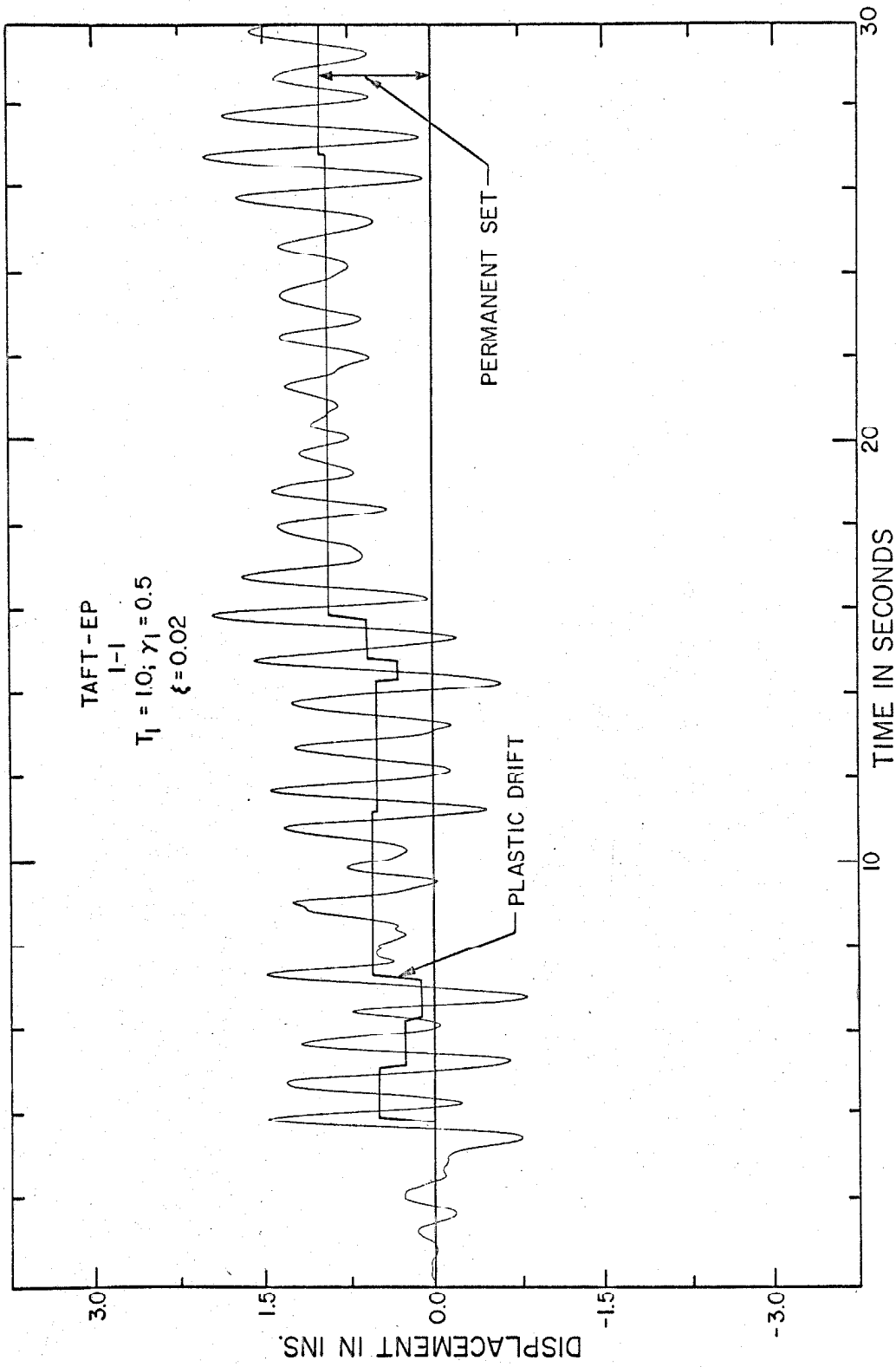


FIG. 5.3 DISPLACEMENT-TIME RESPONSE FOR ELASTO-PLASTIC BEHAVIOR

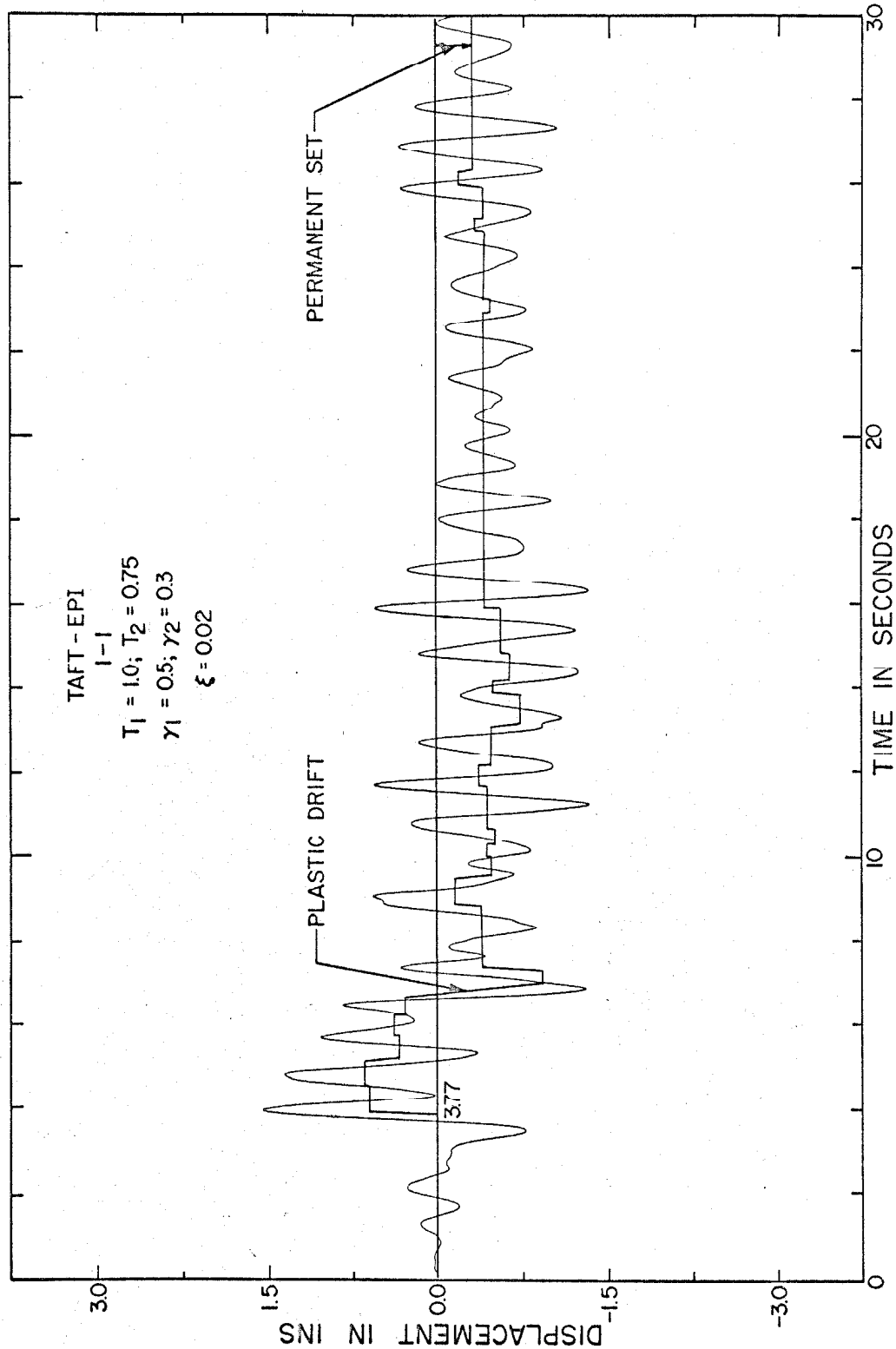


FIG. 5.4 DISPLACEMENT-TIME RESPONSE FOR ELASTO-PLASTIC BEHAVIOR WITH INTERACTION

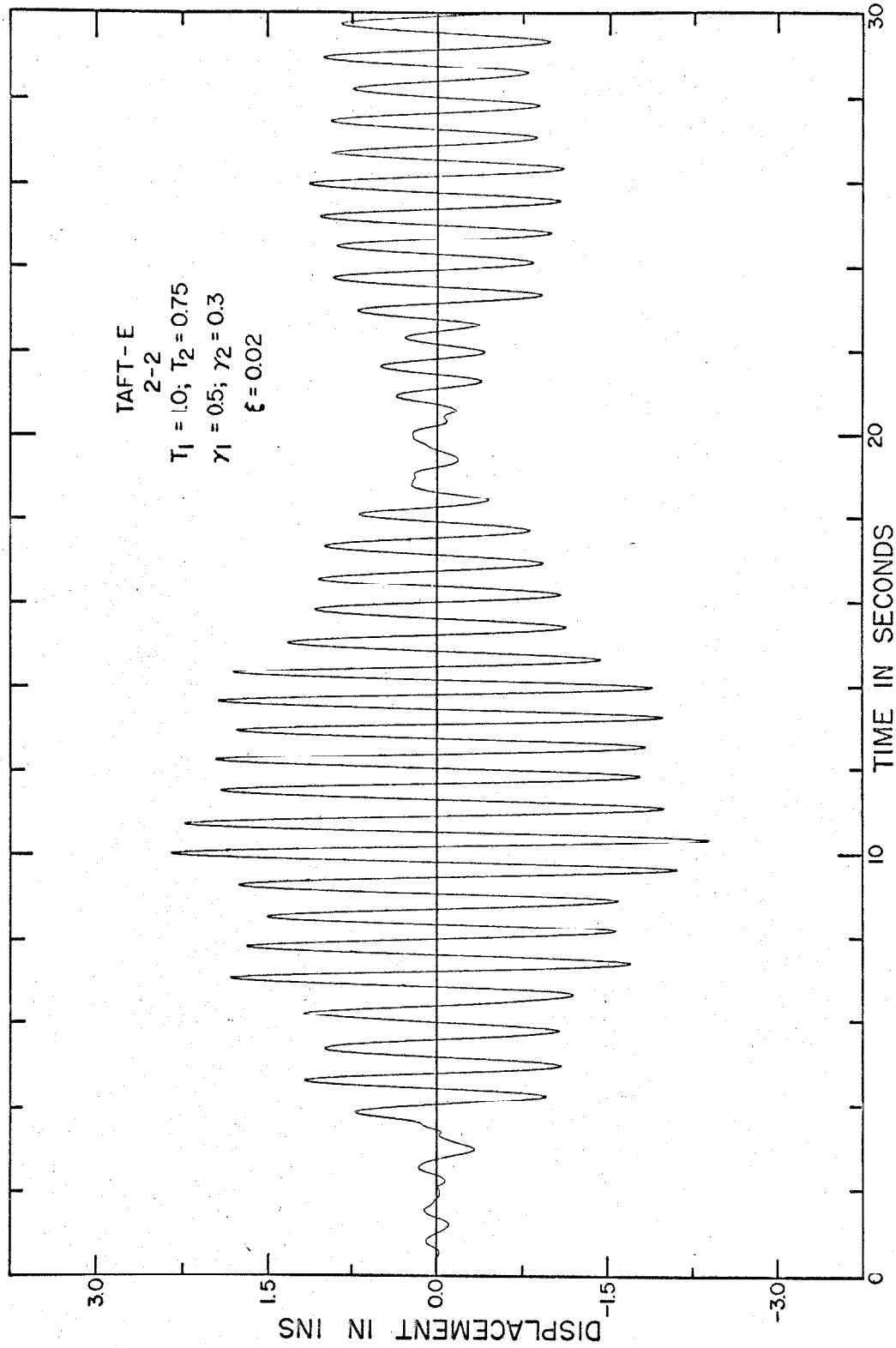


FIG. 5.5 DISPLACEMENT-TIME RESPONSE FOR ELASTIC BEHAVIOR

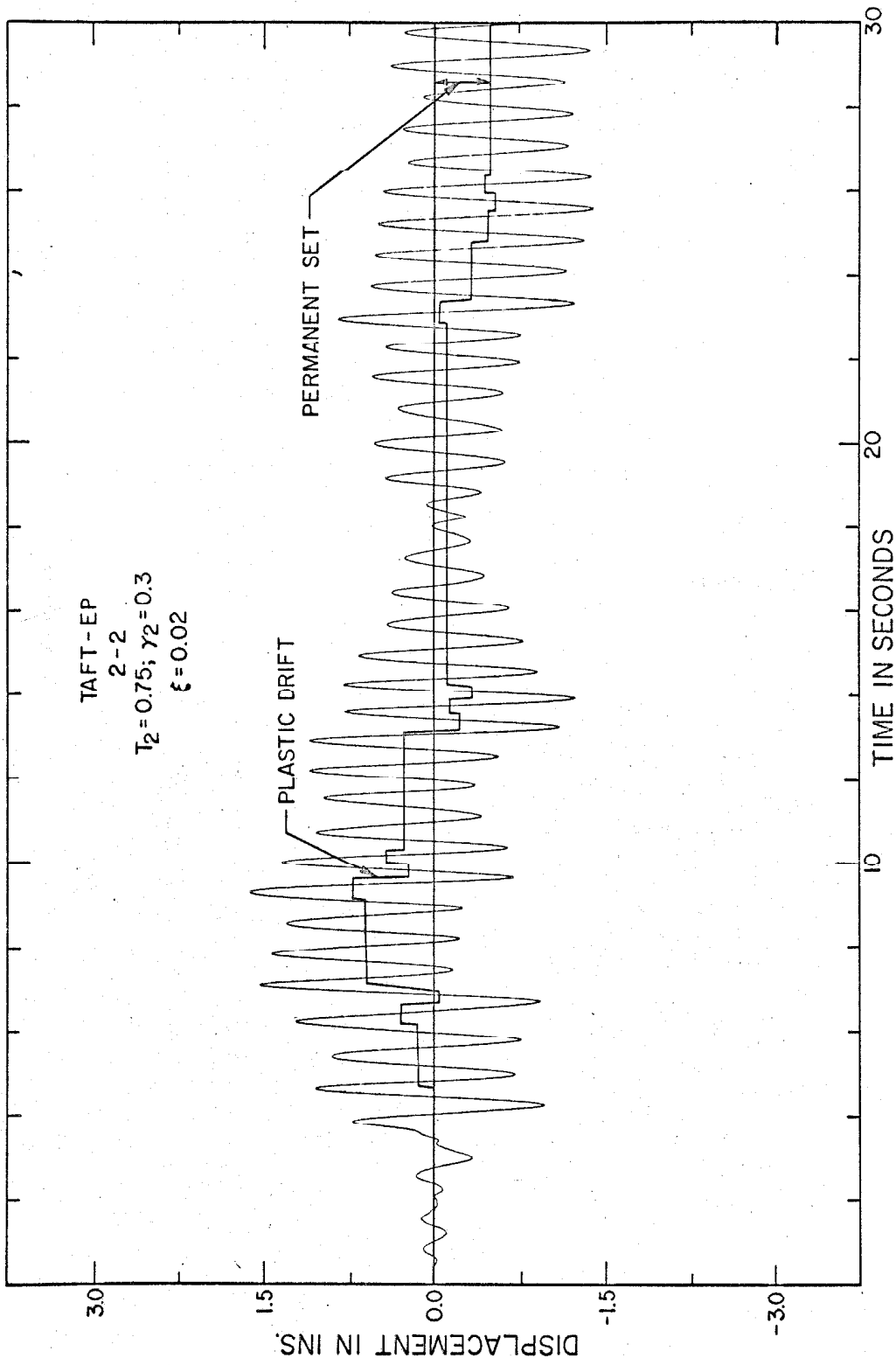


FIG. 5.6 DISPLACEMENT-TIME RESPONSE FOR ELASTO-PLASTIC BEHAVIOR

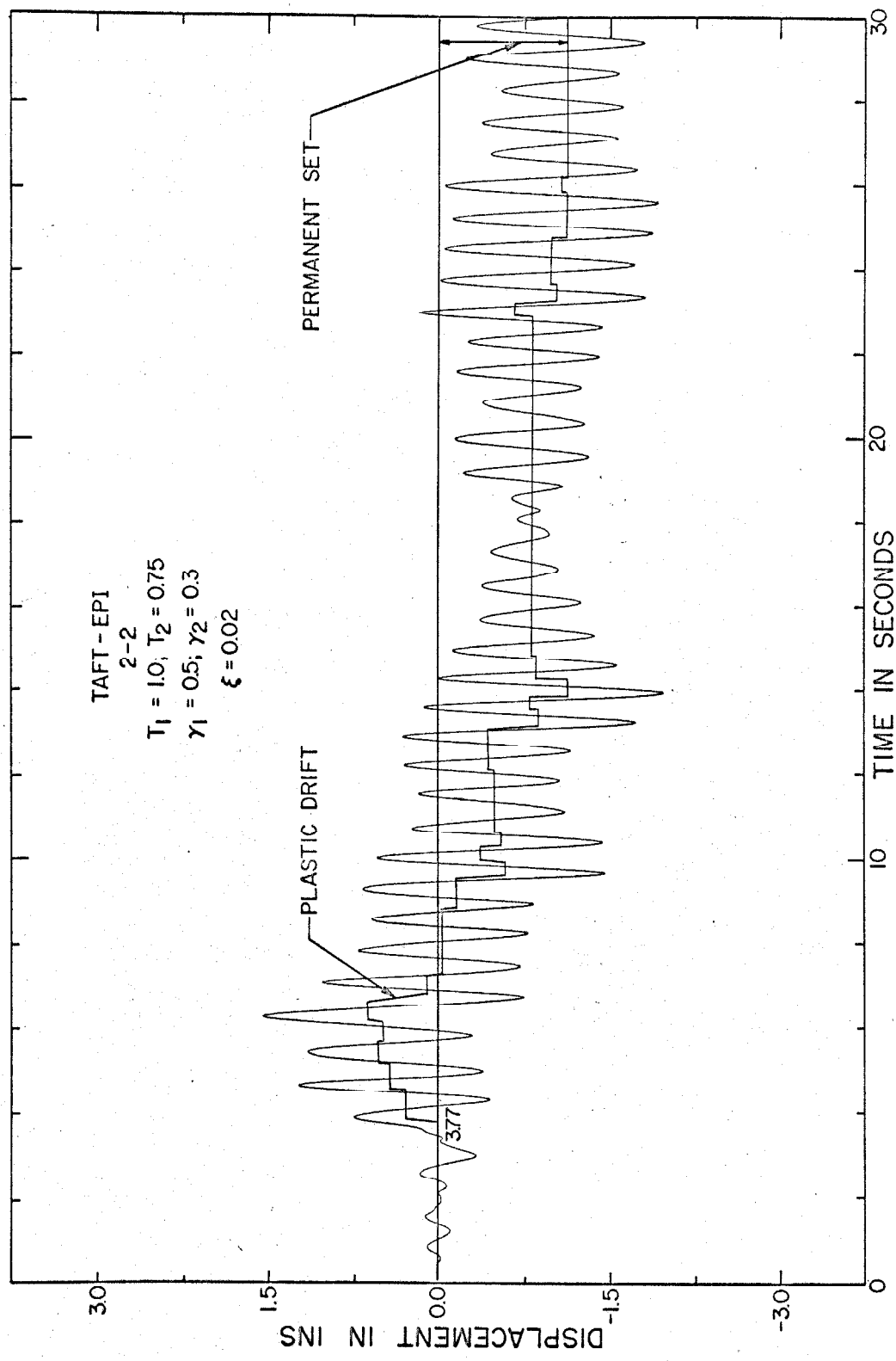


FIG. 5.7 DISPLACEMENT-TIME RESPONSE FOR ELASTO-PLASTIC BEHAVIOR WITH INTERACTION

with interaction. The plastic drift of the frame during yielding is also indicated on these figures. Comparison of these figures shows the following features of the response.

1. The response for elasto-plastic and elasto-plastic behavior with interaction is considerably smaller and much more uniform than the response for elastic behavior. This shows the effectiveness of yielding in reducing the response of structures. Careful comparison of the responses with and without interaction shows that interaction leads to smaller and more uniform response.
2. The oscillatory part of the response for elasto-plastic and interactive elasto-plastic behavior is quite similar but the drift pattern is very different. For response with interaction, yielding occurs at lower force levels and therefore increment in plastic drift occurs many more times than during the response without interaction.
3. The maximum displacement during an earthquake depends both on the plastic drift and on the oscillatory part of the response. Since the drift patterns for response with and without interaction are so different, any estimates of the maximum displacement obtained for the two cases can be very different, in spite of the fact that oscillatory parts of the response are quite similar. This shows the extent of randomness and significance of interaction in the estimates of maximum displacement. This fact is of interest because the ductility ratio, which is the ratio of maximum

displacement to yield displacement, has been suggested as a criterion for inelastic design.[10,13]

Figures 5.8 and 5.9 show the force-displacement relations for the two components of the earthquake, with and without interaction. These figures show, as already pointed out, that interaction causes plastic deformations to occur at yield levels lower than the fixed yield for elasto-plastic behavior (Fig. 5.8). Figure 5.10 shows the locus of the mass of the frame in the horizontal plane. The significant feature of this figure is the fact that large excursions of the mass occur only a few times. Similarity between this figure and the record of the seismoscopes may be noted. Figure 5.11 shows the response in force-space. It is seen that the response during yielding follows the assumed yield curve (a circle) very closely. This is an indication of the accuracy of the numerical integration.

## 5.3 Response of the Frame to the Taft Earthquake and the Ensemble of Artificial Earthquakes

In this section a discussion of the response of the frame to earthquake type excitation is presented in detail. Since the equations of motion 2.36 through 2.39 contain a large number of parameters, it was necessary to impose certain restrictions in order to limit the scope of the study. As in Chapter IV, it was decided to consider only the special case of a symmetrical frame satisfying Eqs. 4.4 and 4.5. Under these restrictions, the equations of motion are considerably simplified and are given by Eqs. 4.6 through 4.9. The response of the frame is obtained by numerical integration of these

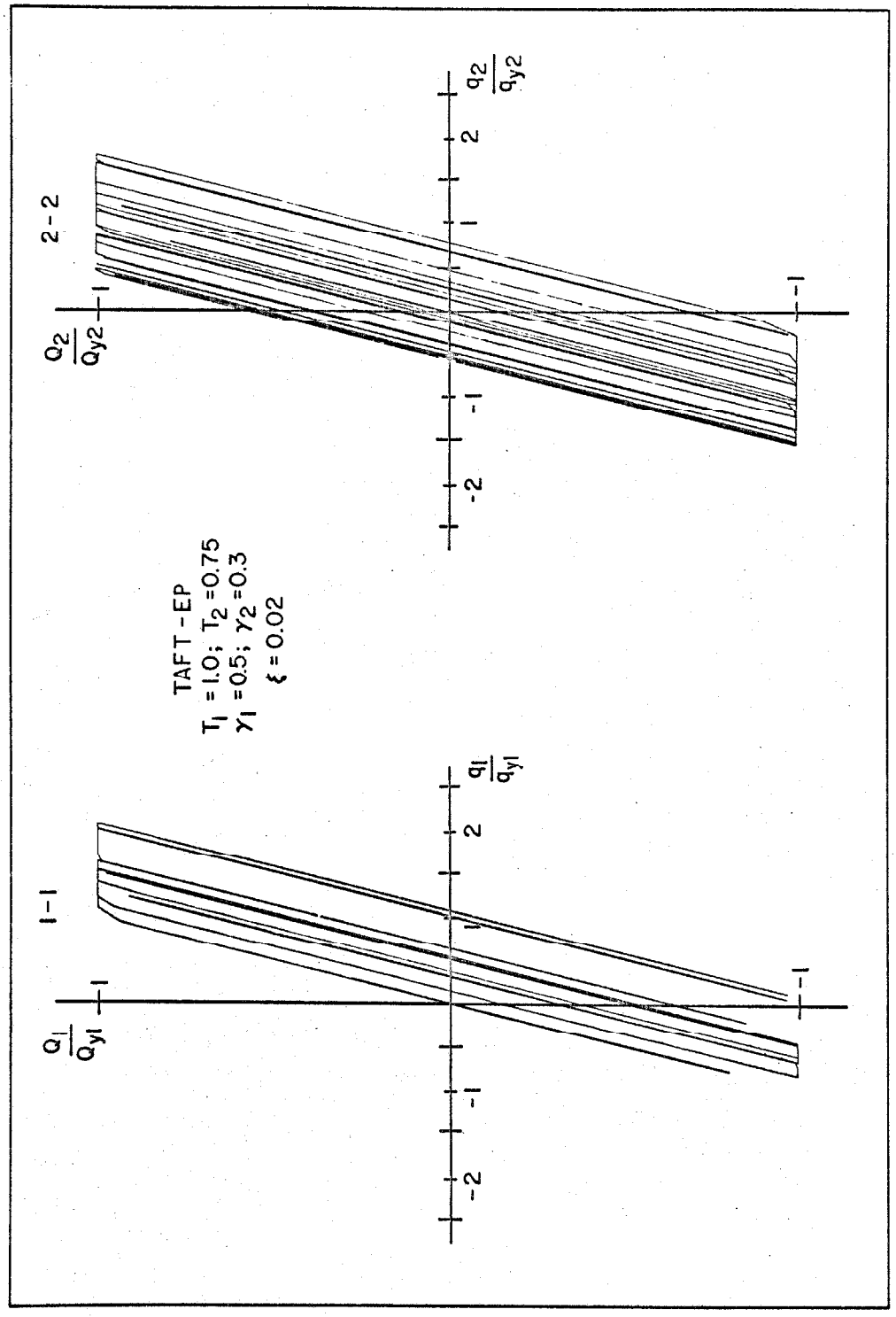


FIG. 5.8 FORCE-DISPLACEMENT RESPONSE FOR ELASTO-PLASTIC BEHAVIOR

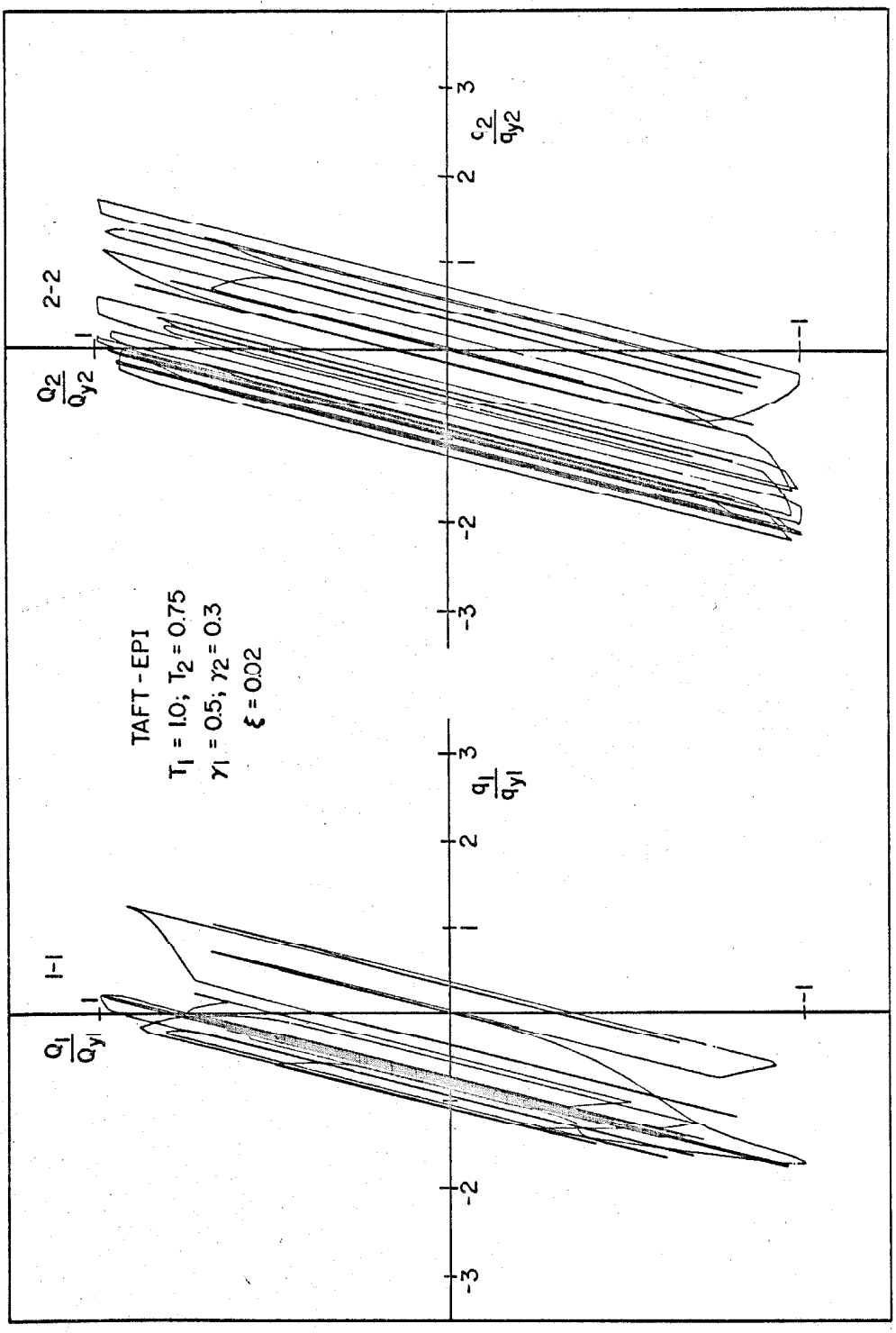


FIG. 5.9 FORCE-DISPLACEMENT RESPONSE FOR ELASTO-PLASTIC BEHAVIOR WITH INTERACTION

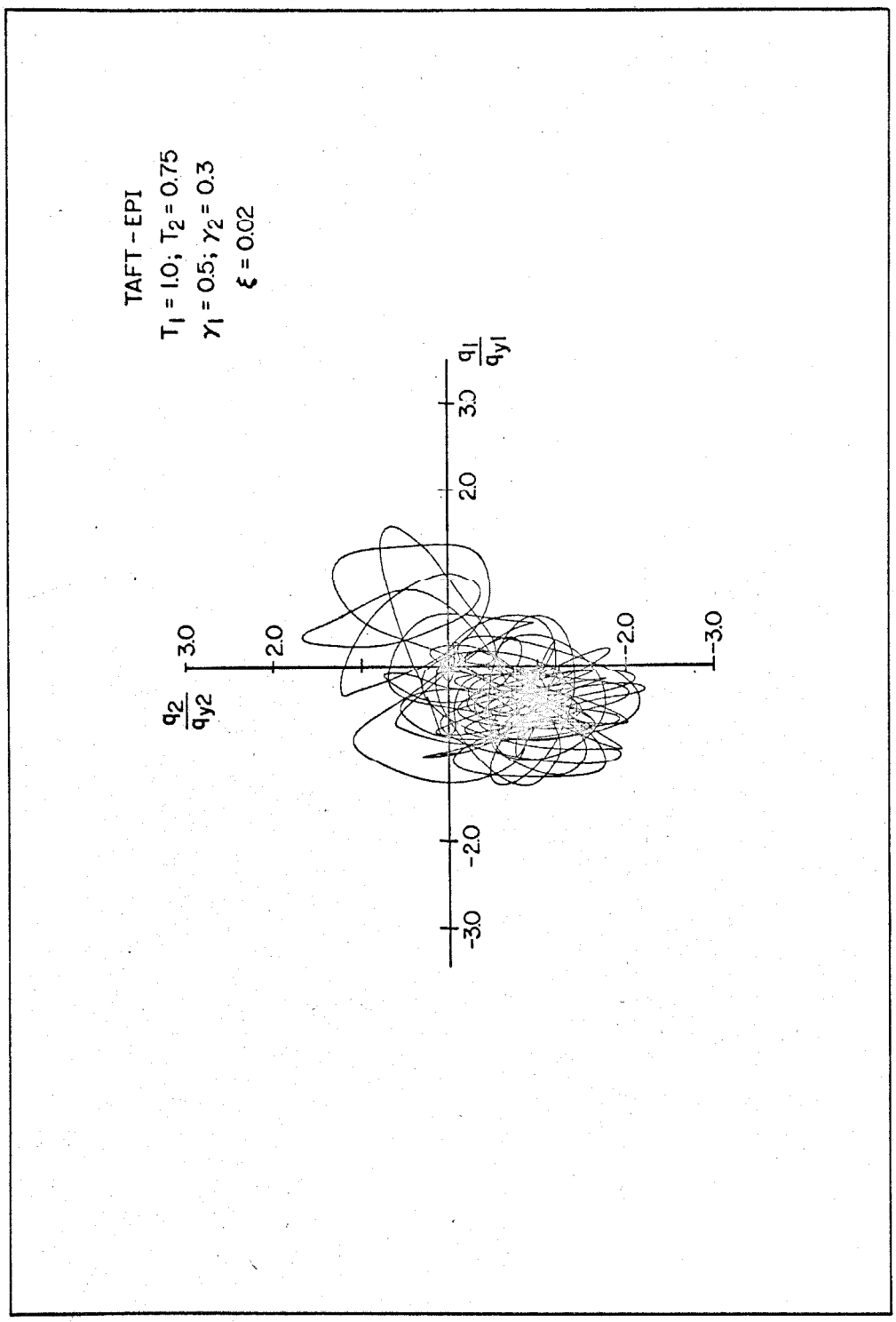


FIG. 5.10 DISPLACEMENT RESPONSE IN THE HORIZONTAL PLANE FOR ELASTO-PLASTIC BEHAVIOR WITH INTERACTION

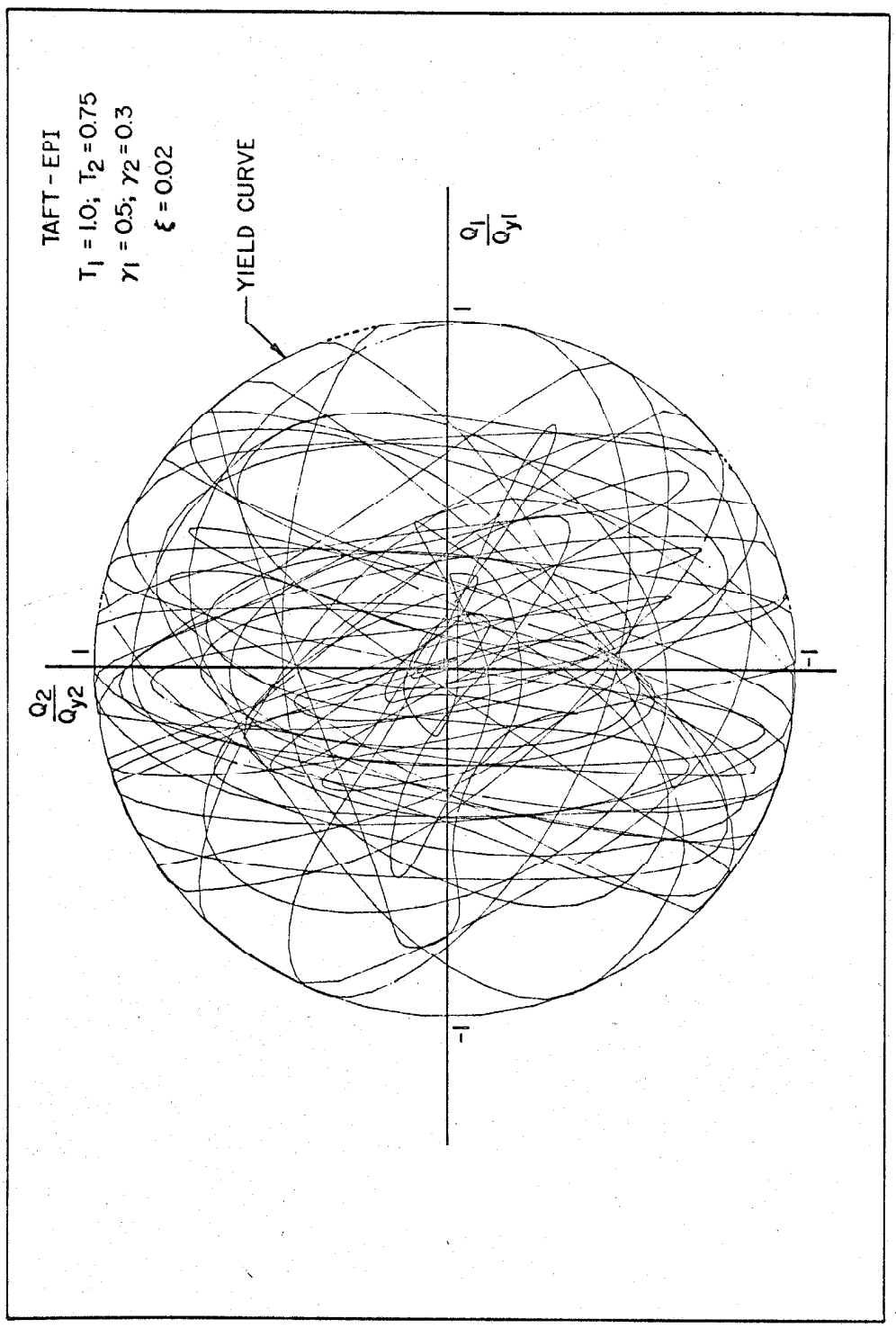


FIG. 5.11 RESPONSE IN THE FORCE-SPACE FOR ELASTO-PLASTIC BEHAVIOR WITH INTERACTION

equations, and curves showing energy input, velocity, displacement, and permanent set are plotted for each case. The special features of these curves are discussed towards the end of the section.

## The Earthquakes

The particulars of the Taft earthquake record and the artificial earthquakes used in this study are shown in Table I. The horizontal components of the ground acceleration recorded during the Taft earthquake are shown in Fig. 5.1. This earthquake record was digitized at the University of Michigan. The artificial earthquakes were generated by Jennings.[16]

## Choice of Parameters

As already pointed out, the discussion in this study is restricted to frames with identical properties along two principal directions, so that $T_1 = T_2$ and $Q_{y1} = Q_{y2}$. The response of the frame to the Taft earthquake has been obtained for seven values of natural period, $T_1 = T_2 = 0.25$, 0.5, 0.75, 1.0, 1.5, 2.0 and 2.5 seconds; and three values of the fraction of critical damping, $\xi = 0.0$, 0.02 and 0.05. The choice of small damping values was made in view of the fact that modern framed structures tend to possess a small amount of damping.[44]

The yield strength of the frame is characterized by the yield accelerations $a_{y1}$ and $a_{y2}$, which represent the acceleration values at which yielding occurs independently in the directions 1-1 and 2-2 respectively. Three values of yield acceleration, $a_{y1} = a_{y2} = 0.247\,g$,

Table I

PARTICULARS OF THE TAFT AND THE ARTIFICIAL EARTHQUAKES

| Sl. No. | Name of the Earthquake | Component/ Number | Duration secs. | Time Step secs. | r.m.s. $ft/sec^2$ | Remarks |
|---|---|---|---|---|---|---|
| 1 | Taft, Calif. July, 1952 | S69E | 30 | 0.02 | 1.134 | Digitized at the University of Michigan |
| | | N21E | 30 | 0.02 | 1.117 | |
| 2 | Artificial Earthquakes | 1 | 30 | 0.025 | 0.665 | Generated by Jennings[16] |
| | | 2 | 30 | 0.025 | 0.684 | |
| 3 | | 3 | 30 | 0.025 | 0.698 | |
| | | 4 | 30 | 0.025 | 0.734 | |
| 4 | | 5 | 30 | 0.025 | 0.689 | |
| | | 6 | 30 | 0.025 | 0.709 | |
| 5 | | 7 | 30 | 0.025 | 0.700 | |
| | | 8 | 30 | 0.025 | 0.694 | |

0.099 g and 0.049 g, have been chosen to cover the range of values likely to occur in properly designed real structures. For the Taft earthquake record of 30 second duration these values correspond to acceleration ratios $\gamma_1 = \gamma_2 = 0.2$, 0.5 and 1.0 respectively. The parameter "acceleration ratio" was introduced by Jennings[16] as the ratio of the r.m.s. value of each component of ground acceleration $(\hat{\ddot{z}}_i)$ to the yield acceleration along that component. In this study the acceleration ratio is defined as the ratio of the r.m.s. value of the ground acceleration vector $(\hat{\ddot{z}})$, which is independent of direction, to the yield acceleration of the structure along a particular direction. The acceleration ratio is a measure of both the strength of the earthquake and yield strength of the structure. It is clear from Eqs. 2.36 through 2.39 and Eq. 5.4 that doubling the strength of the earthquake will produce the same response in terms of $u_i$ $(= q_i/q_{yi})$ as if the yield level had been halved. This permits a more general interpretation of the response and is found to be very convenient in establishing design criteria, as will be shown later.

In this study, the strength of an earthquake is characterized by the r.m.s. value. Since the nature of ground motion during an earthquake is a non-stationary random process, the r.m.s. value is only a partial index of the characteristics of an earthquake. It is known that two earthquakes with the same r.m.s. value may produce widely different response in the same structure. In view of this, it is not meaningful to draw any general conclusions on the basis of a response obtained for a single earthquake. To deal with this prob-

lem, Jennings[16] developed an ensemble of artificial earthquakes, each member of which is a sample of a stationary process, with statistical properties, similar to those of recorded strong-motion earthquakes. By the use of suitable scale factors an ensemble of these earthquakes can be made to match the r.m.s. value of any particular earthquake. The scale factors for the four strong-motion earthquakes, which were used to generate these earthquakes, have been given by Jennings.[16] Using an ensemble of these earthquakes, it is possible to obtain average values and deviations about them of various response parameters and to draw conclusions about the behavior of structures during an earthquake, with some measure of confidence.

For this purpose, eight artificial earthquakes have been used to form an ensemble of four pairs of earthquakes representing the horizontal components of ground acceleration. To match the Taft earthquake (duration 30 seconds), the artificial earthquakes have been multiplied by a scale factor of 1.61, based on the ratio of average r.m.s. of the Taft earthquake to the average r.m.s. of the ensemble. The response of the frame to this ensemble of earthquakes has been obtained for the case having $\gamma_1 = \gamma_2 = 0.6$ and $\xi = 0.02$. The average values and scatter have been computed for each response parameter. The response for the Taft earthquake is compared with the response for the ensemble of artificial earthquakes.

Discussion of Results

The response of the frame to the Taft earthquake and to an ensemble of four pairs of artificial earthquakes is shown in Figs. 5.12 through 5.33. These figures show the variation of energy input, maximum velocity, maximum displacement, and permanent set against the natural period of the frame, for elastic, elasto-plastic and elasto-plastic behavior with interaction. The effect of interaction on each of these response parameters is discussed below.

Energy input and energy loss

Figures 5.12, 5.13 and 5.14 show the variation of the ratio of total energy input to the elastic energy capacity of the frame against its natural period for elasto-plastic and elasto-plastic behavior with interaction. Total energy denotes the sum of the energy input along directions 1-1 and 2-2 and these figures indicate the amount of energy that must be dissipated by the frame through damping and yielding. It is seen from these curves that interaction has the effect of decreasing the energy input to the frame. For $\gamma = 1.0$ and $\xi = 0.0$ the decrease is up to 30 per cent of the energy input without interaction. For lower values of $\gamma$, the reduction in energy input slowly decreases, which must be expected since lower values of $\gamma$ means less yielding. The curves are drawn for three values of damping and it is seen that the increase in damping causes, in general, a small increase in the energy input. It is also seen that decrease in energy input due to interaction is slightly reduced as damping increases.

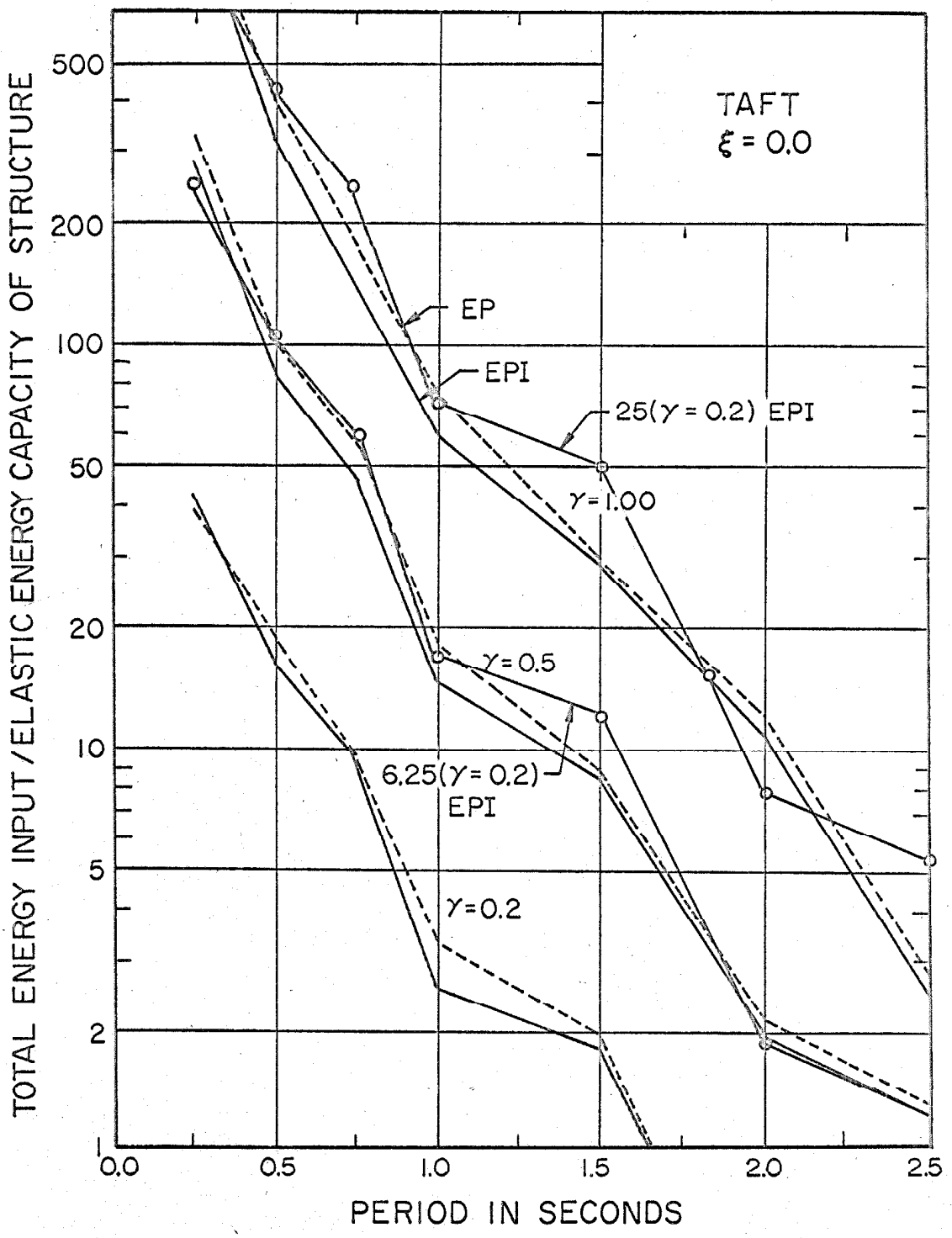


FIG. 5.12 TOTAL ENERGY INPUT SPECTRA

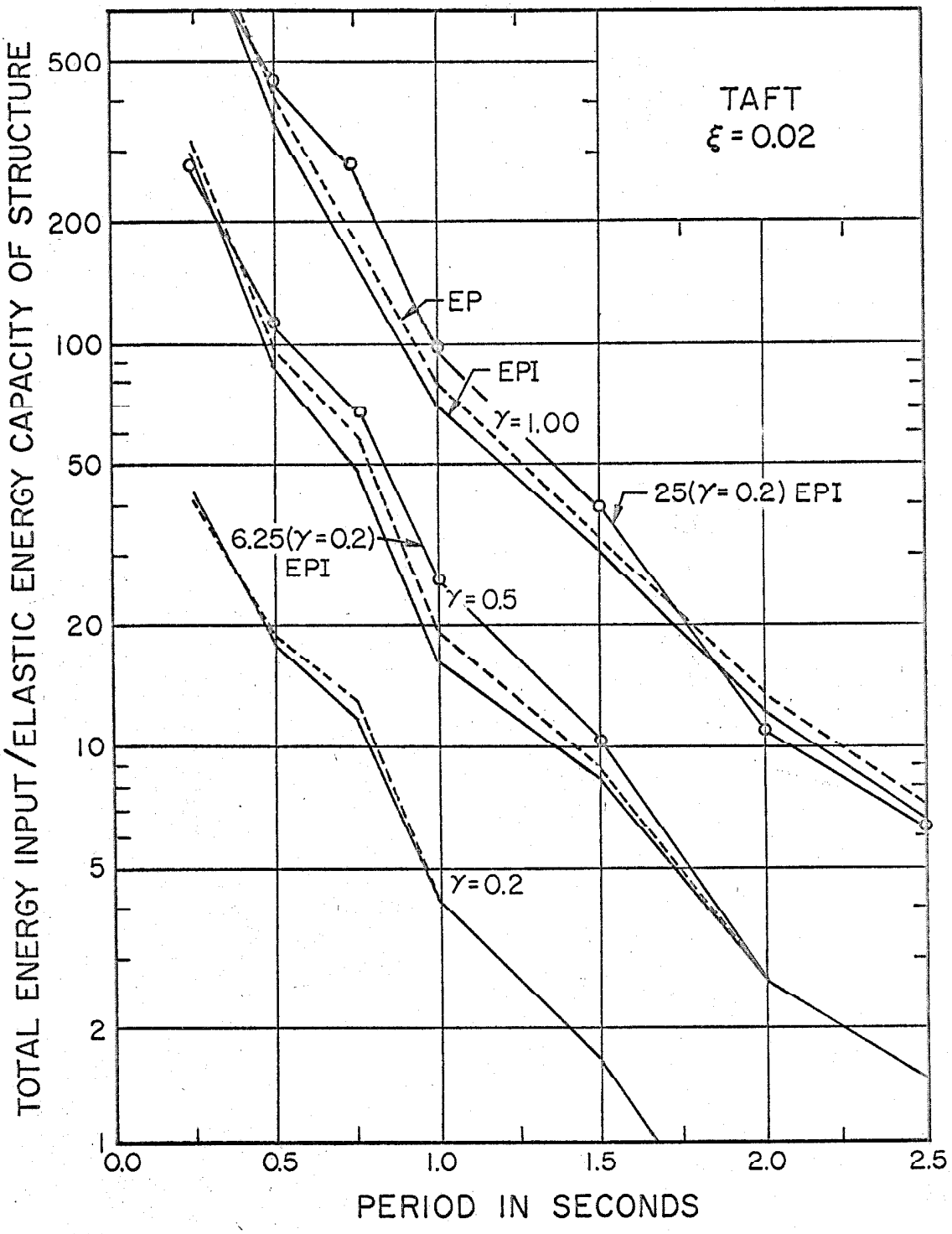


FIG. 5.13 TOTAL ENERGY INPUT SPECTRA

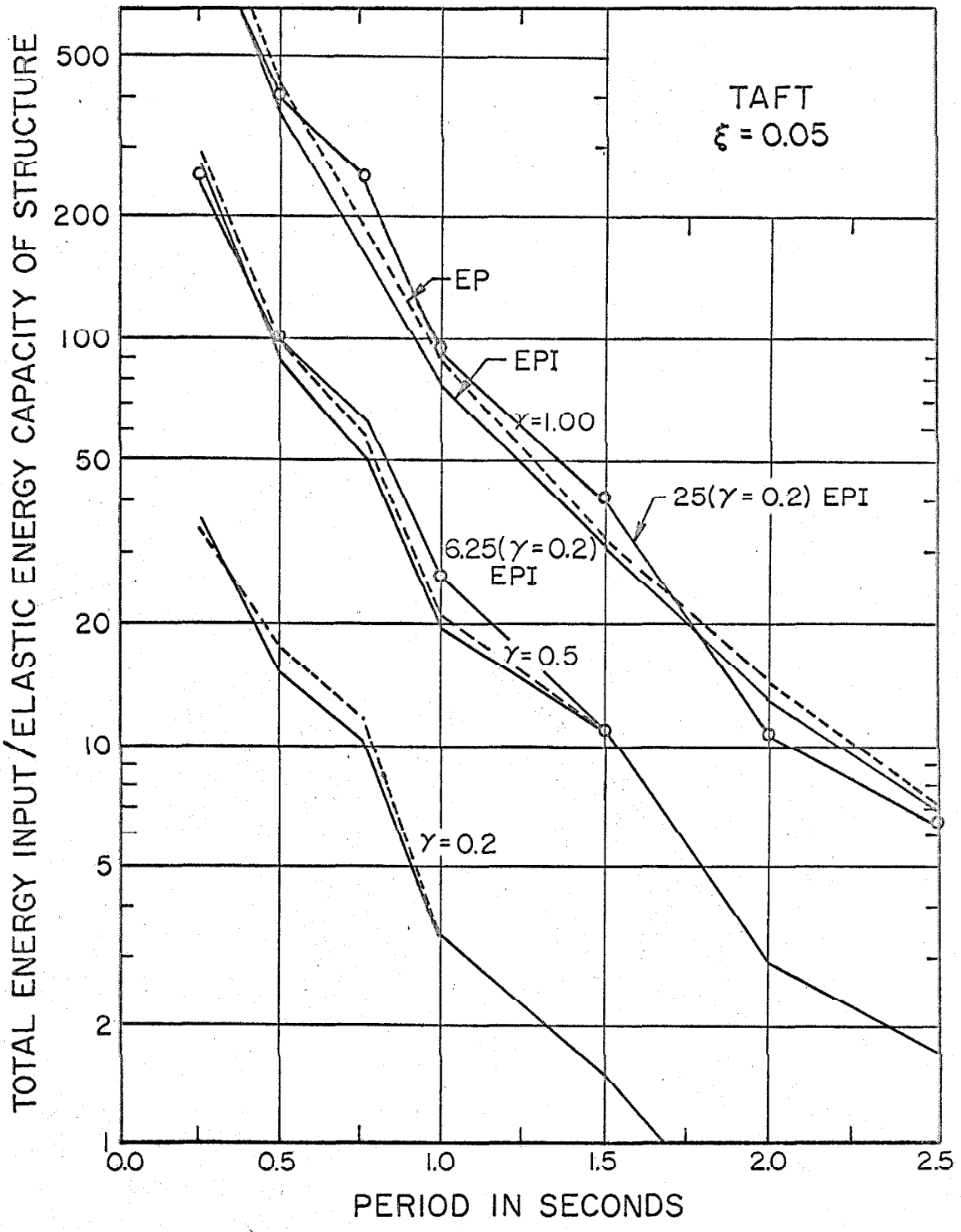


FIG. 5.14 TOTAL ENERGY INPUT SPECTRA

For an elastic frame, multiplying $\gamma$ by a numerical factor n would increase the energy input to the frame $n^2$ times and an interesting comparison is made by multiplying the energy input ratio, for $\gamma = 0.2$, by 6.25 and 25 and comparing it with the energy input ratio for $\gamma = 0.5$ and 1.0 respectively. Curves obtained by multiplying the $\gamma = 0.2$ curve by 6.25 and 25 are shown in Figs. 5.12, 5.13 and 5.14. It is seen that these curves lie, in general, above the actual curves. The actual energy input is seen to be less than the energy input deduced from the $\gamma = 0.2$ curve up to 50 per cent for $\gamma = 1.0$ and 30 per cent for $\gamma = 0.5$. This shows that the energy input to a structure decreases as its yield strength is decreased. It may be pointed out here that Berg[6] found the same behavior for elasto-plastic structures, but Jennings[16] found that for general yielding structures, such a decrease is very small. This fact is of interest in Housner's method of limit design.[7]

Figure 5.15 shows the average energy input curves for elastic, elasto-plastic and elasto-plastic behavior with interaction obtained from the ensemble of artificial earthquakes. The range of energy input for elasto-plastic response with interaction is shown as the shaded area. These curves show that yielding has the effect of decreasing the energy input and interaction decreases it still further. It may be noted that the order of decrease for the ensemble average and for the Taft earthquake is about the same but it is more uniform for the former. It is seen that for $T_1 = T_2 < 0.75$, the energy input curve for elasto-plastic behavior lies outside of the range of the

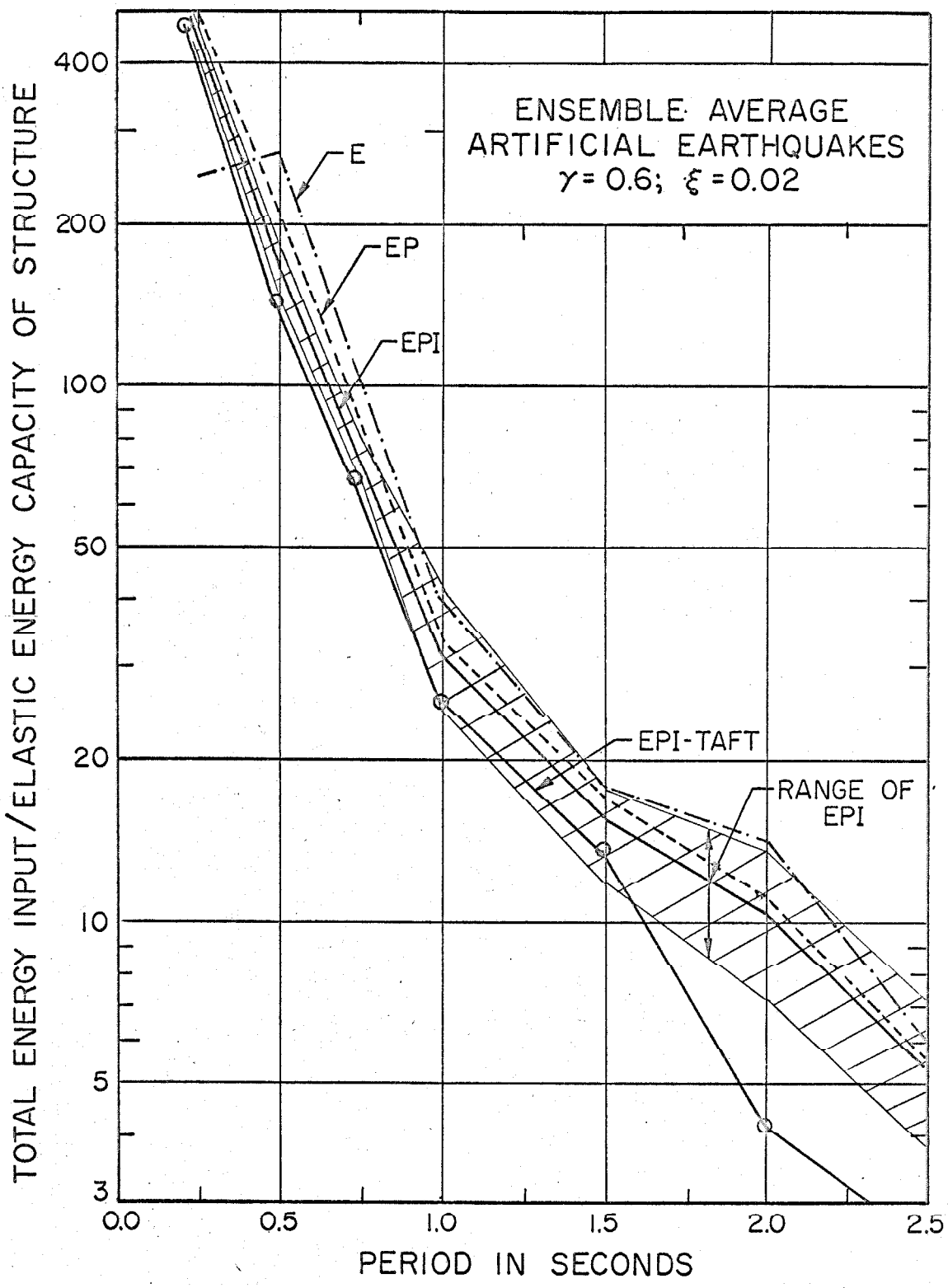


FIG. 5.15 AVERAGE OF TOTAL ENERGY SPECTRA AND RANGE

curves for elasto-plastic behavior with interaction. In this region, therefore, the effect of interaction is more meaningful.

Maximum Velocity

Curves showing the variation of maximum velocity of the frame as a function of its natural period are shown in Figs. 5.16 through 5.19 for the Taft earthquake and the ensemble of artificial earthquakes. It is seen from these curves that yielding reduces the velocity and interaction reduces it still further. It may also be noted from these curves that yielding is more effective in reducing the velocity for low values of period than for higher values. This is due to the fact that as the natural period of a structure decreases its response has greater number of peaks, and yielding occurs more often.

The Ductility Ratio

The ratio of the maximum displacement to the yield displacement in the response of a simple oscillator subjected to earthquake type excitation has been defined[10] as the ductility ratio. If the vibration of a structure is considered independently along its principal directions, the ductility ratio is directly related to the ratio of maximum plastic strain to the yield strain (hereafter called the plastic strain ratio) for each direction and is a convenient measure of the extent of plastic deformation that may be permitted in a structure. If the vibration of the structure occurs simultaneously along the principal directions, as in the case of earthquake type

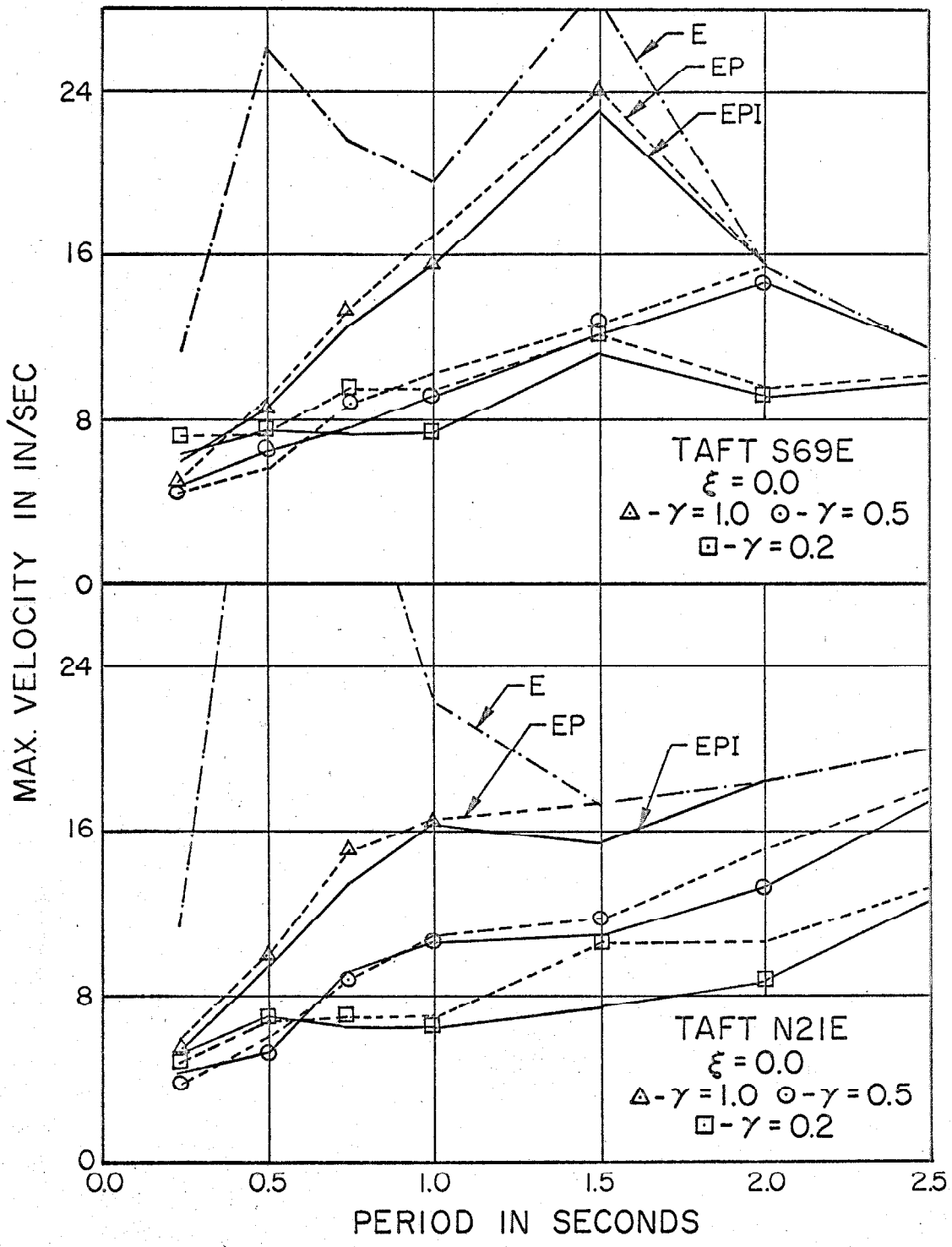


FIG. 5.16 VELOCITY SPECTRA

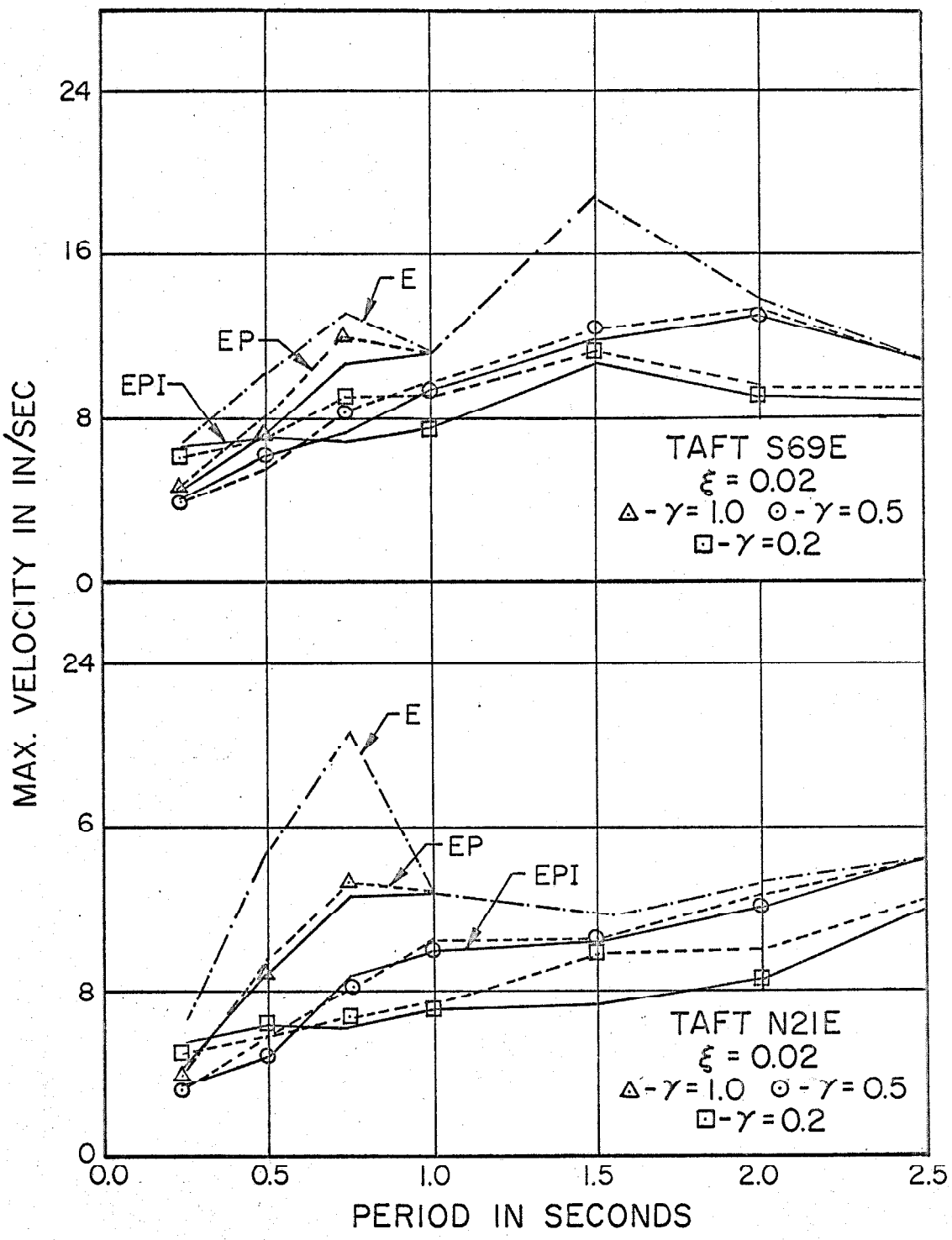


FIG. 5.17 VELOCITY SPECTRA

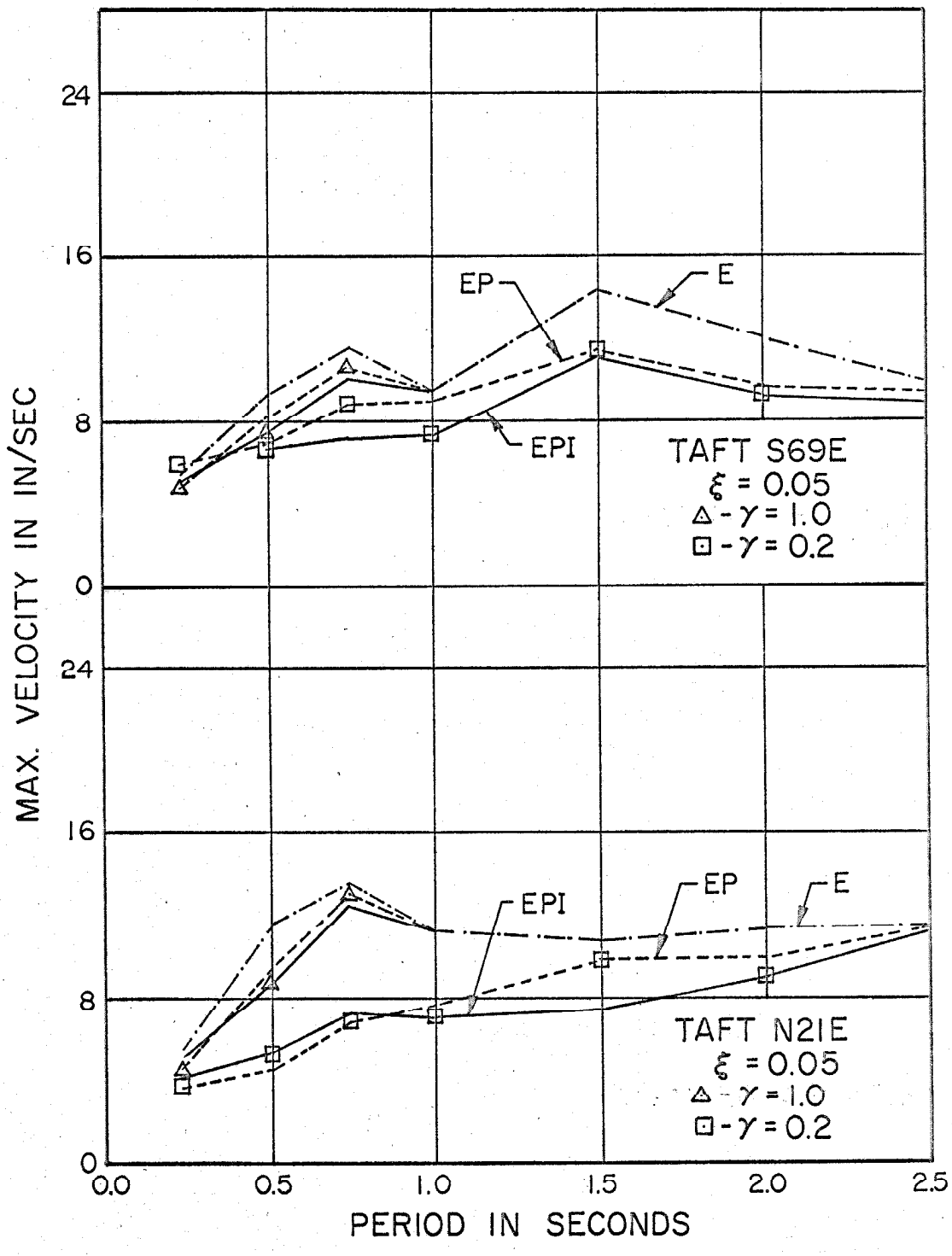


FIG. 5.18 VELOCITY SPECTRA

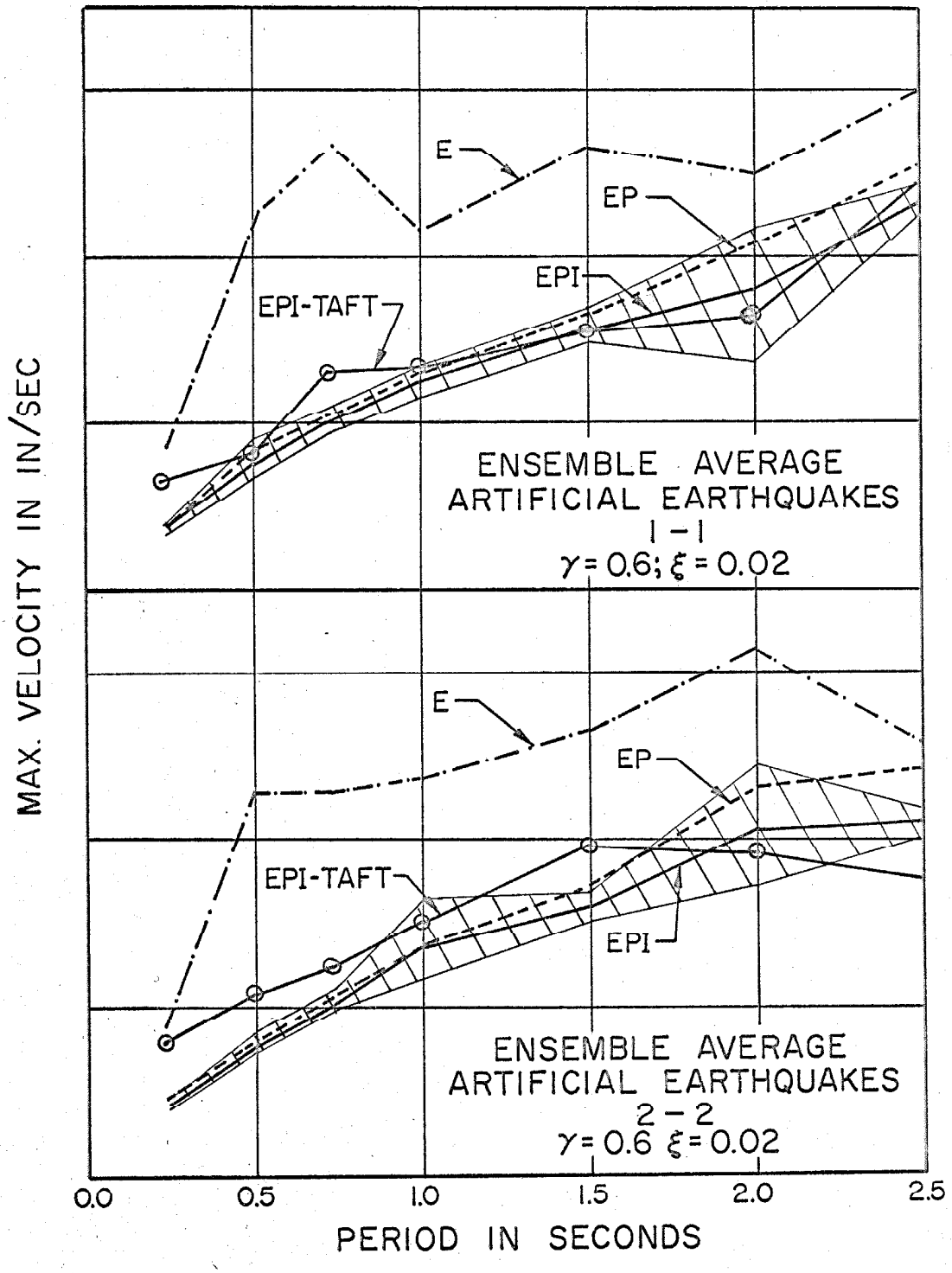


FIG. 5.19 AVERAGE OF VELOCITY SPECTRA AND RANGE

excitation, the total plastic strain ratio will depend on the displacements along both principal directions and it is clear that ductility ratios along each principal direction are not directly related to the total plastic strain ratio. If the ductility ratio along one of the principal directions is considered alone, it will underestimate the total plastic strain ratio and if the sum of the ductility ratios is considered, the total plastic strain will be overestimated. For a frame with columns of circular section, this problem can be resolved by using the ratio of maximum radial displacement and the yield displacement as a measure for plastic strain ratio. For other sections, where yield displacement varies with the direction of displacement, an average value of the yield displacement may be used to divide the maximum radial displacement.

Figures 5.20, 5.21 and 5.22 show the variation of ductility ratio (denoted by $\mu$) against the natural period of the frame. The ratio of maximum radial displacement to the yield displacement (denoted by $\mu^*$) is shown in Figs. 5.23 through 5.25 for the Taft earthquake. It is seen in these figures that the behavior of these curves is somewhat random and it is difficult to find a general trend. This is to be expected because, as pointed out in Section 5.2, the maximum displacement depends on plastic drift, which occurs in a random fashion. These curves indicate that for periods less than 0.5 seconds, interaction causes no significant difference for $\gamma = 1.0$, but for $\gamma = 0.5$ and 0.2, the ductility ratios and the ratio $\mu^*$ are considerably increased. For periods greater than 0.5 seconds,

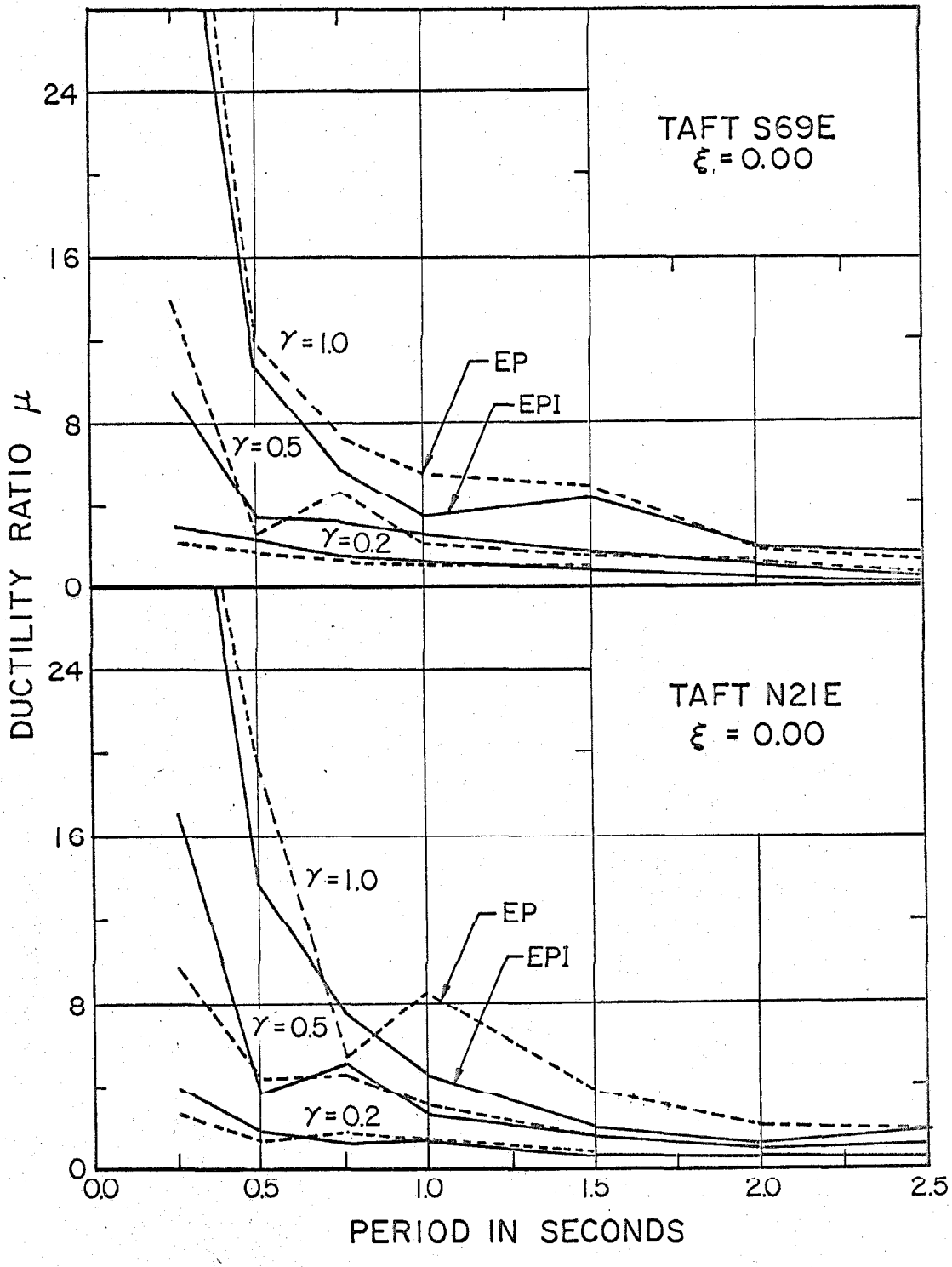


FIG. 5.20 DUCTILITY RATIO

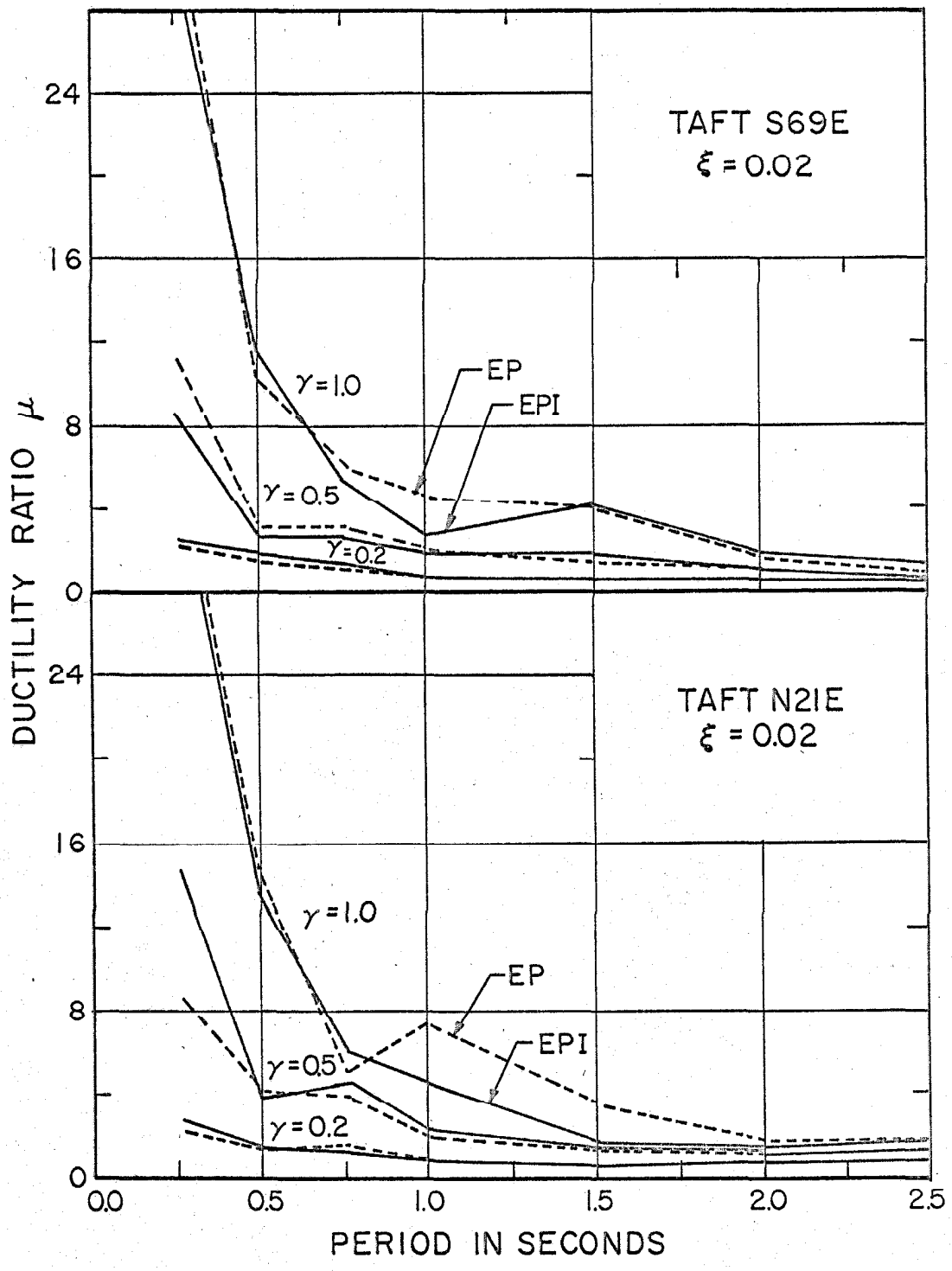


FIG. 5.21 DUCTILITY RATIO

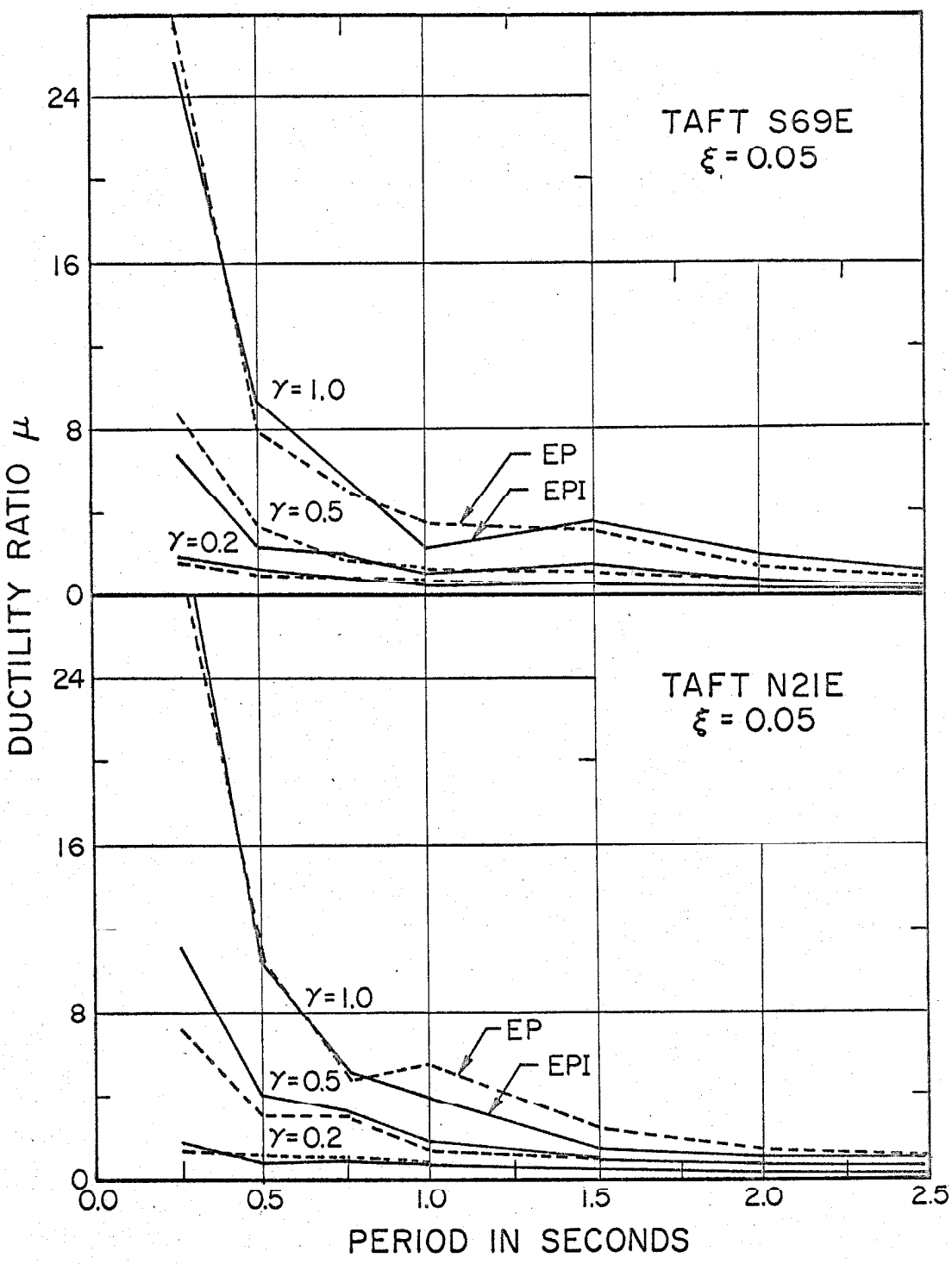


FIG. 5.22 DUCTILITY RATIO

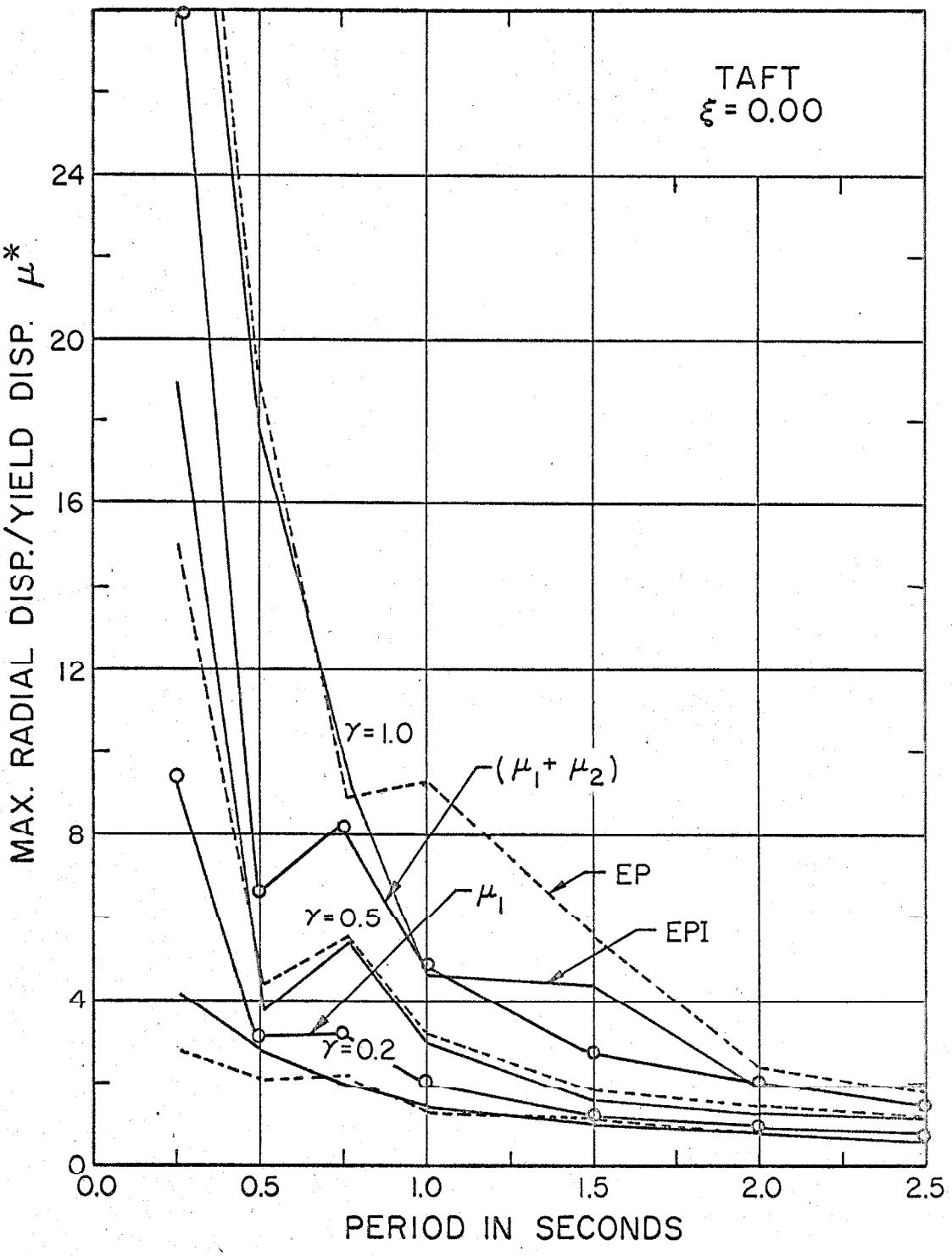


FIG. 5.23 RADIAL DISPLACEMENT SPECTRA

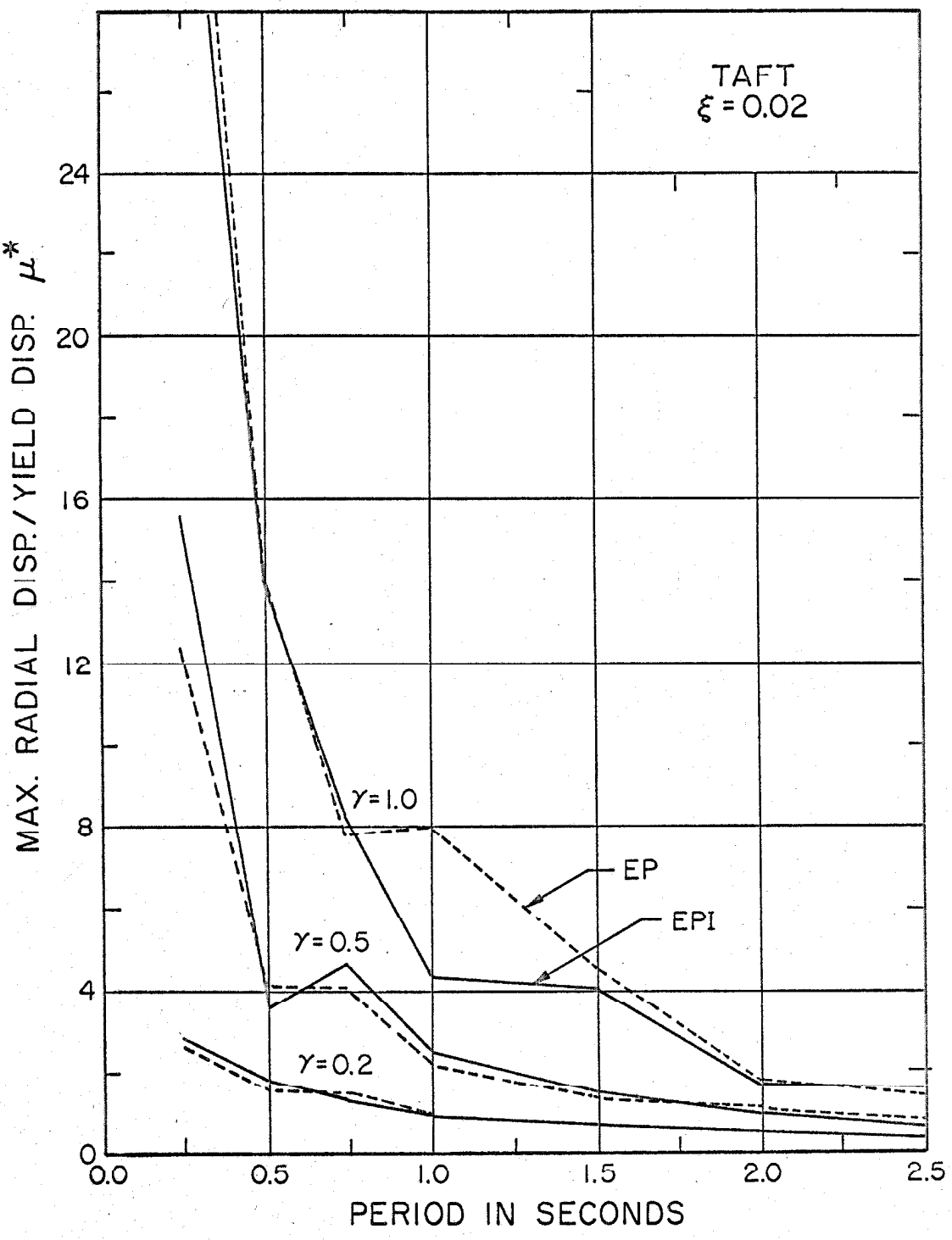


FIG. 5.24 RADIAL DISPLACEMENT SPECTRA

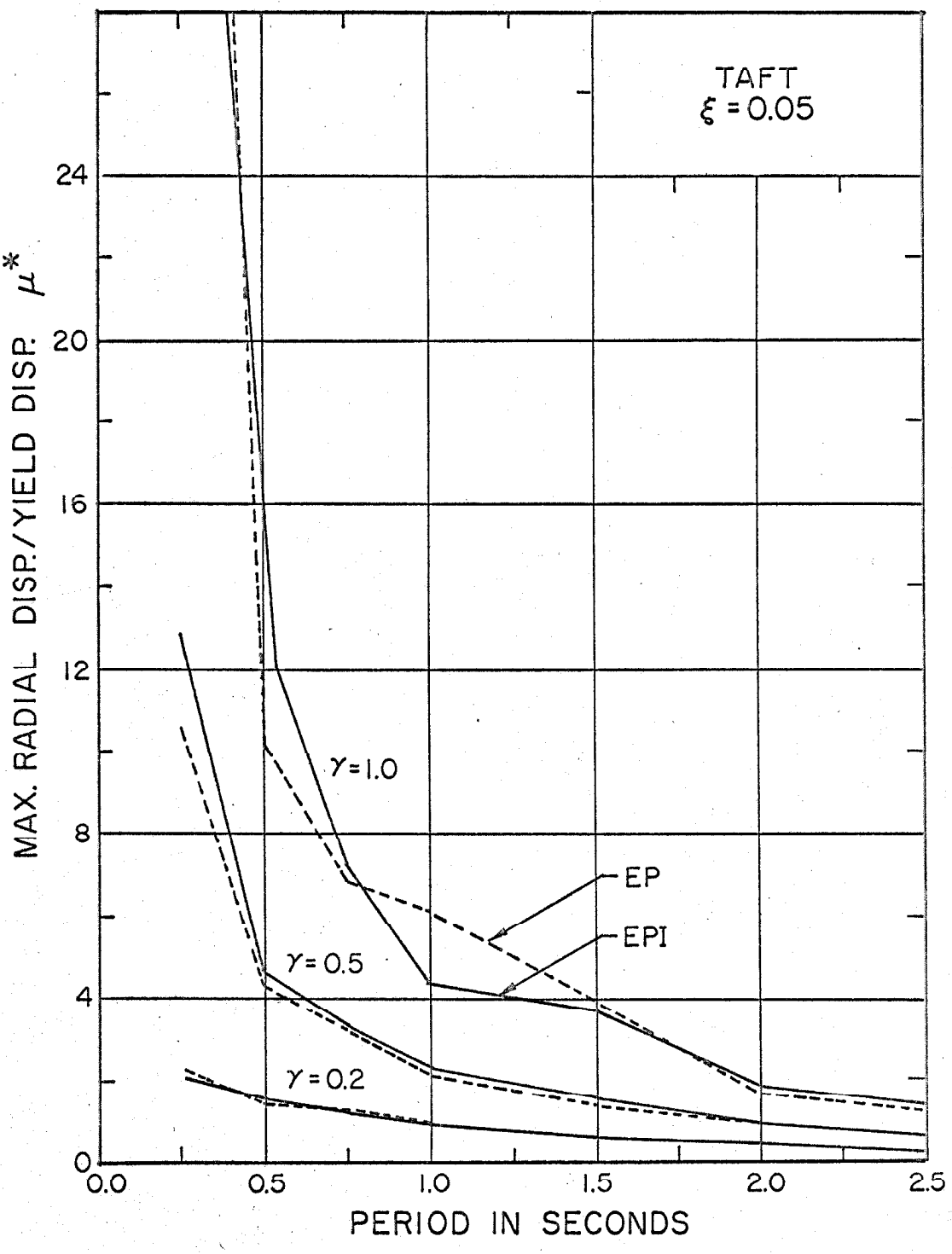


FIG. 5.25 RADIAL DISPLACEMENT SPECTRA

interaction reduces the ductility ratio and the ratio $\mu^*$ if $\gamma = 1.0$, but causes no significant change for $\gamma = 0.2$ and 0.5. In Fig. 5.23, curves for $\mu_1$ and $(\mu_1+\mu_2)$ are drawn for $\gamma = 0.5$ to see how they compare with the curve for $\mu^*$. It is seen from these curves that $\mu_1$ may underestimate the plastic strain ratio by as much as 50 per cent, whereas $(\mu_1 + \mu_2)$ may overestimate it up to 100 per cent of the actual value. Figure 5.26 shows the average curves and range for $\mu^*$. It shows that interaction increases the value of $\mu^*$ considerably for $T_1 = T_2 < 0.5$, but has very little effect for higher values of the natural periods.

Permanent Set

The permanent set is defined as the final position of equilibrium of a structure at the end of an earthquake. It was shown in Figs. 5.3, 5.4, 5.6 and 5.7 that during yielding the frame undergoes plastic drift and moves to a new position of equilibrium every time such drift occurs. The behavior during plastic drift appears to be quite random and therefore estimates of permanent set involve a large degree of uncertainty. Figure 5.27 shows the variation of permanent radial set for the Taft earthquake. It is not possible to draw any precise conclusions from these curves because of their variability. Figure 5.28 shows the average curves and the range. It is seen from these curves that interaction increases the permanent set for natural periods less than 0.5 seconds and has no significant effect for periods greater than 0.5 seconds.

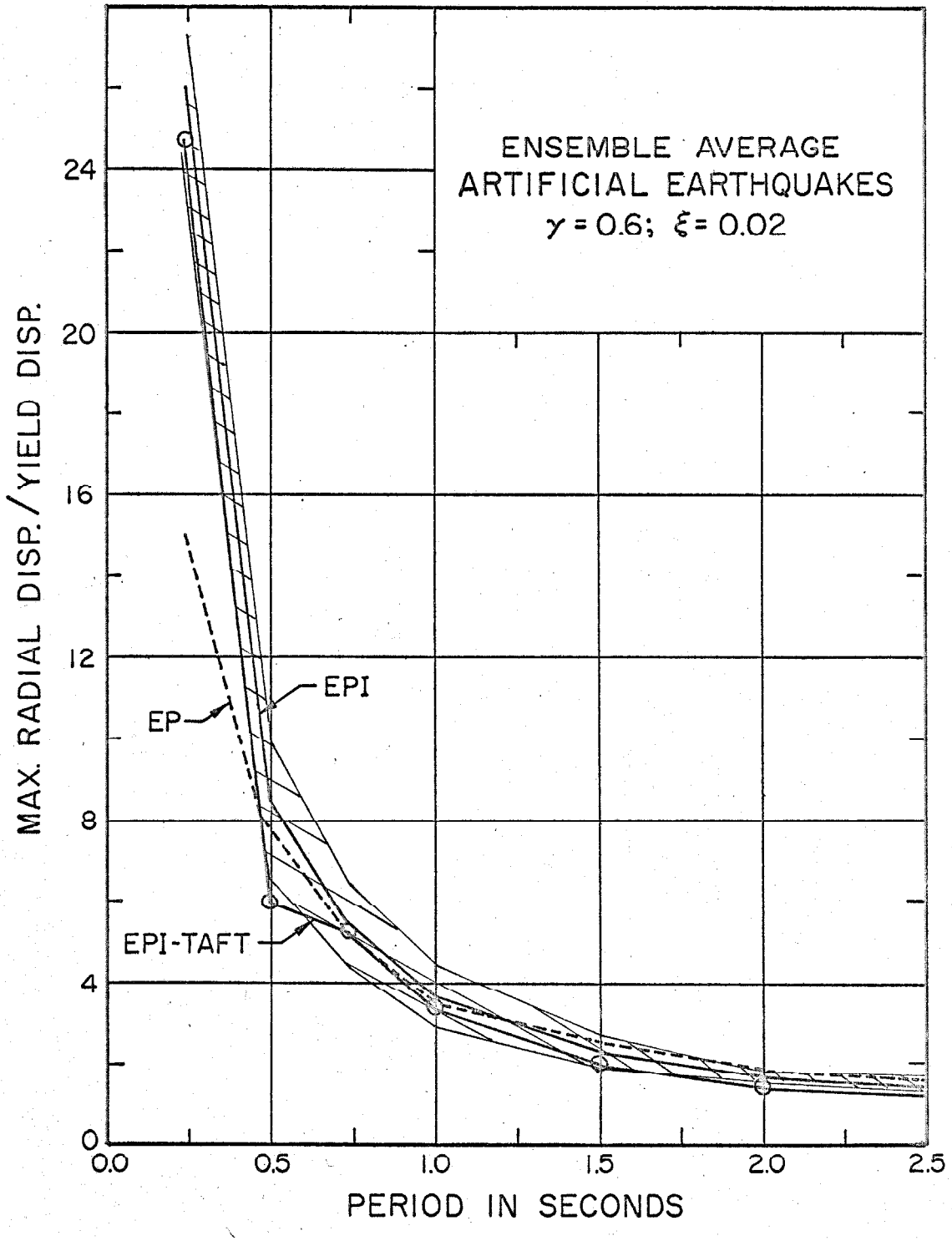


FIG. 5.26 AVERAGE OF RADIAL DISPLACEMENT SPECTRA AND RANGE

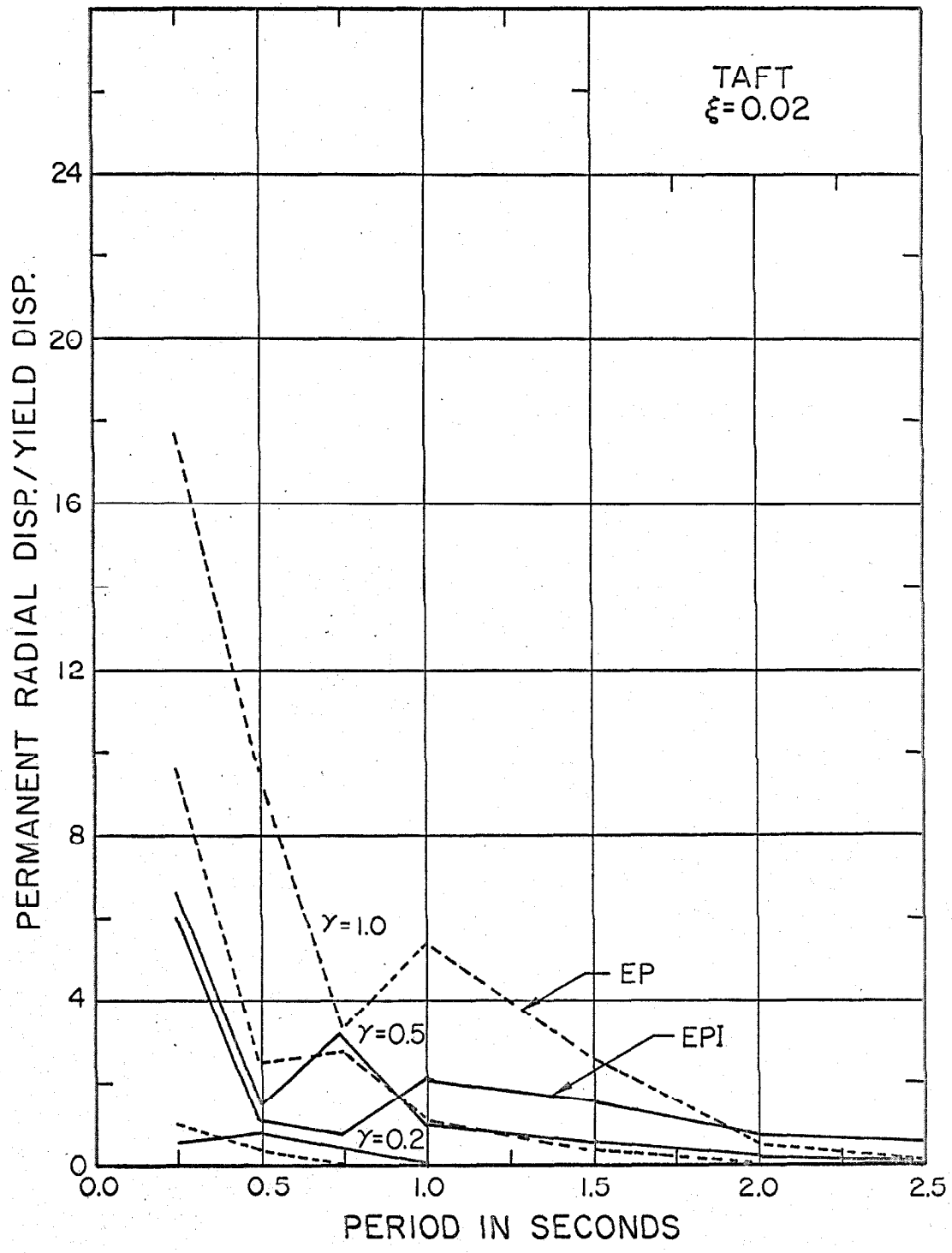


FIG. 5.27 PERMANENT RADIAL SET

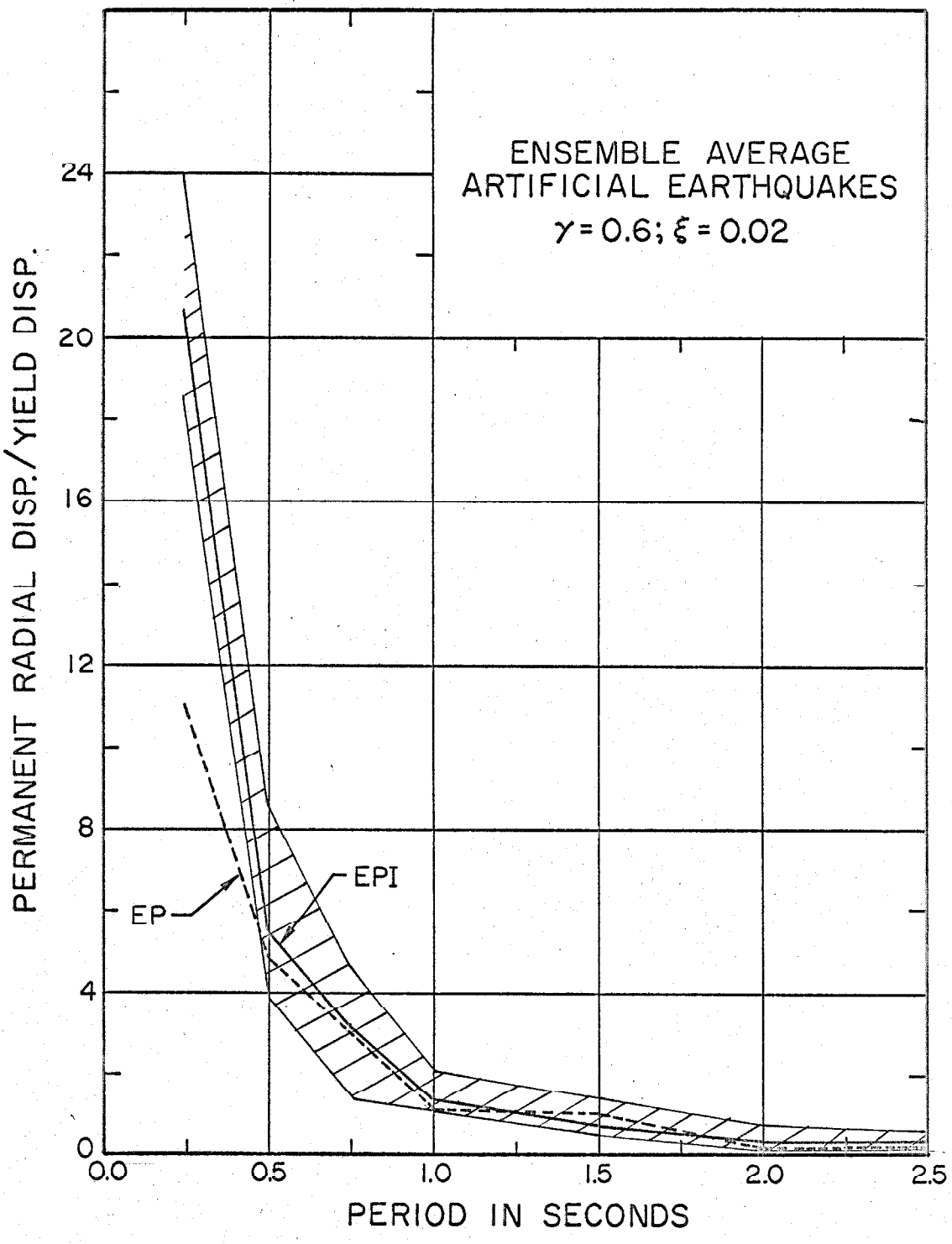


FIG. 5.28 AVERAGE OF PERMANENT RADIAL SET AND RANGE

The Shape of the Yield Curve

The response of the frame discussed so far was obtained for a circular yield curve. Figures 5.29, 5.30 and 5.31 show the response of the frame for three shapes of the yield curve. The upper bound curve represents elasto-plastic behavior without interaction. The lower bound curve permits more interaction as compared to the circular yield curve and this is reflected clearly in all three figures. It is seen that the response curves for the circular yield curve are, in general, bounded from above and below by the response curves for upper and lower bounds.

Comparison of Response for Taft Earthquake and Ensemble of Artificial Earthquakes

The response of the frame to the ensemble of artificial earthquakes was obtained after multiplying the ground acceleration values by a scale factor, so as to match the r.m.s. of the Taft earthquake. Since the artificial earthquakes were generated by obtaining the best fit on the average linear response of four strong-motion earthquakes,[16] it is of interest to see how the response of real and artificial earthquakes compare for nonlinear behavior. For this purpose, the response for the Taft earthquake has been plotted along with the curves showing the average response and range for the ensemble of artificial earthquakes. It is seen from these curves that the energy input curve (Fig. 5.15) for the Taft earthquake lies below the average input curve for all values of natural period. For values of natural period greater than 1.5 seconds, it lies outside the range of values of the ensemble. The curve for maximum radial

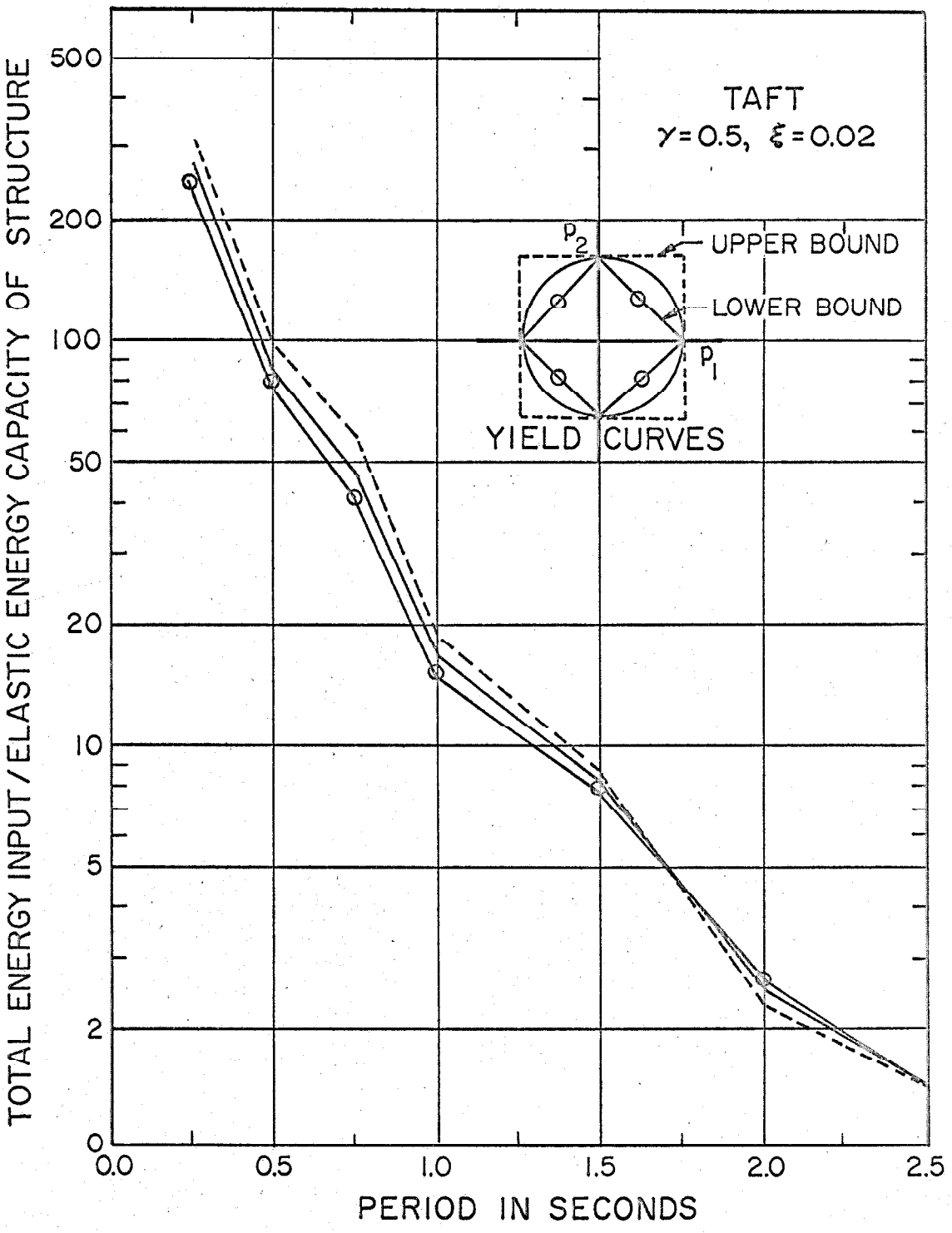


FIG. 5.29 EFFECT OF THE SHAPE OF YIELD CURVE ON TOTAL ENERGY INPUT SPECTRA

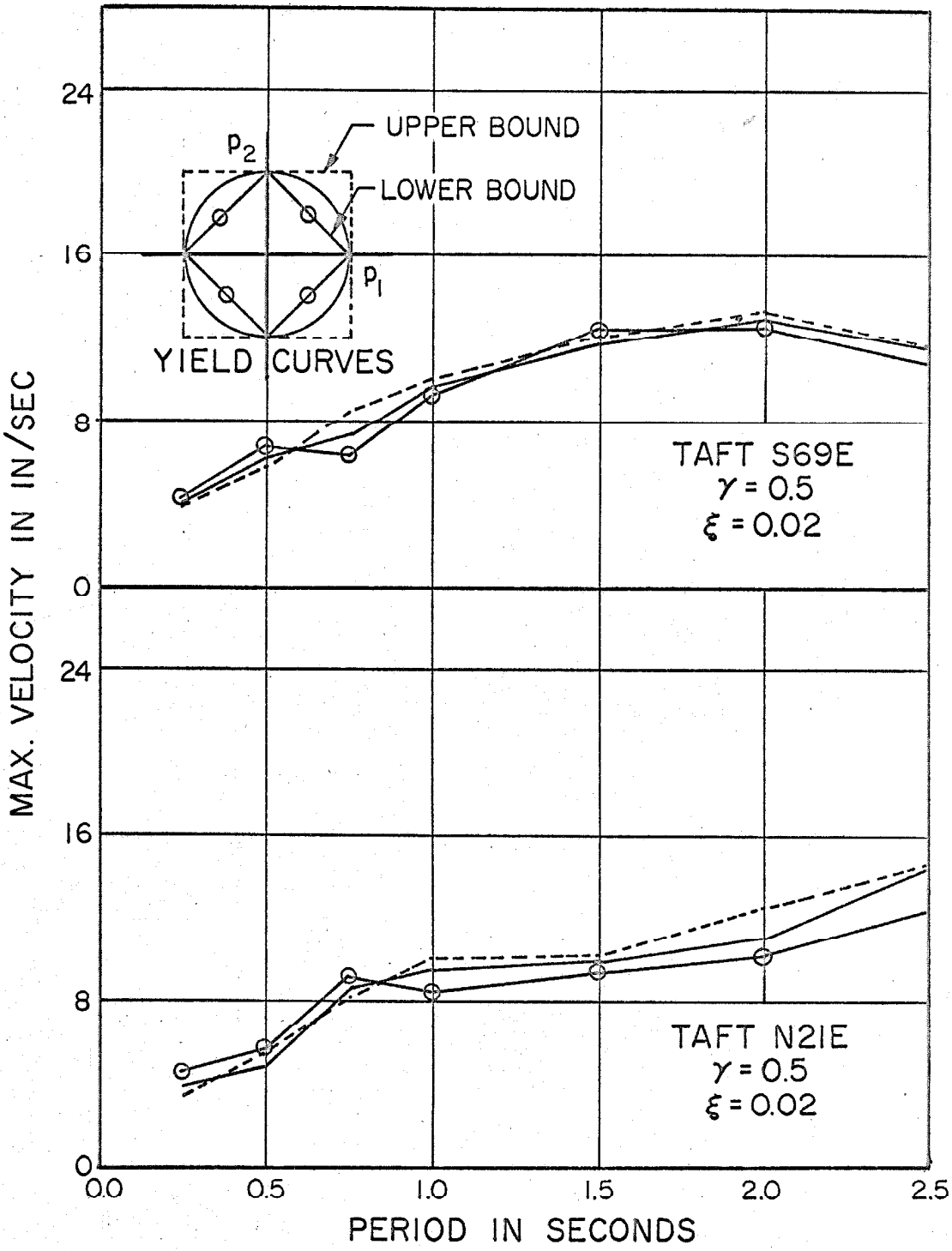


FIG. 5.30 EFFECT OF THE SHAPE OF YIELD CURVE ON VELOCITY SPECTRA

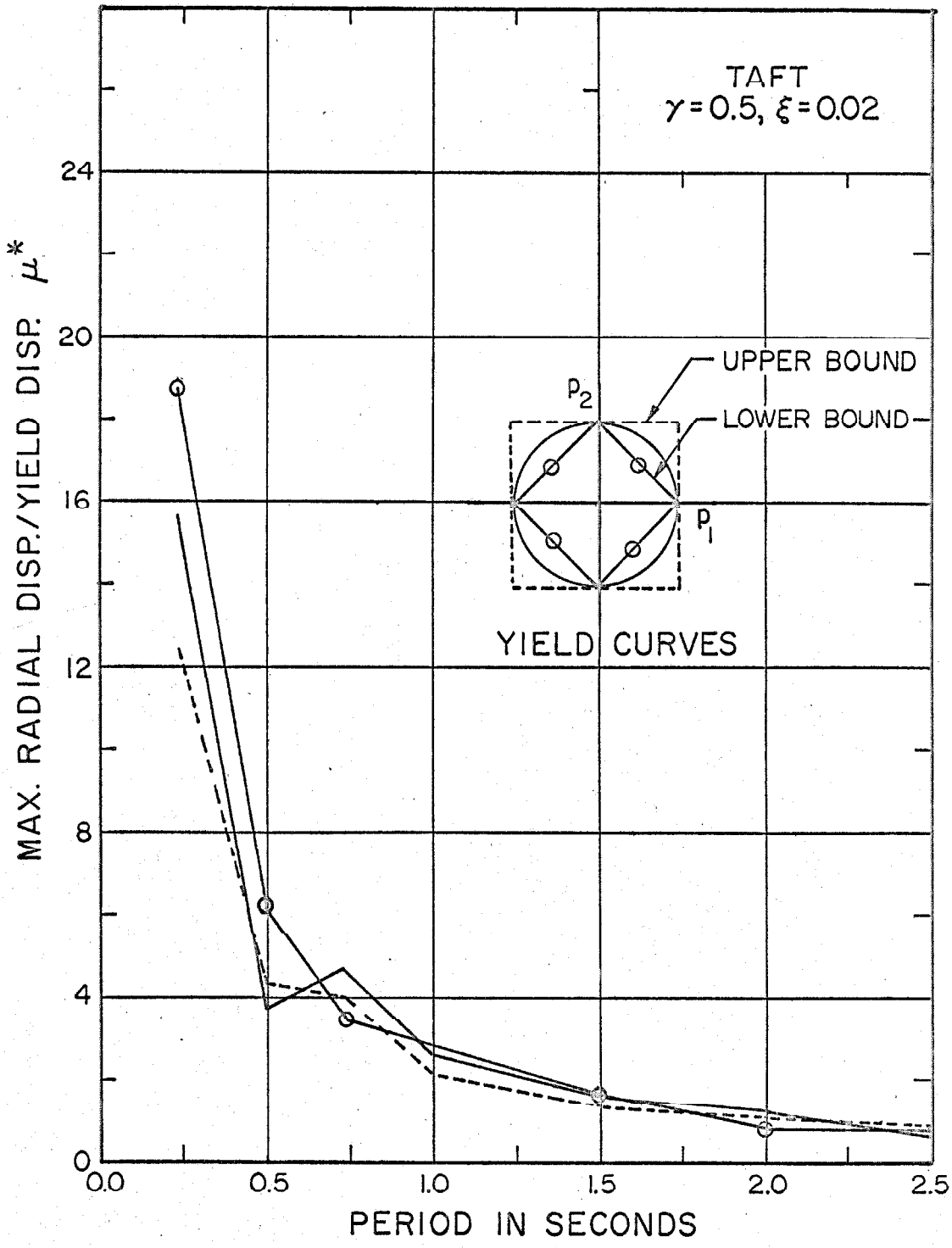


FIG. 5.31 EFFECT OF THE SHAPE OF YIELD CURVE ON RADIAL DISPLACEMENT SPECTRA

displacement (Fig. 5.28) also lies below the average curve, but follows it quite closely and lies within the range of values of the ensemble. The curves for velocity are shown in Fig. 5.19, wherein it is seen that the maximum velocities for the Taft earthquake are higher and outside the range for periods less than 1.5 seconds and lower for periods greater than 1.5 seconds. Considering the non-stationary random nature of real earthquakes the differences pointed out above are considered to be acceptable. These difference could arise because of one or all of the following reasons: 1) The strong part of the Taft earthquake record (Fig. 5.1) is confined to the first 15 seconds, whereas artificial earthquakes are uniform over 30 seconds. 2) The scale factor was based on r.m.s., which is only a partial index of the nature of an earthquake.

Effect of Damping

The response of the frame was obtained for three values of damping, $\xi = 0.0$, 0.02 and 0.05. The effect of damping on various response parameters was pointed out while discussing the response curves for each case. It was shown that the increase in damping has the general effect of reducing the maximum velocities and displacements and smoothing the response curves. The energy input is found to increase by a small amount with increase in damping. The energy loss due to damping, during the Taft earthquake, for elastic and elasto-plastic behavior with interaction, normalized by the damping energy loss in the elastic case, is shown in Fig. 5.32 for $\xi = 0.02$ and 0.05. It is seen from these curves that interaction has the effect

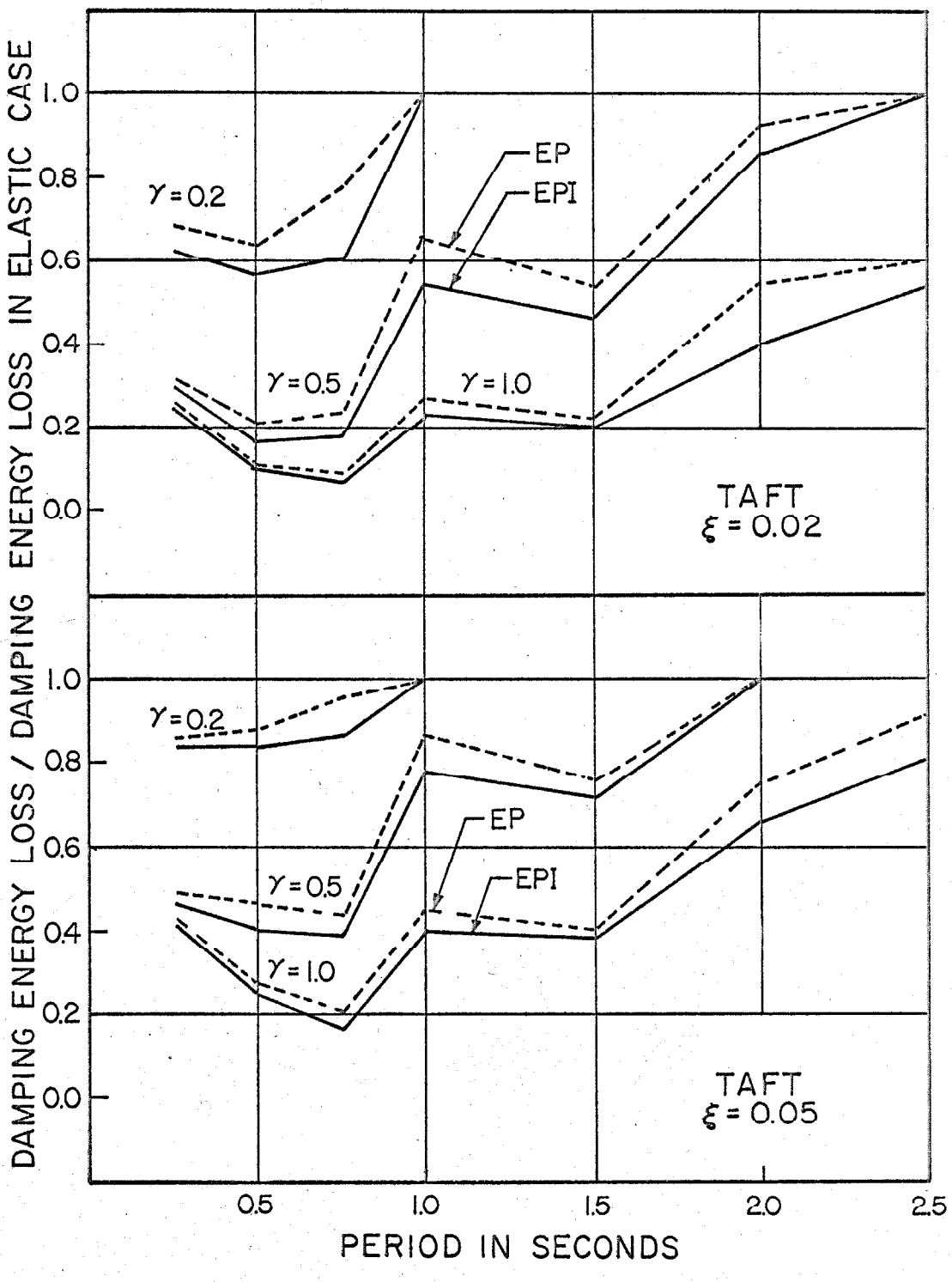


FIG. 5.32 DAMPING ENERGY LOSS SPECTRA

of reducing the energy loss due to damping up to 30 per cent. This shows that interaction reduces the dependence on damping for dissipation of energy. This fact is significant because modern structures are found to possess a small amount of damping.[44]

Yield Displacements and Elastic Energy Capacity of the Frame

Most of the response curves presented in this chapter have been normalized either by the yield displacement or the elastic energy capacity of the frame. The values of these parameters for different values of acceleration ratios and natural periods of the frame are shown in Fig. 5.33. These curves can be used to compute the actual value of a parameter from the response curves presented in this chapter.

## 5.4 Inelastic Design of Structures to Resist Earthquakes

The present concept of inelastic design of structures to resist earthquakes is based on the idea that the structure should remain elastic during small earthquakes, which occur frequently, should undergo limited plastic deformation during moderate size earthquakes, and may undergo large plastic deformations during infrequent large earthquakes. In this section, this basic idea is used to illustrate how the curves presented in the preceding section can be utilized to produce such designs.

In the preceding section, response curves for the Taft earthquake were drawn for three values of acceleration ratio. Since the earthquake was the same in each case, different values of accelera-

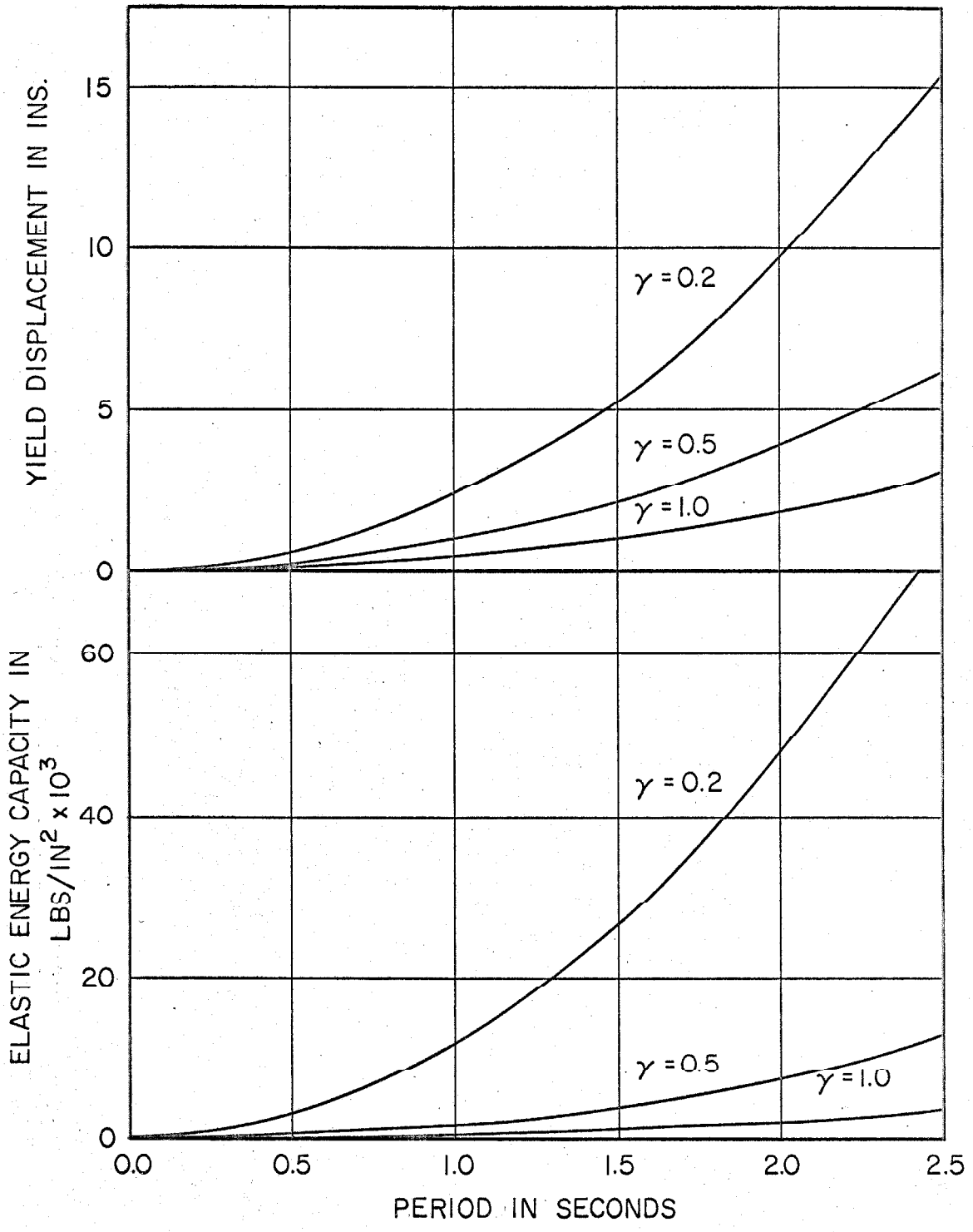


FIG. 5.33 YIELD DISPLACEMENT AND ELASTIC ENERGY CAPACITY

tion ratio represent different yield strengths of the frame. If one considers the yield strength of the frame to be fixed, these curves can be looked upon as response curves for different earthquakes. This interpretation provides a simple way of using these curves in design.

Let us suppose that the Taft earthquake with r.m.s. value $\hat{\ddot{z}} = 1.59$, represents a moderate size earthquake. Let us further suppose that earthquakes with r.m.s. values $\hat{\ddot{z}} = 3.18$ and $\hat{\ddot{z}} = 0.635$ represent large and small size earthquakes respectively. With the size of the earthquakes so specified and considering a frame with yield acceleration $a_{y1} = a_{y2} = 0.1\,g$, it can be shown then that the response curves for $\gamma = 1.0$, 0.5 and 0.2 will represent the response of this frame for large, moderate and small size earthquakes respectively. If "limited" and "large" plastic deformations can be characterized in terms of response parameters such as ductility ratio, permanent set, etc. ( hereafter called design parameters) these curves can be readily used for purposes of design as shown below.

The Ductility Ratio

The ductility ratio has been suggested[10,13] as a measure of permissible plastic deformations. In the preceding section it was shown that the ductility ratio can be redefined as the ratio ($\mu^*$) of the maximum radial displacement and the yield displacement to get a better correlation with plastic strain ratio. Let us use $\mu^*$ as the parameter to specify permissible plastic deformations. It is clear

that $\mu^* \leq 1$ represents elastic behavior. Let us assume, as an example, that $1 < \mu^* \leq 3$ characterizes "limited" plastic deformations and $3 < \mu^* \leq 6$ characterizes "large" plastic deformations. Then, depending upon the damping present in the structure, we can use Fig. 5.23, 5.24 or 5.27 to choose values of yield acceleration which will satisfy the design criteria outlined above. For 2 per cent damping these values are shown below:

| Period ($T_1 = T_2 = T$) | Yield Acceleration ($a_{y1} = a_{y2} = a_y$) |
|---|---|
| $T > 1.0$ | $a_y > 0.1$ g |
| $0.5 < T \leq 1.0$ | $a_y > 0.15$ g |
| $0.25 < T \leq 0.5$ | $a_y > 0.3$ g |

It may be pointed out here that these values of yield acceleration have been estimated on the basis of the three curves shown in Fig. 5.24. If such curves were plotted for a number of acceleration ratios, the appropriate values of yield acceleration could be readily determined. The same procedure can be used for other constraints such as permanent set and values of yield acceleration satisfying all the constraints can be obtained. If the ductility ratio and the permanent set are used as design parameters, it is seen from Figs. 5.24 and 5.28 that interaction has a significant effect on design for $T < 0.5$.

The method of inelastic design outlined above is direct if criteria for permissible plastic deformations can be specified quantitatively in terms of one or more of the response parameters. One of the main considerations in the choice of these parameters and their values is the possibility of fracture or unstable response due to

deterioration of the yield strength of the material during repeated loading. Since it is not possible to include this consideration directly in the suggested design procedure, it is necessary to allow for this through one or more of the response parameters. The ductility ratio is one such parameter and it is of interest to examine its suitability for this purpose.

It was pointed out in the preceding section that under simple loading conditions the ductility ratio is directly related to maximum plastic strain occurring in the structure during an earthquake. Due to this relationship with the maximum plastic strain it has a direct bearing on the possibility of fracture or unstable response due to large strains. Besides this, it has the following additional advantages:

1. The ductility ratio is obtained from the maximum displacement which in itself may be a constraint on design and can be accounted for by a constraint on the ductility ratio.
2. In experimental investigations designed to study the possibility of fracture or unstable response, the ductility ratio can be directly measured. Based on such experiments it can be assigned numerical values to specify permissible plastic deformations for purposes of design.

The use of ductility ratio has the following disadvantages;

1. It was pointed out in Section 5.2 that due to the random nature of plastic drift, estimates of the maximum displacements involve an element of uncertainty. This is

carried over to the estimates of the ductility ratio.

2. The maximum displacement is a transient phenomenon occurring for a short time. Hence, its influence on fracture or deterioration of material may not be significant.

3. For general loading conditions, with torsional moments, shear forces and bending moments acting at a section, the ductility ratio is not directly related to the yield behavior at the section.

The Plastic Energy Ratio

The ratio of the total energy dissipated by yielding during an earthquake to the elastic energy capacity of the structure (hereafter called the plastic energy ratio and denoted by $\Omega$) is another response parameter which can be used as a measure of the possibilities of fracture and deterioration during yielding. Since it represents the overall yield behavior of the structure during an earthquake, including the effects of interaction, it does not have the disadvantages pointed out for the ductility ratio. As compared to the ductility ratio it seems to be a better measure of the deterioration of the yield strength during yielding. The main disadvantage with plastic energy ratio is the difficulty of measuring it in an experimental investigation.

The response curves for plastic energy ratio are shown in Fig. 5.34 and can be used for the purposes of inelastic design by following the procedure outlined earlier. Due to the small number of response curves presented, it is not possible to make a meaningful

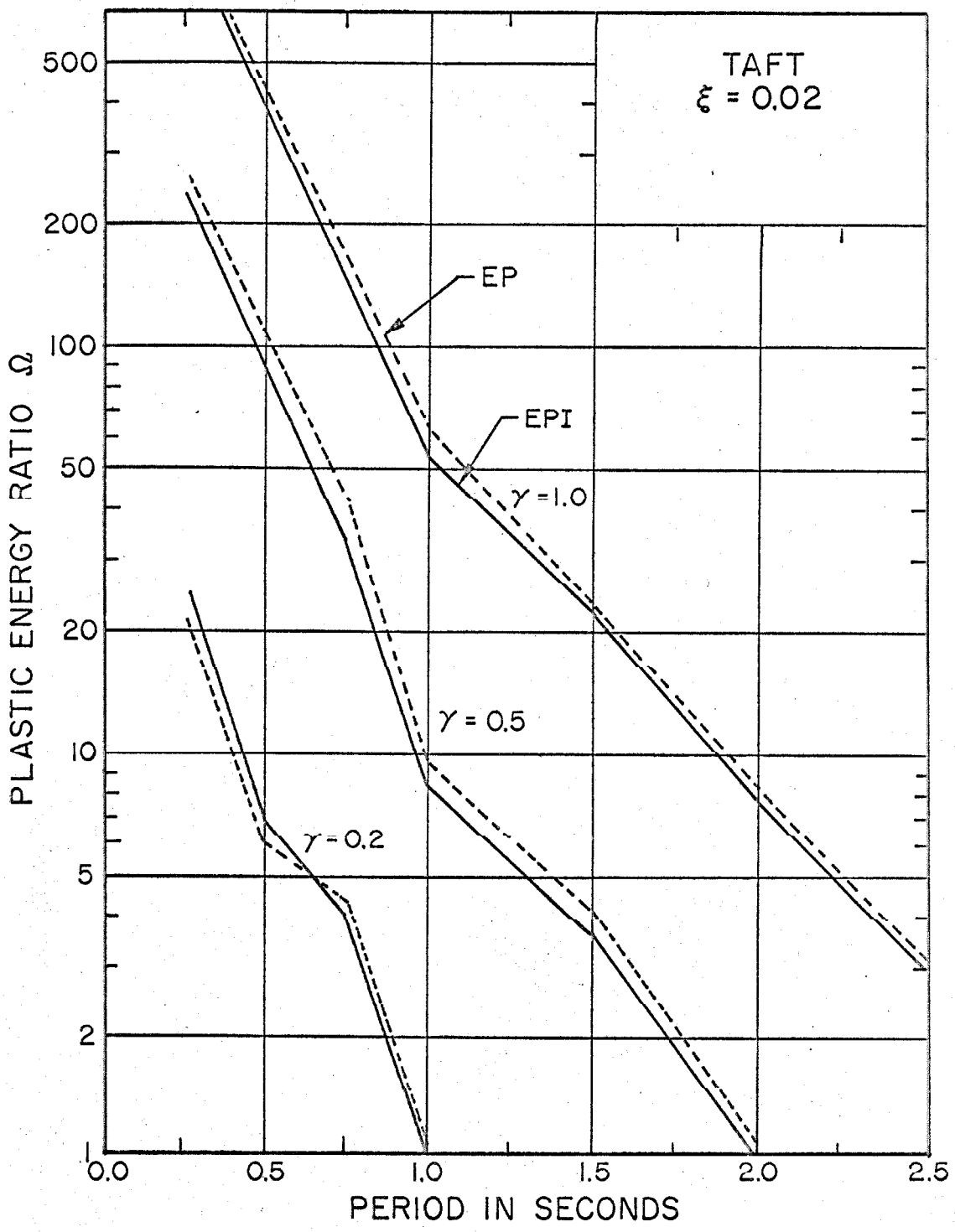


FIG. 5.34 SPECTRA OF THE RATIO OF HYSTERETIC ENERGY LOSS TO THE ELASTIC ENERGY CAPACITY

comparison between designs based on ductility ratio and plastic energy ratio. However, if it is assumed that "limited" plastic deformations are characterized by $0 < \Omega \leq 9$ and "large" plastic deformations by $9 < \Omega \leq 36$, it is seen that designs based on two criteria will be practically the same. From the point of view of interaction, however, there is a significant difference between the two criteria. It is seen from Fig. 5.34 that interaction reduces the plastic energy ratio, for all periods, whereas from Figs. 5.24 and 5.26 it is seen that interaction increases the ductility ratio significantly for $T_1 = T_2 < 0.5$ seconds.

It is clear that a detailed investigation both analytical and experimental, is needed to examine the suitability of these ratios as criteria for inelastic design.

Multi-Story Structures

In this chapter the effects of interaction on the response of structures have been investigated for a single-story frame. It is seen that the interaction does not have a significant effect on the response for natural periods greater than about 1.0 seconds. Since natural periods greater than 1.0 seconds pertain generally to multi-story structures whose behavior is different from the behavior of single-story structures in many respects, these conclusions are not directly applicable in this range. The response of multi-story structures has been investigated[13,15,20] for elasto-plastic behavior and it is of interest to see how interaction can affect the response of these structures. In this connection, the following observations may

be made:

1. The axial force and shear force in the columns of a multi-story structure increase progressively from the top floors to the bottom floors.
2. If the vibration of a structure is considered simultaneously along both principal directions, the interaction between forces coming from the two directions will occur mostly in the columns.

In view of these observations it is clear that if interaction between axial force, shear forces, and bending moments acting at a section is considered, the response must have the following characteristics.

1. The effect of interaction due to axial force and shear force will increase progressively from top to bottom, causing more yielding in the lower stories.
2. The possibility of yielding in columns will increase relative to yielding in girders.

The extent to which such behavior may affect the response of multi-story structures needs to be investigated.

## 5.5 Summary and Conclusions

The dynamic response of a simple frame to earthquake type excitation has been presented. To limit the scope of the study, the investigation was restricted to frames which have identical properties along the two principal directions and a circular yield curve for

bending about the principal axes. Using the equations of motion derived in Chapter II, the response of the frame was obtained for inelastic interaction between bending moments, acting along the principal directions of a section. For purposes of comparison the response was also obtained for elastic and elasto-plastic behavior and changes in the response due to interaction were discussed. A series of curves showing various aspects of the response of the frame were presented for the Taft earthquake and for an ensemble of artificial earthquakes. The existing notions about the inelastic design of structures were examined in the light of results presented in this thesis and use of response curves for such designs was proposed. On the basis of these results the following conclusions can be drawn about the effects of interaction and their implications for earthquake engineering:

1. During earthquakes structures are subjected to general conditions of loading giving rise to inelastic interactions between forces and displacement acting at a section. The theory developed in this thesis makes it possible to consider the effects of such interactions on the dynamic response of structures.

2. The essential feature of interaction is the occurrence of yielding at force-levels lower than the fixed levels for elasto-plastic behavior without interaction. This causes energy to be removed from the system by hysteresis before the response has time to build up, thus resulting in a smaller and more uniform response.

3. The yielding reduces the maximum velocity and energy input

to the system and interaction reduces it still further. This is of significance from the point of view of Housner's method of limit design.

4. The interaction has the effect of increasing the values of ductility ratio and permanent set for structures with natural periods less than 0.5 seconds. This has a significant influence on the designs based on these parameters.

5. The concept of ductility ratio can be redefined, as the ratio of maximum radial displacement to the yield displacement, to obtain better correlation with the plastic strain ratio. The ductility ratio curves, along with curves for other parameters, can be used to design structures in accordance with the current philosophy of earthquake resistant design. The use of ductility ratio to specify permissible plastic deformations is meaningful and convenient, but has certain disadvantages which must be kept in mind.

6. The plastic energy ratio can be used as an alternative to ductility ratio or as an additional design parameter. It has the advantage of representing aggregate yield behavior during an earthquake and seems to be a better measure of deterioration during repeated loading.

7. Extensive experimental and theoretical investigations are needed to incorporate the possibility of fracture or unstable behavior due to large plastic strains, and deterioration of material during yielding, as a constraint on permissible plastic deformations in terms of one or more response parameters.

8. The increase in viscous damping has the effect of reducing

the displacements and velocities and smoothing the response curves. The interaction has the effect of increasing the fraction of the total energy removed by hysteresis, thus reducing the dependence on damping to limit the response. This is significant considering the fact that modern structures possess a small amount of damping.

9. The discussion in this study was confined to a special class of structures. This leaves a number of parameters uninvestigated and these may be responsible for some other significant effects of interaction. Further study is, therefore, needed to investigate the influence of these parameters.

10. Comparisons of the responses to the Taft earthquake and to an ensemble of artificial earthquakes show that artificial earthquakes can be meaningfully employed to obtain average curves, and estimates of the reliability of these averages, well into the nonlinear range of the response.

11. The results of this study, based on the response of a single-story frame, show that interaction does not cause a significant influence on the response of structures with period greater than about 1.0 seconds. This range pertains, mostly, to multi-story structures, whose response differs from the response of single-story structures in many respects. Interaction may cause some change in our present notions about the inelastic response of these structures. This needs to be investigated.

12. In this investigation, the effects of axial force, shear force, gravity,[46] and vertical component of ground motion during

earthquakes, have not been included in computing the response of the frame. The region in force-space, where the structure is partly-elastic and partly-plastic, has been assumed to be elastic. In real structures all the effects are present and will tend to increase the effects of interaction. This must be kept in mind while applying the results of this investigation.

# APPENDIX I

## EXPLANATION OF TERMS

The specific sense in which some of the terms are used in this thesis is stated below.

Force - forces and moments.

Displacement - deflections, rotations and curvatures.

Force-displacement pair - a pair formed by a force and the displacement caused by it.

Simple loading conditions - a single force-displacement pair existing at a section or if more than one force-displacement pairs exist, all except one are disregarded.

General loading conditions - more than one force-displacement pair existing at a section.

Inelastic interaction - influence of forces and displacements acting at a section on yield behavior of the section.

Elastic behavior - linearly elastic force-displacement relationship for each pair.

Elasto-plastic behavior - elastic-perfectly-plastic force displacement relationship for each pair, independent of other pairs.

Elasto-plastic behavior with interaction - a general force-displacement relationship incorporating the effects of inelastic interaction between forces and displacements acting at a section.

Damping energy loss - the energy dissipated in structure due to viscous damping.

Hysteretic energy loss - the energy dissipated in the structure due to yielding.

System parameter - a parameter representing a property of the system.

Response parameter - a parameter representing a property of the response of a system.

Design parameter - a response parameter used as a criterion for design.

Taft earthquake - the ground motion recorded at Taft, California during the earthquake of July 21, 1952.

Artificial earthquake - a sample of a stationary process with statistical properties similar to those of recorded strong-motion earthquakes.

# APPENDIX II

## YIELD CURVES FOR ELLIPTICAL SECTIONS

In Section 3.3 of Chapter III, the equation of the yield curve, for bending about the principal axes of a rectangular section, was derived by determing the highest lower bound. The same approach is now used to determine the equation of the yield curve for elliptical sections. Symbols used are defined wherever they first appear.

Let us consider an elliptical section shown in Fig. A2.1. Let the section boundary be defined by

$$\frac{x^2}{a^2} + \frac{y^2}{b^2} = 1 \qquad \text{(A2.1)}$$

and let $Y = \chi(x)$ be the equation of the curve separating tensile and compressive zones. We have to find $\chi(x)$, which satisfies Eq. 3.7 and is such that given $Q_1$, $Q_2$ is maximised. For such $\chi(x)$, Eqs. 3.6 define the exact yield curve. The axial force at the section is given by Eq. 3.7. Substituting Eq. 3.6 and carrying out the integration it can be shown that

$$N = 2\sigma_y\left\{\int_{x_1}^{a} y\,dx - \int_{-a}^{-x_2} y\,dx + \int_{-x_2}^{x_1} \chi(x)\,dx\right\} \qquad \text{(A2.2)}$$

Substituting for $y$ from Eq. A2.1 and noting that $x_1$ and $x_2$ must satisfy the relations

$$\frac{x_1^2}{a^2} + \frac{\chi^2(x_1)}{b^2} = 1$$

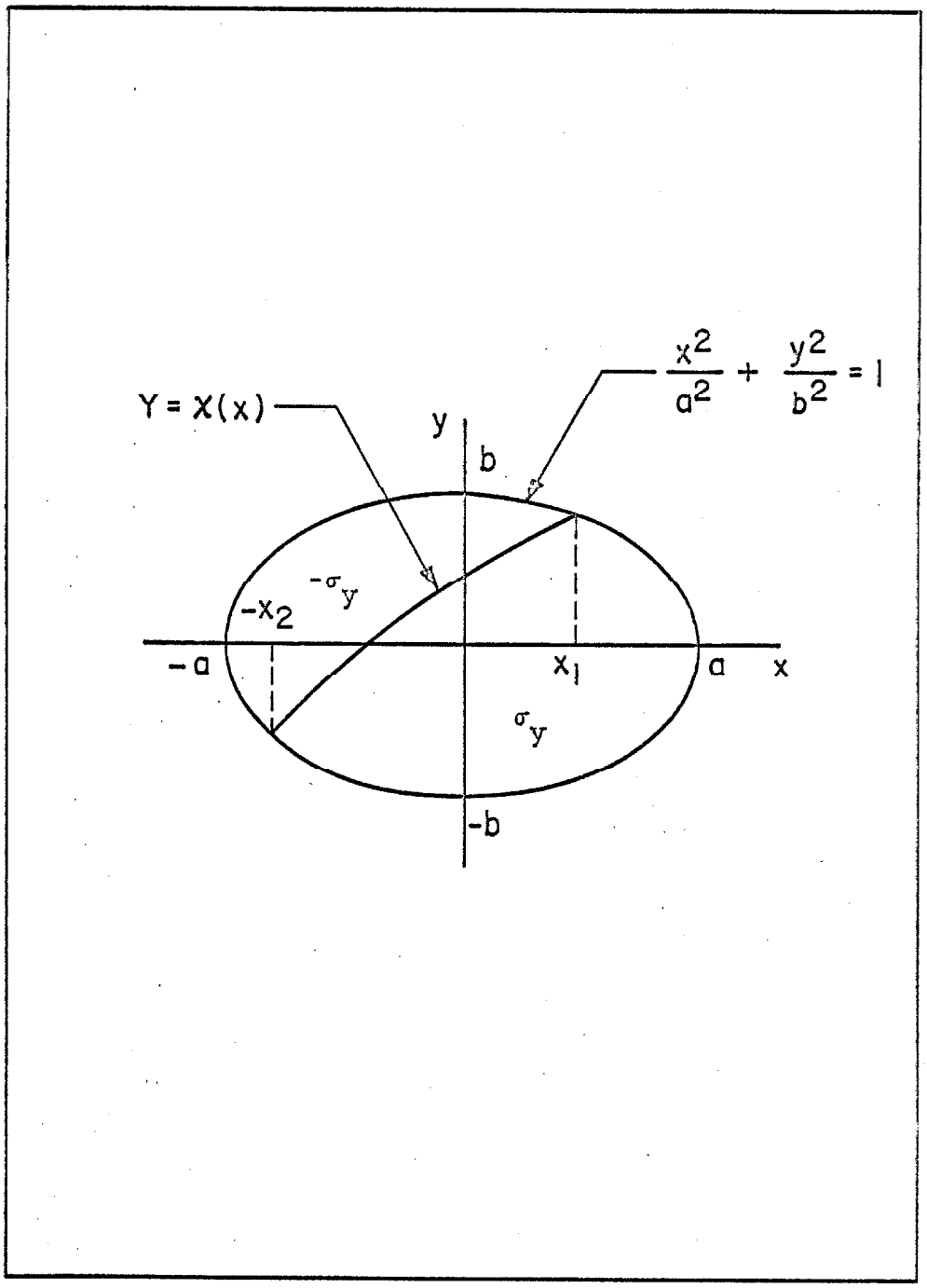


FIG. A2.1 A SOLID ELLIPTICAL SECTION

and (A2.3)

$$\frac{x_2^2}{a^2} + \frac{\chi^2(-x_2)}{b^2} = 1$$

Eq. A2.2 reduces to

$$N = \sigma_y \left\{-x_2\chi(-x_2) - x_1\chi(x_1) - a^2\left(\sin^{-1}\frac{x_1}{a} - \sin^{-1}\frac{x_2}{a}\right)\right\}$$

$$+\int_{-x_2}^{x_1} \chi(x)\,dx \qquad (A2.4)$$

From Eqs. A2.3 and A2.4 it is seen that, if

$$\chi(x) = -\chi(-x) \qquad (A2.5)$$

$x_1 = x_2$ and Eq. 3.7 is identically satisfied.

The generalized forces (bending moments) $Q_1$ and $Q_2$ at the section are given by Eqs. 3.6. Substituting from Eqs. A2.1 and A2.4 and simplifying, it can be shown that

$$Q_1 = \frac{4b\sigma_y}{3a}(a^2 - x_1^2)^{3/2} + 4\sigma_y\int_o^{x_1} x\chi(x)\,dx$$

and (A2.6)

$$Q_2 = 2\sigma_y\int_o^{x_1}\left\{\chi^2(x) - \frac{b^2}{a^2}(a^2 - x^2)\right\}dx$$

To maximize $Q_2$, given $Q_1$, let us define a function

$$\Lambda(x, \chi_1) = \chi^2(x) - 2\nu x\chi(x)$$

where

$\nu$ is a constant

Then a necessary condition, for $Q_2$ to be a maximum, is that $\chi(x)$ satisfies the Euler's equation

$$\frac{d}{dx}\left(\frac{\partial}{\partial \chi'}\right) = \frac{\partial \Lambda}{\partial \chi}$$

where

$\chi'$ denotes $d\chi/dx$

Substituting for $\Lambda(x,\chi)$ gives

$$\chi(x) = \nu x \tag{A2.7}$$

Substituting Eq. A2.7 in Eqs. A2.6 gives

$$Q_1 = \frac{4\sigma_y a^3 b}{3(b^2+a^2\nu^2)^{\frac{1}{2}}}\ \nu$$

and

$$Q_2 = -\frac{4\sigma_y b^3 a}{3(b^2+a^2\nu^2)^{\frac{1}{2}}} \tag{A2.8}$$

The yield moments for the elliptical sections are given by

$$Q_{y1} = \frac{4}{3}\sigma_y a^2 b$$

$$Q_{y2} = \frac{4}{3}\sigma_y b^2 a$$

Dividing Eqs. A2.8 by $Q_{y1}$ and $Q_{y2}$ gives

$$p_1 = \frac{a}{(b^2 + a^2\nu^2)^{\frac{1}{2}}}\,\nu$$

and (A2.9)

$$p_2 = \frac{-b}{(b^2+a^2\nu^2)^{\frac{1}{2}}}$$

Equation A2.9 is the equation of the yield curve in parametric form. Eliminating $\nu$ between Eqs. A2.9 gives

$$p_1^2 + p_2^2 = 1 \qquad \text{(A2.10)}$$

which represents a circle of unit radius in p-space.

Initial Yield Curve

Maximum flexural stress in an elliptical section occurs somewhere on the boundary and is given by

$$\sigma = \frac{Q_1}{I_1}x + \frac{Q_2}{I_2}y \qquad \text{(A2.11)}$$

where

$I_1$ is the moment of inertia of the section for bending along the y-axis

$I_2$ is the moment of inertia of the section for bending along the x-axis

Substituting for $y$ from Eq. A2.1 and taking the partial derivative with respect to $x$ gives

$$\frac{\partial\sigma}{\partial x} = Q_1 - \frac{Q_2 bx}{a(a^2 - x^2)^{\frac{1}{2}}}$$

where

$O_1, O_2$ are the ratios $Q_1/I_1$ and $Q_2/I_2$ respectively

For $\sigma$ to be maximum, $\partial\sigma/\partial x = 0$, which gives

$$x = \frac{a^2 O_1}{(a^2 O_1^2 + b^2 O_2^2)^{\frac{1}{2}}}$$

and (A2.12)

$$y = \frac{b^2 O_2}{(a^2 O_1^2 + b^2 O_2^2)^{\frac{1}{2}}}$$

Substituting in Eq. A2.11 gives

$$\sigma_{max} = (a^2 O_1^2 + b^2 O_2^2)^{\frac{1}{2}} \tag{A2.13}$$

Yielding begins when $\sigma_{max} = |\sigma_y|$ and the equation of the initial yield curve is given by

$$\sigma_y^2 = \frac{a^2 Q_1^2}{I_1^2} + \frac{b^2 Q_2^2}{I_2^2}$$

Substituting for $I_1$ and $I_2$ and using Eq. A2.8 yields

$$p_1^2 + p_2^2 = \left(\frac{3\pi}{16}\right)^2 \tag{A2.14}$$

which is again a circle with radius $3\pi/16$.

# APPENDIX III

# DETAILS OF NUMERICAL COMPUTATION

## Integration of Equations of Motion

In the course of this investigation it was necessary to integrate numerically Eqs. 2.36. The integration was carried out on an IBM 7090 digital computer using a third order Runge-Kutta method attributed to Heun.[45] For a system of n first order differential equations this method can be written in the following form:

Let the system of differential equations be given by

$$\dot{\bar{u}} = \bar{f}(\tau, \bar{u}) \tag{A3.1}$$

where

| | |
|---|---|
| $u$ | is an n-dimensional vector |
| $\bar{f}$ | is an n-dimensional vector function |
| $\tau$ | is related to time by $\tau = \omega t$ |

Then the Runge-Kutta formulae for the $s+1^{st}$ integration step are

$$\bar{u}_{s+1} = \bar{u}_s + \frac{1}{4}(\bar{K}_o + 3\,\bar{K}_2)$$

where

$$\bar{K}_o = \Delta\tau\,\bar{f}(\tau_s, \bar{u}_s) \tag{A3.2}$$

$$\bar{K}_1 = \Delta\tau\,\bar{f}\left\{(\tau_s + \tfrac{1}{3}\Delta\tau), (\bar{u}_s + \tfrac{1}{3}\bar{K}_o)\right\}$$

$$\bar{K}_2 = \Delta\tau\,\bar{f}\left\{(\tau_s + \tfrac{2}{3}\Delta\tau), (\bar{u}_s + \tfrac{2}{3}\bar{K}_1)\right\}$$

where

$\bar{K}_o, \bar{K}_1, \bar{K}_2$ are n-dimensional vectors

$\Delta\tau$ is the interval of integration

Equations 2.36 can be written as a system of first order equations and the above method can be used directly. For elastic and elasto-plastic behavior, Eqs. 2.36 represent two uncoupled second order equations which can be integrated independently. For these cases, let

$$u(1) = u_i$$

and (A3.3)

$$u(2) = \frac{du_i}{d\tau}$$

where i = 1,2. Eqs. 3.6 can then be written

For Elastic Response:

$$\begin{aligned} \dot{u}(1) &= u(2) \\ \dot{u}(2) &= -\left(\frac{\omega_i}{\omega_1}\right)^2 \frac{\ddot{z}_i\left(\frac{\tau}{\omega_1}\right)}{a_{yi}} - 2\left(\frac{\omega_i}{\omega_1}\right)\xi_i u(2) - \left(\frac{\omega_i}{\omega_1}\right)^2 u(1) \end{aligned} \tag{A3.4}$$

For Elasto-Plastic Response:

$$\begin{aligned} \dot{u}(1) &= u(2) \\ \dot{u}(2) &= -\left(\frac{\omega_i}{\omega_1}\right)^2 \frac{\ddot{z}_i\left(\frac{\tau}{\omega_1}\right)}{a_{yi}} - 2\left(\frac{\omega_i}{\omega_1}\right)\xi_i u(2) - \left(\frac{\omega_i}{\omega_1}\right)^2 (u(1) - u_o(1)) \end{aligned}$$

if $p_i < |1|$ ,

or if $p_i = |1|$ and $\dot{W}_i^p < 0$

and (A3.5)

$$\dot{u}(1) = u(2)$$

$$\dot{u}(2)\ \sigma\ -\left(\frac{\omega_i}{\omega_1}\right)^2 \frac{\ddot{z}_i\left(\frac{\tau}{\omega_1}\right)}{a_{yi}} - 2\left(\frac{\omega_i}{\omega_1}\right)\xi_i u(2) - \left(\frac{\omega_i}{\omega_1}\right)^2 |1|$$

$$\text{if } \dot{W}(p) \geq 0$$

When interaction is considered Eqs. 2.36 are coupled and cannot be integrated independently. For this case, let

$$\begin{aligned} u(1) &= u_1 \\ u(2) &= \frac{du_1}{d\tau} \\ u(3) &= u_2 \\ u(4) &= \frac{du_2}{d\tau} \\ u(5) &= p_1 \\ u(6) &= p_2 \end{aligned} \qquad \text{(A3.6)}$$

Equations 3.6 can now be written

For Elasto-Plastic Response with Interaction

$$\dot{u}(1) = u(2)$$

$$\dot{u}(2) = -\frac{\ddot{z}_1\left(\frac{\tau}{\omega_1}\right)}{a_{y1}} - 2\xi_1 u(2) - (u(1) - u_o(1))$$

$$\dot{u}(3) = u(4)$$

$$\dot{u}(4) = \frac{-\ddot{z}\left(\frac{\tau}{\omega_2\zeta}\right)}{\zeta^2 a_{y2}} - \frac{2\xi_2}{\zeta}u(4) - \frac{1}{\zeta^2}(u(3) - u_o(3))$$

if $\Phi(p_1, p_2) < 1$

or if $\Phi(p_1, p_2) = 1$ and $\dot{W}^p < 0$

and (A3.7)

$$\dot{u}(1) = u(2)$$

$$\dot{u}(2) = \frac{-\ddot{z}_1\left(\frac{\tau}{\omega_1}\right)}{a_{y1}} - 2\xi_1 u(2) - u(5)$$

$$\dot{u}(3) = u(4)$$

$$\dot{u}(4) = \frac{-\ddot{z}_2\left(\frac{\tau}{\omega_2\zeta}\right)}{\zeta^2 a_{y2}} - \frac{2\xi_2}{\zeta}u(4) - \frac{u(6)}{\zeta^2}$$

$$\dot{u}(5) = \frac{k_2\left\{\left(\frac{\partial\Phi}{\partial p_2}\right)^2 u(2) - \frac{\partial\Phi}{\partial p_1}\frac{\partial\Phi}{\partial p_2}\frac{q_{y2}}{q_{y1}}u(4)\right\}}{\left\{k_1\left(\frac{\partial\Phi}{\partial p_1}\right)^2 + k_2\left(\frac{\partial\Phi}{\partial p_2}\right)^2\right\}}$$

$$\dot{u}(6) = \frac{k_1\left\{-\frac{\partial\Phi}{\partial p_1}\frac{\partial\Phi}{\partial p_2}\frac{q_{y1}}{q_{y2}}u(2) + \left(\frac{\partial\Phi}{\partial p_1}\right)^2 u(4)\right\}}{\left\{k_1\left(\frac{\partial\Phi}{\partial p_1}\right)^2 + k_2\left(\frac{\partial\Phi}{\partial p_2}\right)^2\right\}}$$

if $\Phi(p_1, p_2) = 1$ and $\dot{W}^p \geq 0$

Equations 2.36 are now in the same form as Eq. A3.1 and can be integrated, step by step, by using Eqs. A3.2. The Runge-Kutta method was chosen because of its long range stability and its self starting feature. It has a truncation error of the order of $(\Delta\tau)^4$.

Integration Interval $\Delta\tau$

The integration interval was determined by the following equation

$$\Delta\tau = \frac{\omega\Delta t}{N} \tag{A3.8}$$

where

| | |
|---|---|
| t | denotes time |
| N | is an integer |

For sinusoidal excitation the integration interval was obtained by setting $\Delta t = 0.0125$ seconds and $N = 1$. Test cases were run for $\Delta t = 0.00625$ seconds and $N = 1$ and it was found that change in displacement values was less than 1 per cent. Hence $\Delta t = 0.0125$ seconds was considered satisfactory. Since it was possible to get exact solution for the phase angle $\rho$ equal to $90^{\circ}$, the numerical accuracy and correctness of the computer program was checked by comparison with exact results. Results of this comparison are shown in Figs. 4.12 and 4.13. The agreement is considered satisfactory.

For earthquake type excitation, $\Delta t$ was taken equal to the interval of digitisation of the earthquake. For the Taft earthquake this value is 0.02 seconds and for the artificial earthquakes it is equal to 0.025 seconds. To determine suitable values of N, a few

test cases were run for $T_1 = T_2 = 0.25$ seconds with $N = 2$ and 4. It was found that the change in displacement values was less than 3 per cent and in energy values less than 5 per cent for these values of N. This difference was considered small and $N = 2$ was adopted. For $T_1 = T_2 = 0.5$ seconds, a few test cases were run with $N = 1$ and $N = 2$ and the differences were found to be of the same order as in the previous case. Hence, a value of $N = 1$ was used for $T_1 = T_2 \geq 0.5$ seconds.

Transitions Between Elastic and Plastic States

From Eqs. A3.5 and A3.7 it is seen that for elasto-plastic and elasto-plastic behavior with interaction the motion is defined by two sets of equations. One set applies, when the response is elastic, and the other when it is plastic. The conditions for transition from one set to another are given in Eqs. A3.5 and A3.7. In any numerical procedure it is not possible to satisfy these conditions exactly and certain tolerances must be permitted. In this study the following criteria were used for such transitions:

For Elasto-Plastic Response:

Change from elastic state to plastic state if $1 \leq |p_i| < 1 + 10^{-4}$

Change from plastic to elastic state if $\frac{\dot{W}_i^p}{Q_{yi}} < -10^{-4}$

For Elasto-Plastic Response with Interaction:

Change from elastic state to plastic state if $1 \leq \Phi(\bar{p}) < 1 + 10^{-4}$

Change from plastic state to elastic state if $\frac{2\dot{W}^p}{Q_{y1} + Q_{y2}} < -10^{-4}$

At each transition, the interval of integration was subdivided until above tolerances were satisfied.

Evaluation of Energy Integrals

The integrals for energy loss due to damping, Eq. 2.50, were computed by Simpson's rule on the IBM 7090 computer. The interval of integration was the same as in the integration of the equations of motion. Energy loss due to hysteresis was obtained for each step of integration by computing the product $\Delta HE = \langle Q, \Delta\bar{q}^p \rangle$. The accuracy of Simpson's rule was checked by a few test runs and was considered satisfactory.

# REFERENCES


1. Neal, B. G., Plastic Method of Structural Analysis, New York: John Wiley & Sons, Inc., (1963).

2. Hodge, P. G., Jr., Plastic Analysis of Structures, New York: McGraw Hill Book Company, Inc., (1959).

3. Hodge, P. G., Jr., Limit Analysis of Rotationally Symmetric Plates and Shells, Englewood Cliffs, N.J.: Prentice-Hall, Inc., (1963).

4. Housner, G. W., "Reporter's Summary -- Theme II," Proceedings of the Third World Conference on Earthquake Engineering, Vol. II, Auckland and Wellington, New Zealand (January, 1965), pp. 1-20.

5. Housner, G. W., "Behavior of Structures During Earthquakes," Proceedings, ASCE, Vol. 85, No. EM4 (Oct., 1959), pp. 109-129.

6. Berg, G. V. and Thomaides, S. S., "Energy Consumption by Structures in Strong-Motion Earthquakes," Proceedings of the Second World Conference on Earthquake Engineering, Vol. II, Tokyo and Kyoto, Japan, (July, 1960), pp. 681-698.

7. Housner, G. W., "Limit Design of Structures to Resist Earthquakes," Proceedings of the World Conference on Earthquake Engineering, Berkeley, U.S.A., (June, 1956),

8. Housner, G. W., "The Plastic Failure of Frames During Earthquakes," Proceedings of the Second World Conference on Earthquake Engineering, Vol. II, Tokyo and Kyoto, Japan, (July, 1960), pp. 997-1012.

9. Blume, J. A., "A Reserve Energy Technique for the Earthquake Design and Rating of Structures in the Inelastic Range," Proceedings of the Second World Conference on Earthquake Engineering, Vol. II, Tokyo and Kyoto, Japan, (July, 1960), pp. 1061-1084.

10. Velestos, A. S., and Newmark, N. M., "Effect of Inelastic Behavior on the Response of Simple Systems to Earthquake Motions," Proceedings of the Second World Conference on Earthquake Engineering, Vol. II, Tokyo and Kyoto, Japan, (July, 1960), pp. 895-912.

11. Newmark, N. M., et al., "Deformation Spectra for Elastic and Elasto-Plastic Systems Subjected to Ground Shock and Earthquake Motions," Proceedings of the Third World Conference on Earthquake Engineering, Vol. II, Auckland and Wellington, New Zealand, (January, 1965), pp. 663-682.

12. Berg, G. V. and Da Deppo, D. A., "Dynamic Analysis of Elasto-Plastic Structures," Proceedings, ASCE, Vol. 86, No. EM2, (April, 1960), pp. 35-58.

13. Clough, R. W., et al., "Inelastic Earthquake Response of Tall Buildings," Proceedings of the Third World Conference on Earthquake Engineering, Vol. II, Auckland and Wellington, New Zealand, (January, 1965), pp. 68-89.

14. Penzien, J., "Dynamic Response of Elasto-Plastic Frames," Proceedings, ASCE, Vol. 86, ST7, (July, 1960), pp. 81-94.

15. Penzien, J., "Elasto-Plastic Response of Idealized Multi-Story Structures Subjected to a Strong Motion Earthquake," Proceedings of the Second World Conference on Earthquake Engineering, Vol. II, Tokyo and Kyoto, Japan, (July, 1960), pp. 739-760.

16. Jennings, P. C., "Response of Simple Yielding Structures to Earthquake Excitation," Ph.D. Thesis, California Institute of Technology, Pasadena, U.S.A. (1963).

17. Tanabashi, R., "Nonlinear Transient Vibrations of Structures," Proceedings of the Second World Conference on Earthquake Engineering, Vol. II, Tokyo and Kyoto, Japan, (July, 1960), pp. 1223-1238.

18. Hisada, T., et al., "Earthquake Response of Idealized Twenty Story Buildings Having Various Elasto-Plastic Properties," Proceedings of the Third World Conference on Earthquake Engineering, Vol. II, Auckland and Wellington, New Zealand, (January, 1965), pp. 168-184.

19. Saul, W. E., et al., "Dynamic Analysis of Bilinear Inelastic Multiple Story Shear Buildings," Proceedings of the Third World Conference on Earthquake Engineering, Vol. II, Auckland and Wellington, New Zealand, (January, 1965), pp. 533-551.

20. Giberson, M. F., "The Response of Nonlinear Multi-story Structures Subjected to Earthquake Excitation," Ph.D. Thesis, California Institute of Technology, Pasadena, U.S.A. (1967).

21. Hanson, R. D., "Post-Elastic Dynamic Response of Mild Steel Structures," Ph.D. Thesis, California Institute of Technology, Pasadena, U.S.A., (1965).

22. Berg, G. V., "A Study of the Earthquake Response of Inelastic Systems," Proceedings 34th Annual Convention Structural Engineers Association of California, Coronado, California (Oct. 1965), pp. 63-67.

23. Hill, R., The Mathematical Theory of Plasticity, London: Oxford University Press, (1950).

24. Prandtl, L., "Ein Gedankenmodell Zur Kinetschen Theory der Festen Korper," Z. Angew Math. Mech., Vol. 8, (1928), pp. 85-106.

25. Koiter, W. T., "Stress-Strain Relations, Uniqueness and Variational Theorems for Elastic Plastic Materials with a Singular Yield Surface," Quarterly of Applied Mathematics, Vol. 11, (1953), pp. 350-354.

26. Sadowsky, M. A., "A Principle of Maximum Plastic Resistance," Journal of Applied Mechanics, Vol. 10, No. 2, (1943), pp. 65-68.

27. Prager, W., Discussion of "A Principle of Maximum Plastic Resistance," by M. A. Sadowsky, Journal of Applied Mechanics, Vol. 10, No. 4, (1943), pp. 238-239.

28. Handelman, G. H., "A Variational Principle for a State of Combined Plastic Stress," Quarterly of Applied Mathematics, Vol. 4, (1944), pp. 351-353.

29. Hill, R., "A Variational Principle of Maximum Plastic Work in Classical Plasticity," Quarterly of Applied Mathematics, Vol. 1, (1948), pp. 18-28.

30. Imegwu, E. O., "Combined Plastic Bending and Torsion," Journal of Mechanics and Physics of Solids, Vol. 10, (1962), pp. 277-282.

31. Imegwu, E. O., "Plastic Flexure and Torsion," Journal of Mechanics and Physics of Solids, Vol. 8, (1960), pp. 141-146.

32. Steele, M. C., "The Plastic Bending and Twisting of Square Section Members," Journal of Mechanics and Physics of Solids, Vol. 8, (1954), pp. 156-166.

33. Hill, R. and Siebel, M. P. L., "Combined Bending and Twisting of Thin Tubes in the Plastic Range," Philosophical Magazine, Vol. 42, (1951), pp. 722-733.

34. Hill, R., and Siebel, M.P.L., " On the Plastic Distortion of Solid Bars by Combined Bending and Twisting," Journal of Mechanics and Physics of Solids, Vol. 1, No. 3, (1953), pp. 207-214.

35. Siebel, M. P. L., "The Combined Bending and Twisting of Thin Cylinders in the Plastic Range," Journal of Mechanics and Physics of Solids, Vol. 1, No. 3, (1953), pp. 189-206.

36. Drucker, D. C., "Plasticity," Proceedings of the First Symposium on Naval Structural Mechanics, California, (Aug., 1958), pp. 407-455.

37. Iwan, W. D., "A Distributed-Element Model for Hysteresis and Its Steady-State Dynamic Response," Journal of Applied Mechanics, Vol. 33, No. 4, (Dec., 1966), pp. 893-900.

38. Naghdi, P. M., "Stress-Strain Relations and Thermo-plasticity," Proceedings of the Second Symposium on Naval Structural Mechanics, Rhode Island, (April, 1960), pp. 121-169.

39. Phillips, A., "Pointed Vertices in Plasticity," Proceedings of the Second Symposium on Naval Structural Mechanics, Rhode Island, (April, 1960), pp. 202-214.

40. Shield, R. T., and Ziegler, H., "On Prager's Hardening Rule," Z. Ang. Math. and Phys., (1958), pp. 260-276.

41. Tse, F. S., et al., Mechanical Vibrations, Boston: Allyn and Bacon, Inc., (1964).

42. Iwan, W. D., "The Dynamic Response of Bilinear Hysteretic Systems," Ph.D. Thesis, California Institute of Technology, Pasadena, U.S.A., (1961).

43. Caughey, T. K., "Sinusoidal Excitation of a System with Bilinear Hysteresis," Journal of Applied Mechanics, Vol. 27, No. 4, (Dec., 1960), pp. 640-643.

44. Nielsen, N. N., "Dynamic Response of Multi-Story Buildings," Ph.D. Thesis, California Institute of Technology, Pasadena, U.S.A., (1964).

45. Hildebrand, F. B., Introduction to Numerical Analysis, New York: McGraw Hill Book Company, Inc., (1961).

46. Husid, R., "Gravity Effects on the Earthquake Response of Yielding Structures," Ph.D. Thesis, California Institute of Technology, Pasadena, California, U.S.A. (1967).